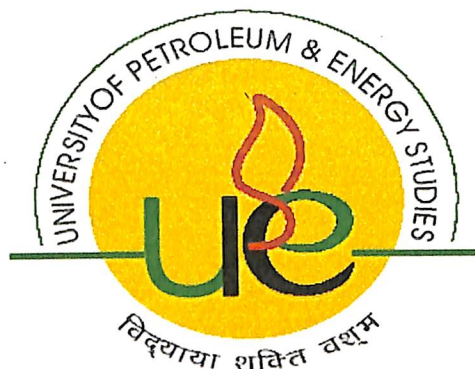


EFFECT OF RESERVOIR HETEROGENEITY ON WELL TESTING AND FIELD DEVELOPMENT

By
REEMA WADHAWAN
&
SHREYANSH DIVYANKAR



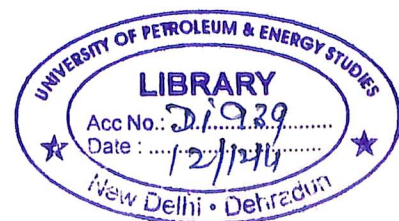
College of Engineering
University of Petroleum & Energy Studies
Dehradun
May, 2009

UPES - Library



D1939

WAD-2009BT



EFFECT OF RESERVOIR HETEROGENEITY ON WELL TESTING AND FIELD DEVELOPMENT

A dissertation submitted in partial fulfillment of the requirements for the Degree of
Bachelor of Technology

By
(REEMA WADHAWAN
&
SHREYANSH DIVYANKAR)

Under the guidance of

Dr. B.P. Pandey
(Project Guide & Dean Emeritus COE)
UPES

Approved

.....
Dean


College of Engineering
University of Petroleum & Energy Studies
Dehradun
May, 2009



UNIVERSITY OF PETROLEUM & ENERGY STUDIES
(ISO 9001:2000 Certified)

CERTIFICATE

This is to certify that the work contained in this thesis titled "Effect of Reservoir Heterogeneity on Well Testing and Field Development" has been successfully carried out by Mr. Shreyansh Divyankar and Ms. Reema Wadhawan, students of B.Tech Applied Petroleum Engineering- final year under my mentorship and has not been submitted elsewhere for a degree.


Dr. B.P. Pandey 07.05.09
Dean Emeritus & Professor of Eminence

Corporate Office:
Hydrocarbons Education & Research Society
3rd Floor, PHD House,
4/2 Siri Institutional Area
August Kranti Marg, New Delhi - 110 016 India
Ph.: +91-11-41730151-53 Fax: +91-11-41730154

Main Campus:
Energy Acres,
PO Bidholi Via Prem Nagar,
Dehradun - 248 007 (Uttarakhand), India
Ph.: +91-135-2102690-91, 2694201/ 203/ 208
Fax: +91-135-2694204

Regional Centre (NCR) :
SCO, 9-12, Sector-14,
Gurgaon 122 007
(Haryana), India.
Ph: +91-124-4540 300
Fax: +91-124-4540 330.

Regional Centre (Rajahmundry):
GIET, NH 5, Velugubanda,
Rajahmundry - 533 294,
East Godavari Dist., (Andhra Pradesh), India
Tel: +91-883-2484811/ 855
Fax: +91-883-2484822

Email: info@upes.ac.in URL: www.upes.ac.in

Acknowledgment

First and foremost, we are thankful to University of Petroleum & Energy Studies for giving us opportunity to carry out our major project on “Effect of Reservoir Heterogeneity on Well Testing and Field Development”.

We are indebted to our mentor, Dr. B.P. Pandey (Dean Emeritus, College of Engineering), for his constant support and guidance during this study. We would like to express our sincere gratitude for his patience and encouragement throughout this work, without which this work would not have been possible.

We take immense pleasure in thanking Mr. K.K Jha, (General Manager, Reservoir), Jubilent Petroleum Limited who has been a source of inspiration and for his timely guidance in the conduct of our project work. His contributions are infused throughout this report.

We are extremely grateful to the entire UPES faculty for their significant contribution to my academic and intellectual development.

Date:

Reema Wadhawan
&
Shreyansh Divyankar
(UNIVERSITY OF PETROLEUM & ENERGY STUDIES, Dehradun)

ABSTRACT

The prospect of a heterogeneous reservoir is not alien to a reservoir engineer who has studied the core samples of such a reservoir. Geological processes themselves dictate that rock to be non-uniform. The process of sedimentation, erosion, glaciation etc. all work towards creating a reservoir which is heterogeneous in nature, although the non-uniformity is to an extent predictable. In terms of well testing, reservoir heterogeneities are identified by variations in the pressure response. Sometimes the pressure data deviates from the homogeneous behaviour only during the first minutes of the test period under investigation, in other cases it takes from several hours to several days before the heterogeneity becomes evident. Heterogeneous Reservoirs have a signature pattern on pressure draw down curves and derivative plot. This is because of the flow regime prevailing in the reservoir. With the introduction of pressure derivative analysis and development of complex interpretation models that are able to account for detailed geological features, well test analysis has become a powerful tool for reservoir characterization. Heterogeneities which are hardly visible on the conventional well testing plots are amplified on the derivative plot.

Heterogeneity in reservoirs has resulted in paradigm shifts concerning the field development practices from the point of view of a reservoir engineer. We would like to highlight these new changes and use them to highlight the differences between a homogeneous and a heterogeneous reservoir. The project will also cover the condition and methods of application of the Schilthius Material Balance Equation to such reservoirs.

The project consists of an extensive literature survey on the types of non-uniformities generally encountered in oil and gas reservoirs. New practices and developments in well testing procedures would also be discussed and the role of well testing in determining the extent and nature of heterogeneity will be highlighted. In addition to this, we have presented the detailed analysis of the well testing results obtained; highlight the type of heterogeneity present and its origin.

CONTENTS

TITLE PAGE.....	i
CERTIFICATE.....	iii
ACKNOWLEDGEMENT.....	iv
ABSTRACT.....	v
TABLE OF CONTENTS.....	vi
LIST OF FIGURES.....	ix
LIST OF TABLES.....	x
1. INTRODUCTION TO RESERVOIR HETEROGENEITY.....	1
1.1 Classification of Reservoir Heterogeneity.....	1
1.2 Faults.....	3
1.3 Genetic Unit Boundaries.....	3
1.4 Shale Baffles and Permeability Streaks.....	3
1.5 Natural Fractures.....	4
2. CARBONATE RESERVOIRS.....	5
2.1 Environment of sedimentary formation.....	5
2.2 Rock Texture	6
2.3 Diagenesis and Porosity.....	8
2.3.1 Dolomatization.....	9
2.3.2 Stilolite.....	9
2.3.3 Dissolution.....	9
2.3.4 Fracturing.....	10
3. ANALYSIS OF NATURALLY FRACTURED RESERVOIR	11
3.1 Definition.....	11
3.2 Basic Types of Evaluation.....	12

3.3 Fracture System Origin.....	13
3.4 Experimental Fracture Classification.....	14
3.4.1 Shear Fractures.....	14
3.4.2 Extension Fractures.....	15
3.4.3 Tension Fractures.....	15
3.5 Geological Classification of Naturally Occurring Fractures.....	16
3.5.1 Tectonic Fractures.....	17
3.5.1.1 Fault related Fracture Systems.....	17
3.5.1.2 Fold related Fracture Systems.....	19
3.5.2 Regional Fractures.....	22
3.5.3 Contractional Fractures.....	24
3.5.3.1 Dessication Fractures.....	24
3.5.3.2 Syneresis Fractures.....	24
3.5.3.3 Thermal Contractional Fractures.....	26
3.5.3.4 Mineral phase change Fractures.....	26
3.5.4 Surface related Fractures.....	27
3.6 Fracture Properties affecting Reservoir Performance.....	28
3.6.1 Fracture Morphology.....	29
3.6.1.1 Open Fractures.....	30
3.6.1.2 Deformed Fractures.....	31
3.6.1.3 Mineral filled Fractures.....	33
3.6.1.4 Vuggy Fractures.....	35
3.6.1.5 Morphology/ Permeability Summary.....	36
3.6.2 Fracture Width and Permeability.....	36
3.6.2.1 Equation for Fluid Flow.....	36
3.6.2.2 Direct Effect of Fractures on Fluid Flow.....	42
3.6.2.3 Fracture Permeability vs. Confining space.....	43
3.6.2.4 Fracture Width vs. Confining Space.....	44
3.6.2.5 Fracture Spacing.....	45
3.6.3 Fracture and Matrix Porosity Communication.....	47

3.6.3.1 Basics.....	48
3.6.3.2 Porosity- Permeability Relationship.....	49
3.6.3.3 Compressibility Differences.....	49
3.6.3.4 Magnitude Difference.....	50
3.6.3.5 Significance of Fracture Porosity.....	51
3.6.3.6 Fracture Porosity Estimation.....	51
3.6.3.6.1 Core Analysis.....	51
3.6.3.6.2 Fracture Porosity- Fracture Permeability Relations.....	52
3.6.3.6.4 Log-Log Suits.....	54
3.6.3.6.5 Multiple Well Tests.....	54
3.7 Estimation of Porosity Interaction.....	55
4. BASICS OF WELL TEST ANALYSIS.....	56
4.1 Introduction.....	56
4.2 Methodology: The Inverse Problem.....	56
4.3 Plots used in Well Testing.....	57
4.4 Types of Flow Behavior.....	58
5. PRESSURE BEHAVIOR IN NATURALLY FRACTURED RESERVOIRS.....	59
5.1 Fissured Reservoir.....	59
5.2 Double Porosity Model.....	60
5.2.1 Restricted Interporosity Flow Model.....	63
5.2.2 Unrestricted Interporosity Flow Model.....	66
5.3 Matrix Skin.....	68
6. PRESSURE BEHAVIOR IN LAYERED RESERVOIR.....	69
6.1 Introduction.....	69
6.2 Pressure Decline Curves.....	70
6.3 Pressure Build-up.....	71
7. PRESSURE BEHAVIOR IN HYDRAULICALLY FRACTURED WELLS.....	74

7.1 Hydro-fractured Wellbore Models.....	74
7.2 Infinite Conductivity Fractured Wells.....	74
7.3 Finite Conductivity Fractured Wells.....	78

8. A CASE STUDY- WELL TEST INTERPRETATION OF HYDRO-FRACTURED WELLS.....	83
8.1 Introduction.....	83
8.2 Input Data for Interpretation.....	83
8.3 Plots.....	84
8.4 Results and Discussion.....	87
8.5 Software Run.....	87

9. RECOVERY AND MATERIAL BALANCE EQUATIONS OF DOUBLE POROSITY RESERVOIR.....	89
9.1 Determination of imbibition using empirical correlations.....	90
9.2 Flow between fracture and matrix: analytical analysis.....	94
9.2.1 Unidirectional one dimensional displacement.....	94
9.2.2 Counterflow In 3D.....	98
9.3 Material Balance Equation for Double Porosity Reservoirs.....	107

CONCLUSION.....	110
REFERENCES.....	111

LIST OF FIGURES

1.1: Types of reservoir heterogeneity	1
1.2: Impact of reservoir heterogeneity on oil recovery	4
3.1: Potential fracture planes developed in laboratory compression tests. Extension fractures (A) and shear fractures (B and C) are shown	15
3.2: Rose diagram of shear fractures associated with normal fault.....	18
3.3: Relationships between stress states, the fault and fracture orientations derived from those stress states, and the resultant dip histograms subsequently obtained from core analyses. After Price (1966) and Friedman (1969), courtesy of Pergamon Press, Ltd., and the American Association of Petroleum Geologists	19
3.4: Typical fold-related fracture orientation diagrams depicting a portion of the total fracture geometry on folds. After Price (1966) and Price (1967).....	20
3.5: A generalization of dominant fold-related fracture sets according to Stearns.....	20
3.6: A block diagram showing the geometry of the major conjugate fracture patterns observed on folds in rock.....	20
3.7: Contractional (chicken-wire) fractures in core sample	25
3.8: Contrasting characteristics of desiccation and syneresis.....	26

3.9: Example of 3-D whole-core permeability associated with an open fracture.....	30
3.10: Example of 3-D whole-core permeability associated with a gouge-filled fracture.....	32
3.11: Gouge texture in shales and carbonates.....	32
3.12: Example of 3-D whole-core permeability associated with a slickensided fracture.....	33
3.13: Example of 3-D whole-core permeability associated with mineralized fractures.....	33
3.14: vertical vs. horizontal permeability.....	43
3.15: Matrix (k_r) and fracture (k_f) and total (k_{fr}) permeability versus hydrostatic confining.....	44
3.16: calculation of fracture width (e) versus hydrostatic confining pressure (P_c) plot for several North Sea chalk samples.....	45
3.17: Fracture permeability as a function of fracture width and fracture spacing.....	46
3.18: Fracture porosity as a function of fracture width and fracture spacing.....	47
3.19: Normalized porosity (ϕ/ϕ_{500}) and permeability (k/k_{500}) are shown as a function of P_c	50

3.20: Fracture porosity as a function of fracture spacing and flow test permeability	53
5.1 Example of double porosity reservoir, fissured and multiple layer formation.....	59
5.2 Semi log plot of a well in a double porosity reservoir.....	65
5.3 Pressure and derivative plot of a well in a double porosity reservoir, pseudo steady state interporosity flow.....	66
5.4 Pressure and derivative plot of a reservoir in a double porosity reservoir, transient State interporosity flow.....	67
5.5 Matrix skin. Slab and sphere matrix blocks.....	68
6.1 Layered reservoir System.....	69
6.2 Well pressure decline and fractional flow rate from one layer for a two layer reservoir	70
6.3 Theoretical Pressure Build up curve for a two layer reservoir.....	71
6.4 Build up in two layer reservoir.....	72
6.5 Schematic cross section of a portion of a two layer reservoir with inter-layer crossflow	72
6.6 Pressure Performance at a constant production rate with and without crossflow.....	73

7.1 Fracture Geometry.....	74
7.2 Infinite Conductivity Fracture.....	75
7.3 Response of a well intercepting a high conductivity fracture. Infinite conductivity and Uniform Flux Model.....	76
7.4 Responses for a fractured well with wellbore storage.....	77
7.5 Responses of a well intercepting a high conductivity damaged fracture.....	77
7.6 Finite Conductivity Fracture.....	78
7.7 Finite Conductivity Fracture Pressure vs. fourth root of time.....	79
7.8 Response of a well intercepting a Finite Conductivity Fracture	80
9.1- Model of double porosity reservoir.....	89
9.2- Reservoir being considered as a series of blocks.....	91
9.3- Determination of recovery parameters.....	93
9.4- Birk's model.....	94
9.5- Displacement if matrix is gradually submerged in water.....	97
9.6- Pressure of fracture and matrix.....	101
9.7- Approximation of gravitational force.....	105
9.8- Displacement mechanism of double porosity reservoir.....	108

Chapter 1

Introduction to Reservoir Heterogeneity

Reservoir heterogeneities are small to large scale geological features that may or may not be significant from a strictly static reservoir characterization point of view, but do have a significant impact on fluid flow. Therefore, reservoir heterogeneity is not a truly static issue. An interesting and possibly surprising implication of such an observation is that the impact of reservoir heterogeneity is related to non-geological parameters, like mobility ratio, PVT properties, aquifer strength and development strategy. In other words, the same degree of geological reservoir heterogeneity may be important, for example, when the reservoir fluid is oil but may not be relevant in the case of a gas reservoir.

1.1 Classification of reservoir heterogeneities: A reservoir is intrinsically heterogeneous. Differences in lithology, texture and sorting, as well as the presence of fractures, faults, baffles and diagenetic effects of different nature are the principal factors responsible for what we call, reservoir heterogeneity. The existence of these features affects the fluid flow at different scales, from the micro to the mega scale. In particular, they have a considerable impact on the effectiveness of the displacement process and, consequently, on the value of the residual oil saturation and the final recovery factor. A correct evaluation of reservoir heterogeneity is therefore an essential issue in field development and exploitation, and must be explicitly taken into account in the construction of the reservoir simulation model.

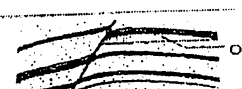
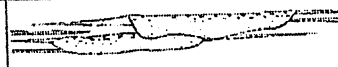
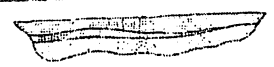
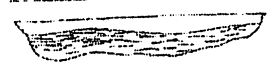


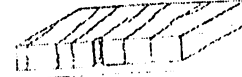
Reservoir heterogeneity type	
Sealing fault Semi-sealing fault Non-sealing fault	
Boundaries genetic units	
Permeability zonation within genetic units	
Baffles within genetic units	
Lamination, cross-bedding	
Microscopic heterogeneity, textural type, mineralogy	
Fracturing tight, fracturing open	

Figure 1.1: Types of Reservoir Heterogeneity



Small scale heterogeneity: At the scale of the pore (micro scale) the heterogeneity is clearly evident in the existence of different porosities, i.e. in carbonate reservoirs. At the core level (macro scale) the heterogeneities are often related to lamination and cross bedding. In fact, from a sedimentary point of view the only depositional unit that can be considered intrinsically homogeneous is the lamina. Being the product of a single, geologically instantaneous depositional system, the lamina is internally free of significant heterogeneities. These small scale heterogeneities have a significant impact on microscopic flow efficiency, hence on the overall recovery due to capillary trapping phenomenon. Inevitably these observations raise a question: how do we deal with such heterogeneities and how do we represent them in the much larger numerical simulation grid-blocks?

Several papers of Heriot- Watt University researchers have addressed the problem of small scale heterogeneity and its impact on fluid flow. Ideally, small scale heterogeneities should be explicitly taken into account, and proper up-scaling procedures should be applied to preserve at higher scale the impact of such heterogeneities on fluid flow. This phase, however, can be very time consuming, since it requires the use of numerical modeling to correctly describe the process and derive adequate pseudo-functions. In practice, it is very seldom performed and facies are characterized at the macro-scale with average petrophysical values that are computed without much concern about small scale heterogeneities. The implicit assumption is therefore that the rock can be considered homogeneous at smaller scale.

Large scale heterogeneity: Large scale (mega-scale) heterogeneities are the most important types of internal reservoir discontinuity. They can represent barriers to fluid flow and be responsible for the compartmentalisation of the reservoir. Alternatively, they may represent preferential flow paths with respect to a homogeneous, lower permeability background rock. In either case, their impact in the reservoir dynamics may be strong enough to dominate field performance; therefore their assessment is a mandatory task in all reservoir studies.

Referring to Fig. 1 the main types of large scale heterogeneities are faults, either sealing or not, boundaries of genetic units, high or low permeability streaks and shale baffles. Fractures, either open or sealed, represent another important type of reservoir heterogeneity. In this report, special emphasis has been given to fractured reservoirs as there have been numerous developments in the field of analysis of fractured reservoirs due to the all new discoveries being pre-dominantly fractured carbonate reservoirs.



The main characteristics of these large scale heterogeneities are briefly discussed as following:

1.2 Faults: Faults are typical structural discontinuities. A fault can be sealing, partially sealing or conductive and therefore it may represent a barrier, an impediment or a conduit to fluid flow. Hence when faults are concerned, the geoscientists are faced not only with the problem of identifying them, but also with the assessment of their seal potential. Four main mechanisms of faulting are described:

- *Juxtaposition:* reservoir units are juxtaposed against low permeability units, i.e. shales.
- *Clay smear:* entrainment of clay in fault plane creating a low permeability surface
- *Cataclasis:* crushing of sand grains to form a surface with high capillary entry pressure
- *Diagenesis:* preferential cementation that creates a seal by completely or partially removing the original porosity.

When faults are recognised, several theoretical methods have been developed to assess their seal potential. Juxtaposition for example, can be studied by means of graphs that allow for the reconstruction of the fault throw and predict the occurrence of given lithologies along the fault plane.

1.3 Genetic unit boundaries

Always encountered in real depositional systems. They represent stratigraphic discontinuities whose sealing potential is variable and dependent on a number of parameters such as contrast in lithology and petrophysical properties of adjacent units etc. Isolated bars or channels, sand or conglomerate lenses in shales is an example of this heterogeneity.

1.4 Shales baffles and permeability streaks

In clastic reservoirs, presence of shale baffles is often observed within the main genetic unit. These features can be detected from cores or well logs and their lateral extension



depends on the sedimentary environment. Carbonate streak represents another major heterogeneity and is formed usually at the interface of deposition cycles.

Both shale baffles and carbonate streaks affect vertical communication in the reservoir.

1.5 Natural fractures: a detailed analysis of natural fractures is provided in chapter 3.

Reservoir heterogeneity type	Reservoir continuity	Sweep efficiency		
		Horizontal	Vertical	Microscopic
Large scale				
Sealing fault	x	x		
Partially sealing fault	o	x	x	
Non-sealing fault	o	x	x	
Boundaries of genetic units	x	x	x	
Permeability zonations		o	x	o
Baffles and streaks		o	x	o
Open fractures		x	x	
Tight fractures		x	x	
Small scale				
Laminations and crossbedding		o	o	x
Mineralogy and texture			x	
Open microfractures		x	x	x
Tight microfractures		x	x	x

o = moderate effect x = strong effect

Figure 1.2: impact of heterogeneity on oil recovery



Chapter 2

Carbonate Reservoirs

About one half of the world's hydrocarbon reserves are trapped in carbonate reservoirs. Carbonate reservoirs are different from Silliclastic reservoirs in many aspects: they originate where the sediments are formed and hence transport plays a minimal role. In general, they are of biogenic origin and the carbonate is very soluble in (acidic) water. Furthermore, diagenesis has a greater role in the development of porosity, the carbonate is more brittle and compared to sandstone, fractures easily and because of carbonate solubility significant sized caverns can be formed.

2.1 Environment of Sedimentary Formation

The basic difference between carbonate and sandstone reservoirs is that carbonate reservoirs are basically of biological origin. This fact determines the process of diagenesis and the rock texture. The formation of present carbonate sediments indicates that 90% of them are of biological origin in marine environment.

The spread of the carbonate rock is determined in areas where the living condition for the associated organisms is guaranteed: i.e. temperature, light, salinity and availability of nutrient. During the lives of such organisms, using their organic framework they build coral reefs, which can resist the destructive effects of water. Today the coral reefs result from living corals and red algae. They are dependant on each other and thus they live in symbiosis. The algae draw out carbon dioxide from water and CaCO_3 is deposited; the corals build their framework from CaCO_3 .

The living conditions for corals include clean water and light. This is why the water depth favourable for their existence is less than 75 meters. For corals, the tropical waters between the 30 degree North and 25 degree South latitudes are favourable. Coral reefs are biogenic constructions which are formed in shallow water from the living corals 'settled' in colonies. The forms of reefs are the following after Link P.K. (1982):

- Fringe reef: it is located directly on the coastline; it forms where there is no or very little debris and no mud
- Barrier reef: it is separated from the coastline by a lagoon, it has a long shape and its other side faces the sea



- Atoll: circular or elliptical shaped reef which is on the edge of a submerged volcano and as soon as it sinks downward with the rising sea level, the corals build up the reef at the same velocity as that of the submerging of the volcano
- Pinnacle: due to rapid rise in sea level the reef is built vertically; its areal extent is small and its height can be up to 100 metres

In general, reef has an irregular surface considering that the shape is influenced by the changing life conditions of the living organisms. If the sea level decreases the reef comes to the surface and its destruction and disintegration begins; this results in the formation of carbonate debris, carbonate sand and mud. If the sea level rises the construction of reef continues once again. Reservoirs originating from reefs generally have excellent parameters. The morphology and geology of coral reefs can also be classified in other ways:

- Bioherm: reefs build by corals, elliptical or circular in shape and made up of the remains of corals or shellfish
- Biostrom: stratified, partially eroded reef, it originates during the course of the disintegration of the Bioherm
- Stratigraphical reef: a series of Bioherm reefs built one upon another

That part of the coral reef, which faces the open sea, is permanently subject to the effect of strong waves and this results in disintegration and breaking down of the reef itself. The debris has a porosity which improves the reservoir parameters. Various types of carbonate formation are possible on the continental shelf. The limestone mud, which occurs here, results in carbonate formations that have poor properties (except in the case of Dolomitization). Deep sea carbonate sediments are very finely graded. Given this fact and there is no oxygen in this environment, these sediments can be effective source rock. The carbonate mud deposited in the lagoons (between the barrier reef and the coastline) is not suitable for reservoir because such a reservoir has unfavourable properties in the absence of dolomitization.

In general, there is no debris from the shore in the lagoons and it is mainly different evaporates (e.g. gypsum, salt, etc.) that are formed.

2.2 Rock Texture

The biological origin of the carbonate reservoirs does not make it easy to classify the rock texture. In the case of siliciclastic reservoirs the grain size of sediments and their grading and energy of the transporting agent determines the rock texture; with carbonate reservoirs the particle size and the grading of the particles is influenced by the dynamics



of the activities of the living organisms and the shape of the framework of their bodies (e.g. circular, bristles, etc.). After the formation of carbonate sediments, if those sediments are then independent of the activities of the living organisms, then the transport and sedimentation are the same as in the case of silicate sediments (i.e. beds, layers, laminae, cross bedding, ripples, turbidites etc.) although there is less resistance for transport.

For easier understanding of the classification of the rock texture the following terminology (after Balogh K. 1992) is used:

- **Micrite:** this describes opaque carbonate rock which is formed by 1-4 μm diameter calcite crystals (lime mud). Its origin is explained by the activity of bacteria and/or algae, inorganic deposition of carbonate or the mechanical degradation of the carbonate rock.
- **Algae- stromalites:** in general thin disc shaped (laminae) carbonate sediments are called stromalites. Some of these are inorganic in origin but the majority are the result of the living functions of blue and green algae.
- **Pellets:** spherical or egg shaped, consisting sometimes of slightly stretched micro or kryptocrystallised calcites and sometimes of carbonate silt with diameter 0.02-2.0 mm. This type of rock has good reservoir parameters. They originate primarily from mollusc and worm faecal pellets.
- **Ooides:** spherical or egg shaped carbonate particles, which are created from the inner core and one or more multi layered CaCO_3 crystal shells concentrated around the core. The thickness of layers of the covering is 3-15 μm . The number of concentric layers reaches up to 200. Ooides can measure 0.2-2.0 mm but in general their size is between 0.2-0.6 mm. The core of the Ooides can be of any matter like terrigenous sand particles. Reservoirs with good porosity can be formed with Ooides.
- **Oolites:** similar to Ooides with the difference that there are one or two CaCO_3 shell layers only.



In 1913 Grabau A.W. classified carbonate reservoirs according to particle size, which is summarised in the following table-

Table 2.1: classification according to particle size

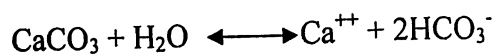
Name	Particle diameter (mm)	Remark
Calcilutite	<0.004	
Calcsiltite	0.004-0.06	Fine and coarse
Calcarenite	0.06-2.00	From very fine to very coarse particles
Calcirudite	2.00-8.00	

However, Folk's classification is the preferred one: he classified carbonate reservoirs according to components, i.e. grains, matrix and cement.

Dunham classified carbonate reservoirs in the following way: what is the proportion of the lime mud and carbonate particles with diameters over 0.02 mm. If the proportion of lime mud is large then the grains are mud supported. However, if the particles are larger in volume then the rock is supported by grains. If the quantity of grains is around 10% then the particles are submerged in lime mud. If the particles are present in such a quantity that they are actually in contact with one another then the rock is grain supported.

2.3 Diagenesis and Porosity

The diagenesis of carbonate sediments is a complex process. After the sediment has been deposited, it changes due to physical and chemical processes. Thus it is difficult to draw conclusions from the rock texture about the environment in which it is deposited. The precipitation of the carbonate sediments in water can be described by the following equation:



Calcium carbonate is crystalline, while the calcium and hydrogen carbonate ions are present in the dissolved form. If the organisms draw out the CO_2 in order to sustain their life processes then CaCO_3 is deposited. If the CO_2 is dissolved in water in the form of H_2CO_3 (acid) then the earlier deposited carbonates are dissolved, resulting in the formation of caves, caverns and vugs. This process is determined by the pressure, temperature and ionic concentration. Attention needs to be paid to the fact that the environment where the process takes place is very complex in all aspects. This is why

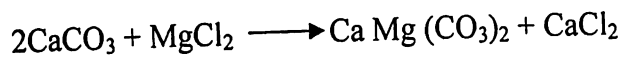


very heterogeneous reservoir formations can occur. The concentration of the hydrogen ions (pH) has an important role in the formation of the rock.

The reservoir parameters are influenced by dolomitization, formation of stilolites, dissolution and by fracturing.

2.3.1 Dolomitization

The limestone can partly or completely turn into dolomite if, after deposition, water, which is rich in magnesium ions can be filtered through it:



From the point of view of crystallization, dolomite $\text{Ca Mg} (\text{CO}_3)_2$ is similar to limestone; however, its density is greater, it is less soluble in water and more brittle. During the course of recrystallization there is decrease in volume and from the Micrite (sugar texture), in a reservoir with generally good parameters a dolomite rock is formed if a dense interlocking crystal fabric does not originate. Moore C.H. (1989) analyzed the relation between degree of dolomitization and porosity. In the example which he presented (after Murray, 1960), with the dolomitization of limestone the porosity linearly decreased until the fraction of dolomite in the rock increased from 0% to 50%. At 50%, the dolomite rhombs act as the framework which prevented further compaction of the lime mud. After that as the fraction of dolomite increased over 50%, the porosity also increased. From the point of view of reservoir parameters, it is most favourable if the degree of dolomitization is around 80% with regard to the rock volume.

2.3.2 Stilolite

The formation of stilolites can be attributed to the solubility of rock particles due to high pressure and this can occur in silicate type rocks as well. Stilolite is essentially a rock suture, which has irregular sealing surface and basically it can influence fluid filtration if this suture is continuous and extend over a large area.

2.3.3 Dissolution

If the limestone is exposed to the surface it will crack and the water that absorbs the CO_2 from the air forms an acid which will dissolve the limestone; moreover at a given depth caves develop up to the height of the outflow of surface water. If the height of the outflow of the surface water changes (e.g. it sinks), then a new cavern system can occur which is hydrodynamically connected with the previous system. If the sediment does not



fill up the cavities, then a very complex reservoir forms, although with excellent parameters. For example, during drilling the 'fall' of drilling pipes to some metres can prove the presence of caverns. Due to the effects of unbalanced forces, the cave zone might also collapse. In this case the reservoir structure is quite different.

2.3.4 Fracturing

Carbonate rocks are brittle and hence fracturing can occur due to the combined effect of different force systems. Fractures usually improve the reservoir parameters and determine the well pattern and production technology. Frequently, the fractures can be filled in and various minerals can be crystallized.



Chapter 3

Analysis of Naturally Fractured Reservoirs

3.1 Definition

The word "fracture" has been defined in various ways. Some definitions are purely descriptive (Dennis, 1967) while others are mechanical (Ranalli and Gale, 1976). The range in definitions generally reflects the different interests of the authors. A reservoir fracture is a naturally occurring macroscopic planar discontinuity in rock due to deformation or physical diagenesis. If related to brittle failure, it was probably initially open, but may have been subsequently altered or mineralized. If related to more ductile failure, it may exist as a band of highly deformed country rock. As a result, natural reservoir fractures may have either a positive or negative effect on fluid flow within the rock.

This broad definition allows this report to address fluid flow anisotropy created by numerous features regardless of any mechanical differences in their generation and propagation (extension versus shear, mode 1 versus mode 2, fracture versus microfault, etc.). This definition also makes it possible to treat effects of various fracture morphologies on fluid flow. For example, one can look at the effect of highly permeable open fractures on reservoir behavior, but can also consider the strong anisotropy in rock permeability created by low-permeability deformed fractures. The definition of a reservoir fracture is a broad one and the definition of a "fractured reservoir" even more so. Because natural fracture systems can have a variety of effects on reservoir performance in primary, secondary, and tertiary recovery, and because these effects must often be predicted long before they are evidenced in production data, an operational definition of a fractured reservoir becomes a necessity. A fractured reservoir is defined as a reservoir in which naturally occurring fractures either have, or are predicted to have, a significant effect on reservoir fluid flow either in the form of increased reservoir permeability and/or reserves or increased permeability anisotropy. The qualifier, or "are predicted to have a significant effect," is important operationally because the data necessary to quantify a fractured reservoir must be collected very early in the life of a reservoir. We must often, therefore, predict the "significant effect" and treat the formation as a fractured reservoir prior to true substantiation by production history.



3.2 Basic types of evaluation

Exploration and production cannot be separated from evaluation in fractured reservoirs. It is of paramount importance to know what we are looking for and what we have found in terms of reservoir properties. There are three basic types of evaluation to be addressed in fractured reservoir analysis (Nelson, 1982). They are listed in order of increasing complexity, amount of data, and time to completion:

- Early exploration evaluations to determine or predict gross reservoir quality.
- Evaluations of economic potential (reserves, flow rates, etc.).
- Evaluations for recovery planning and detailed reservoir modeling

The early exploration evaluation data most often used are:

- General geological/geophysical data on structural forms.
- A good lithologic description of the stratigraphic section.
- Mechanical data on the particular rocks of interest or on similar lithologies.
- Matrix properties from logs or as interpreted from nearby areas.
- Drill stem test (DST) or initial potential (IP) flow rates.
- Core analysis (standard or whole core).
- Borehole imaging logs.
- In situ stress data.

In addition to early exploration data, other information should include:

- Extended time pressure tests.
- 3-D whole-core permeability analyses (oriented if possible), borehole imaging logs.
- Laboratory data on matrix and fracture properties under simulated depth and depletion conditions.
- Estimations of fracture/matrix interaction.

The types of data most often used in recovery planning evaluations are:

- Detailed structure maps covering several horizons above and below the producing formation.
- Detailed core descriptions including lithology, mineralogy, textures and a foot-by-foot documentation of fracture occurrence, orientation, and morphology.
- Interpreted borehole imagery logs in all wells, especially those that are uncored.



- 3-D whole-core analyses with at least one oriented core in the field.
- Mechanical data derived from core samples of interest.
- Geologic Analysis of Naturally Fractured Reservoirs
- Long-term flow tests and multiple well tests.
- Estimation of initial in situ stress state in the reservoir.
- Laboratory data on both matrix and fracture properties under simulated depth and depletion conditions.
- Laboratory data on fracture/matrix interaction.

3.3 Fracture System Origin

The origin of the fracture system is postulated from data on fracture dip, morphology, strike (if available), relative abundance, and the angular relationships between fracture sets. These data can be obtained from full-diameter core (oriented or conventional), borehole imaging log output, or other less oriented logging tools, and applied to empirical models of fracture generation. Available fracture models range from tectonic to others of primarily diagenetic origin (Stearns and Friedman, 1972; and Nelson, 1979). It is only by a proper fit of fracture data to one of these genetic models that any effective extrapolation or interpolation of fracture distribution can be made. The interpretation of fracture system origin involves a combined geological/rock mechanics approach to the problem. It is assumed that natural fracture patterns depict the local state of stress at the time of fracturing, and that subsurface rocks fracture in a manner qualitatively similar to equivalent rocks in laboratory tests performed at analogous environmental conditions. Natural fracture patterns are interpreted in light of laboratory-derived fracture patterns (Handin and Hager, 1957) and in terms of postulated paleo-stress fields and strain distributions at the time of fracturing.

In general, any physical or mathematical model of deformation that depicts stress or strain fields can, by various levels of extrapolation, be used as a fracture distribution model (Hafner, 1951; Odé, 1957; and Lorenz and others, 1993). A genetic classification scheme for natural fracture systems, which is an expansion of that found in Stearns and Friedman (1972), permits separation of complicated natural fracture systems into superimposed components of different origin. Such partitioning can make delineation of structure (Friedman, 1969; and Friedman and Stearns, 1971) and prediction of increased fracture-related reservoir quality (McCaleb and Willingham, 1967; and Stearns and Friedman, 1972) from fracture data more tractable. Stearns and Friedman (1972) classify fractures into those observed in laboratory experiments and those observed in outcrop and subsurface settings. Their classification scheme, together with modifications suggested by this book, forms a useful basis for fracture models (Table 1-1). The major



modification to Stearns' and Friedman's scheme is the addition of two categories of naturally occurring fractures: contractional fractures and surface-related fractures. A minor modification to the experimental fracture classification is the addition of a category similar to extension fractures in morphology and orientation, but having a different stress state at generation and rock strength: tension fractures.

Experimental fracture classification:

- Shear fractures
- Extension fractures
- Tensile fractures

Naturally occurring fracture classification:

- Tectonic fractures (due to surface forces)
- Regional fractures (due to surface or body forces)
- Contractional fractures (due to body forces)
- Surface related fractures (due to body forces)

3.4 Experimental fracture classification:

3.4.1 Shear Fractures

Shear fractures have a sense of displacement parallel to the fracture plane. They form at some acute angle to the maximum compressive principal stress direction (σ_1) and at an obtuse angle to the minimum compressive stress direction (σ_3) within the rock sample. Potentially, two shear fracture orientations can develop in every laboratory fracture experiment, one on either side of, and oriented at the same angle to, σ_1 . In laboratory experiments, these fractures form parallel to σ_2 and at an obtuse angle to σ_3 . Shear fractures form when all three principal stresses are compressive (compressive stresses are considered positive). The acute angle between shear fractures is called the conjugate angle and is dependent primarily on:

- The mechanical properties of the material.
- The absolute magnitude of the minimum principal stress (σ_3).
- The magnitude of the intermediate principal stress (σ_2) relative to both the maximum (σ_1) and minimum (σ_3) principal stresses (as σ_2 approaches σ_1 the angle between σ_1 and the fracture plane decreases).

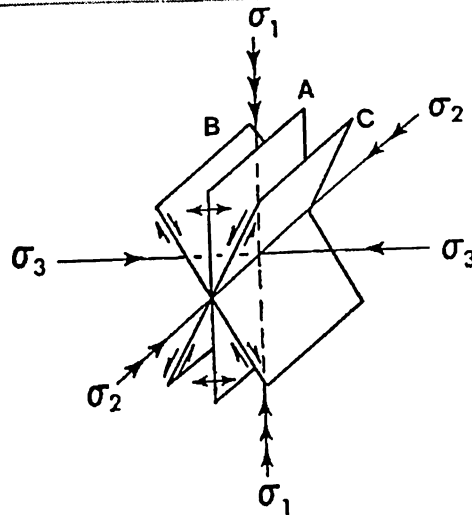


Figure 3.1: Potential fracture planes developed in laboratory compression tests. Extension fractures (A) and shear fractures (B and C) are shown.

3.4.2 Extension Fractures

Extension fractures have a sense of displacement perpendicular to and away from the fracture plane. They form parallel to σ_1 and σ_2 and perpendicular to σ_3 (Figure 3.1). These fractures also form when all three principal stresses are compressive. In laboratory fracture experiments, extension fractures can and often do form synchronously with shear fractures.

3.4.3 Tension Fractures

Tension fractures also have a sense of displacement perpendicular to and away from the fracture plane and form parallel to σ_1 and σ_2 . In terms of orientation of σ_1 and sense of displacement, these fractures resemble extension fractures. However, to form a tension fracture, at least one principal stress (σ_3) must be negative (tensile). To form an extension fracture, all three principal stresses must be positive (compressive). The distinction between the two is important because rocks have a much lower (10 to 50 times lower) fracture strength in tension tests than they do in extension tests. This becomes important in mathematical prediction of subsurface fracturing. Also, it is likely that true tensile fractures only occur in near subsurface environment, while extension fractures can occur in all low mean stress subsurface conditions. In general, we will call extension fractures those that are parallel to σ_1 and perpendicular to σ_3 when σ_3 is compressive (positive) or when its sign is unknown; tensile fractures will be referred to only when evidence suggests σ_3 is negative.



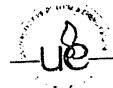
3.5 Geological Classification of Naturally Occurring Fractures

The genetic natural fracture classification presented in Stearns and Friedman (1972) and expanded here is built on two fundamental assumptions:

- Natural fracture patterns (conjugate shear and extension or tensile fractures) faithfully depict the local state of stress at the time of fracturing.
- Subsurface rocks fracture in a manner qualitatively similar to equivalent rocks in laboratory tests performed at analogous environmental conditions.

Thus, it is assumed that natural fracture patterns reflect the same geometry with respect to applied loads as do fractures generated in laboratory experiments. If these assumptions are correct, then naturally occurring fractures can be classified on the basis of the origin of their causative forces as determined from laboratory data and fracture system geometry. Therefore, this classification relies heavily on the previously presented experimental or generic fracture classification. There are two schools of thought on the best means to observe and describe complex natural fracture systems in outcrop. One assumes that fracture data must be handled statistically to be meaningful. Thus, by combining large amounts of data from many outcrops together and searching for preferred orientations, it is believed that objectivity in interpretation can be obtained (Currie and Reik, 1977). While this combining of data is necessary at some stage of a fracture study, our research indicates this approach to be inefficient due to the great loss of interpretive precision when data are lumped together prior to interpretation.

For example, an orientation plot containing 10,000 fracture measurements from many places on a fold will display gross trends in the data but will not allow description of subtle changes in orientation and inferred stress states from outcrop to outcrop. A second approach involves the interpretation of individual outcrop data with respect to the mode of origin prior to statistical treatment (Stearns and Friedman, 1972). These interpreted data sets can then be added together sequentially to arrive at a combined description. The combined data set will have more statistical meaning and is also more easily interpreted for stress analysis due to prior interpretation of the statistically less significant individual data sets. This approach to fracture interpretation necessitates the use of a genetic natural fracture classification such as that used in this report. Determining the origin of loads that caused fracturing at the outcrop scale increases the precision of structural interpretation on all scales. This can be accomplished because fractures form in a consistent geometry with respect to the three principal stress directions, thus delineating the paleo-stress field at the time of fracture. The geologic classification described below has important ramifications to pervasiveness, or the degree to which the fracture system is developed



over multiple scales of size. For example, tectonic fractures related to folding are pervasive because the same fracture types and orientations are seen from aerial photographs of the outcrop, to hand samples from the outcrop, to thin sections taken from the outcrop or core. On the other hand, regional fractures are non-pervasive because they can usually be seen on only a limited number of scales, i.e., down to outcrop scale only.

3.5.1 Tectonic Fractures

Tectonic fractures are those whose origin can, on the basis of orientation, distribution, and morphology, be attributed to or associated with a local tectonic event. They are formed by the application of surface forces. This author has observed that the majority of tectonic fractures in outcrop tend to be shear fractures according to the literature reviewed. However, locally there have been examples of folds in compressive environments where the deformation is dominated by extension fractures. Tectonic fractures form in networks with specific spatial relationships to folds and faults.

3.5.1.1 Fault related Fracture Systems

Fault planes are, by definition, planes of shear motion. The majority of fractures developed in the vicinity of faults are shear fractures parallel to the fault, shear fractures conjugate to the fault, or extension fractures bisecting the acute angle between these two shear directions (the zone of fault slip or gouge is complex, and has its own internal deformation morphology). These three orientations (Figure 3.2) correspond to the three potential fracture directions during laboratory fracture experiments (Figure 3.1) and are developed relative to the local state of stress causing the fault. The fault is a result of the same stress field that caused the fractures. The fracture swarm predates the through-going fault and acts as a process zone conditioning the rock mass for the eventual fault offset. There are cases where large-scale slip did not occur, leaving only the precursive fracture swarm. In these cases, the orientation of the swarm itself, as well as the internal fracture orientations is needed to ascribe a fault-related origin. Several authors have noted and documented the fault-fracture relationship: Stearns (1964), Yamaguchi (1965), Norris (1966), Stearns (1968a, 1968b, 1972), Skehan (1968), Friedman (1969, 1975), Tchalenko and Ambraseys (1970), Stearns and Friedman (1972), and Freund (1974). Because of the relationship between faulting and fracturing, it is possible to determine the direction of the principal stresses or loads at the time of formation. Also, knowing the orientation of a fault plane and the fractures associated with it, the sense of movement of the fault can be determined (Figure 3.3). The relationship of fractures to faults exists on all scales. Indeed, Friedman (1969) was able to use the orientation of microscopic fractures from oriented cores in the Saticoy Field of California to determine the orientation and dip of a nearby fault.

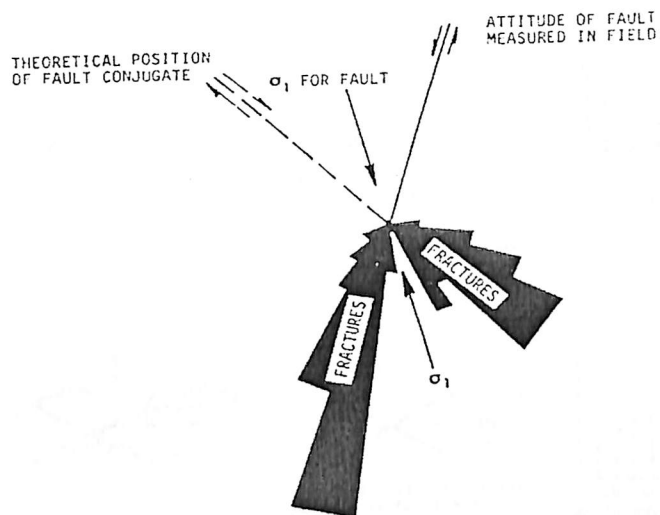


Figure 3.2: Rose diagram of shear fractures associated with normal default.

While, under ideal conditions, it is now possible to determine the orientation and sense of displacement of a nearby fault by the analysis of fractures, it is difficult to determine the proximity of the fault (Skehan, 1968; Pohn, 1981; Shepherd and others, 1982). The intensity of fracturing associated with faulting appears to be a function of lithology, distance from fault plane, amount of displacement along the fault, total strain in the rock mass, depth of burial, and possibly the type of fault (thrust, growth, etc.). Which of these parameters will dominate fracture intensity varies from fault to fault. There are other less frequent fracture orientations associated with faulting of various scales. One group of grain-sized fractures occurs at acute angles to the fault plane and is called microscopic feather fractures (Friedman and Logan, 1970), Conrad (1974) relates these to displacement along the fault and the normal stress across the fault plane. While these feather fractures are important in determining a faulting origin and in microscopic examination of fault planes for the sense of shear motion, their importance in macroscopic fracture production of hydrocarbons is probably minimal. Other fractures associated with faults occur within the slip zone itself. These reflect complex and changing stress and strain states inherent in the slip zone or mylonite zone itself.

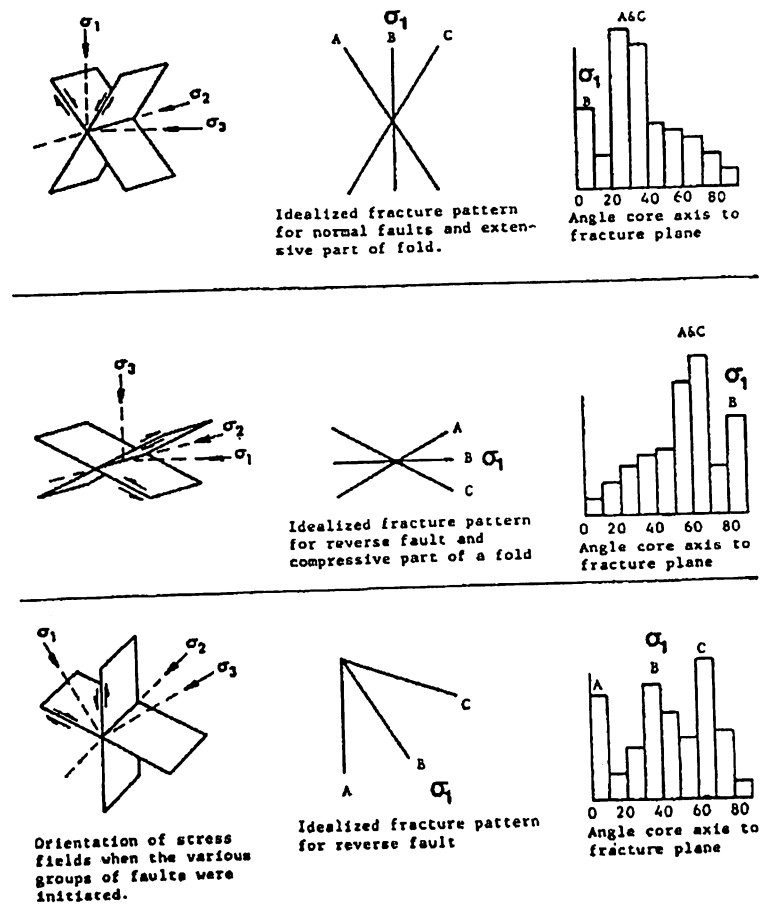


Figure 3.3: Relationships between stress states, the fault and fracture orientations derived from those stress states, and the resultant dip histograms subsequently obtained from core analyses. After Price (1966) and Friedman (1969), courtesy of Pergamon Press, Ltd., and the American Association of Petroleum Geologists

3.5.1.2 Fold related Fracture Systems

The stress and strain history during the initiation and growth of a fold in rock is very complex. Therefore, the fracture patterns that develop within the fold are also complex. A significant amount of literature has been published describing the orientation of fractures on folds: Martin (1963), Stearns (1964, 1968a, 1968b), Muecke and Charlesworth (1966), Price (1966), Roberts (1966), Nickelson and Hough (1967, 1969), Norris (1966), Price (1967), Charlesworth (1968), Parker (1942, 1969), Arndt and others (1969), Burger and Thompson (1969, 1970), Friedman and Stearns (1971), Stearns and Friedman (1972), McQuillan (1973, 1974), and Reik and Currie (1974). The majority of these papers describe only portions of the total fracture geometry (Figure 3.4). Stearns (1964, 1968a,

1968b) presents the most useful description of the total fracture geometry of folds (Figures 3.5 and 3.6).

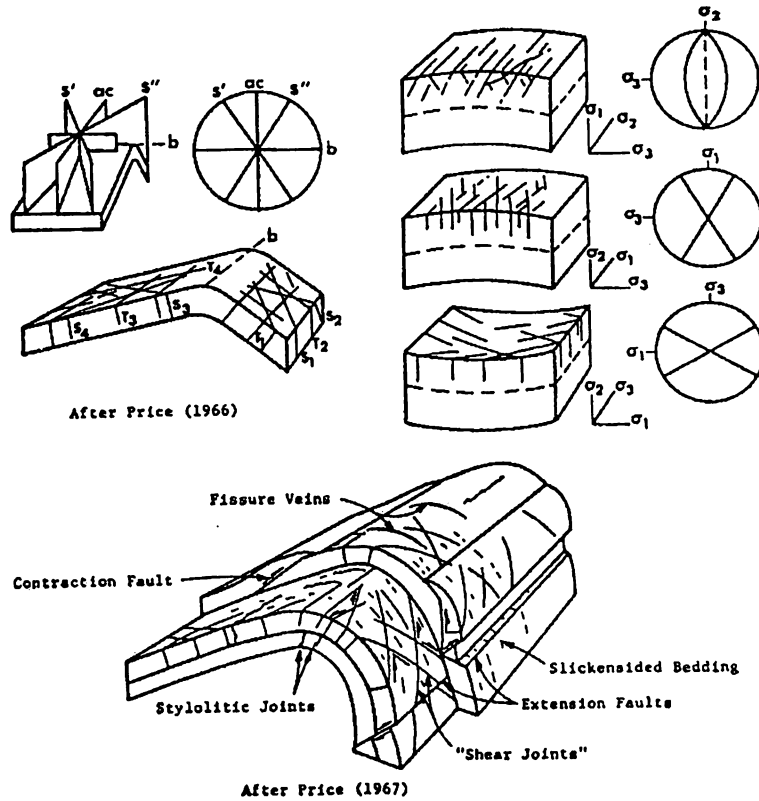


Figure 3.4: Typical fold-related fracture orientation diagrams depicting a portion of the total fracture geometry on folds. After Price (1966) and Price (1967)

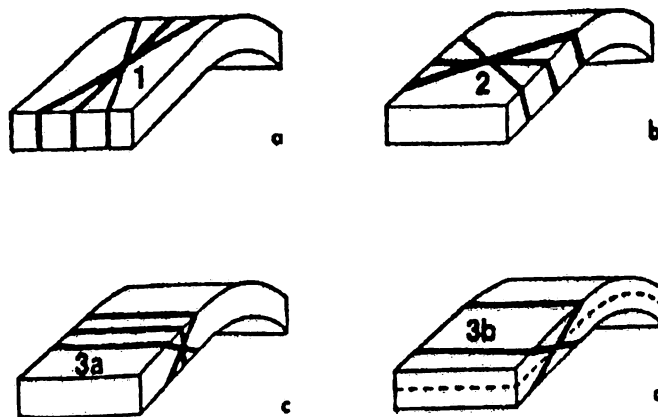


Figure 3.5: A generalization of dominant fold-related fracture sets according to Stearns

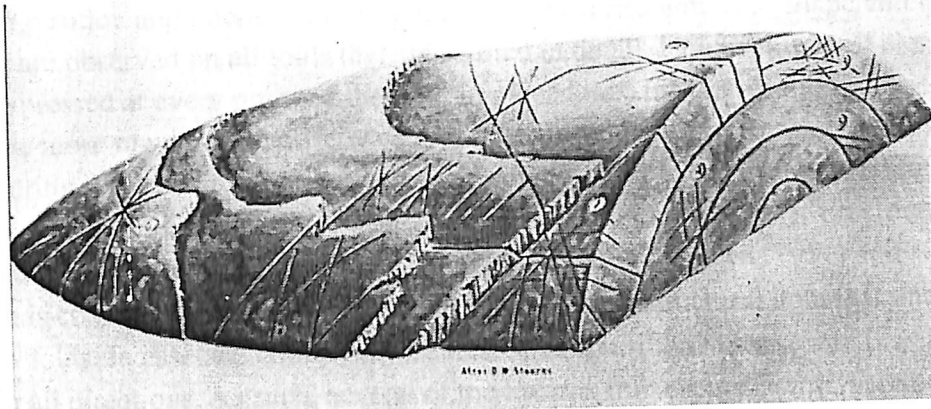


Figure 3.6: A block diagram showing the geometry of the major conjugate fracture patterns observed on folds in rock

Table 3.1: Fracture geometry of folds

Type set	σ_1	σ_2	σ_3
1	Parallel to dip direction	Perpendicular to bedding	Parallel to bedding
	Parallel to bedding		
2	Perpendicular to dip direction	Perpendicular to bedding	Parallel to bedding
	Parallel to bedding		
3. a	Perpendicular to bedding	Parallel to bedding strike	Parallel to dip direction
3. b	Parallel to the dip direction	Parallel to bedding strike	Perpendicular to bedding
4	Parallel to bedding	Parallel to bedding strike	Perpendicular to bedding
5	At an angle to bedding plane (dihedral angle)	Parallel to bedding strike	At an angle to bedding plane (90 degree dihedral angle)

- 1- Associated with bending in strike section
- 2- Associated with bending in dip section
- 3- Associated with bending in cross section; (a) extension, (b) compression
- 4- Associated with fold related thrusting
- 5- Associated with bedding plane slip



While the position and intensity of these fracture sets varies with fold shape and origin, most sets are observed on all folds that are studied in detail. However, not all elements will be expressed at every point on the fold. In other folds, the distribution of orientations tends to be more regular. The difference is that each fold has uniqueness in its strain pattern during folding. The distribution of various elements of the fold-related fracture geometry that are utilized on the structure during deformation will vary. Fractures associated with domes have been briefly investigated by Nakagawa (1971) and Nelson (1975). It is concluded that the distribution of fractures on structural domes is analogous to that on folds. In essence, domes may be treated as equi-dimensional anticlines that plunge in all directions. As such, several of the Stearns fracture sets, which are defined with respect to the strike and dip of the beds, become coincident on domes.

3.5.2 Regional Fractures

Regional fractures are those that are developed over large areas of the earth's crust with relatively little change in orientation, show no evidence of offset across the fracture plane, and are always perpendicular to major bedding surfaces. Regional fractures differ from tectonic fractures in that they are developed in a consistent and simple geometry, have a relatively large spacing, and are developed over an extremely large area crosscutting local structures. These fracture systems have (1)

- Orientation variations of only 15–20° over 80 mi.;
- Fracture spacing ranging from just under 1 ft. to over 20 ft.
- Consistent development in large areas

The descriptive terms of Hodgson (1961a) are the most commonly used. He describes the longer and more through-going fracture set as the “systematic” set (usually 90° Azimuth [AZ] from the first) and the shorter more discontinuous fracture set as the “non-systematic” set. Because the non-systematic set often abuts or terminates against the systematic set, they are considered to have formed sometime after the systematic set. However, the time delay may have been milliseconds or many years. Regional fractures in the stratigraphic section generally parallel cleat directions in coal beds in an area, with the face cleat corresponding to the systematic regional fracture set and the butt cleat corresponding to the non-systematic regional fracture set. Regional fractures are commonly developed in orthogonal sets (Price, 1959, 1966; Stearns, 1968a; and Holst, 1982) and often change strike slightly from formation to formation. It has been suggested that the two orthogonal orientations which are parallel to the long and short axes of the basin in which they form are due to the loading and unloading history of the rock. The



origin of regional fractures is obscure. Many theories have been proposed, ranging from plate tectonics to earth tides (fatigue); however, none have proven conclusive.

At present, they are considered to be due to the application of external or surface forces. They are probably developed with respect to vertical earth movements, but their distribution indicates that the scale of this movement is much larger in areal extent than anything we see in local structures. One proposal of regional fracture origin that has gained support in the last 10 years is that of Lorenz et al. (1993). In their model, regional fractures are thought to be related to tectonic loading at the basin edges. It is postulated that these fractures owe their orientation to the compression or shortening directions of the belt at the basin edge and on the belt's geometric variation. Variations in the shape of the indenter or compressing block are envisioned to give variations in the strike of the resulting regional fractures within the basin. A convincing argument can be made for this idea. However, several features of regional fractures worldwide do not fit this model:

- The intensity of regional fracture systems does not vary dramatically from the active basin margin to the basin centre; they should decrease noticeably in intensity toward the basin centre.
- There are many basins that have well-developed regional fractures that have no structural belts at their edges to cause the fracturing.

As an alternate hypothesis, regional fractures are seen as part of the normal basin compaction process. The fractures are an artifact of the loss of vertical dimension of the sediments, and the pattern and azimuth of the extension fractures are imparted by the geometry of the basin itself. Price (1966) contends that the two perpendicular orientations of most regional fracture sets are rotated to basin shape. As most basins are elliptical to some degree he rightly pointed out that one orientation of the orthogonal pattern parallels the long axis of the basin and the other parallel the short axes of the sedimentary basin.

Regional fracture systems produce hydrocarbons in numerous fields including Big Sandy and Altamont-Blue Bell. Regional fracture systems are second in importance only to tectonic fractures in hydrocarbon production. Excellent fractured reservoirs occur when later tectonic fracture systems are superimposed over a strong regional system. This relative importance of regional fractures will probably increase as large stratigraphic traps (off structure) become more prevalent.



3.5.3 Contractional fractures

This class is a collection of tension or extension fractures associated with a general bulk volume reduction throughout the rock. These fractures are the result of:

- Desiccation
- Syneresis
- Thermal gradients
- Mineral phase changes

The importance of these volume reduction-related features to hydrocarbon production has long been overlooked. Because these fractures are initiated by internal forces to the body (body forces) rather than external forces (surface forces), their distribution is not necessarily restricted to local geologic structures as in tectonic. Herein lies their great value to production. Under the right depositional and diagenetic circumstances, contractional fractures can occur throughout the reservoir independently of the trapping mechanism.

3.5.3.1 Desiccation Fractures (*mud cracks*)

In the contractional class, mud cracks are the most familiar to geologists, but they may also have the least economic significance. This fracture system is known to be due to shrinkage upon loss of water in sub-aerial drying. These tensile fractures are generally steeply dipping (with respect to bedding), wedge-shaped fractures often filled with later deposited material. The fracture system forms cusped-shaped polygons of several nested sizes. Desiccation fractures are generally developed in clay-rich sediments. These fractures are important in reconstructing depositional environments because they indicate sub-aerial drying. However, because they are restricted to thin topographic exposure surfaces or unconformity surfaces, they are probably of minimal importance to direct hydrocarbon production.

3.5.3.2 Syneresis Fractures

Syneresis is a chemical process that brings about bulk volume reduction within sediments by subaqueous or subsurface dewatering. This can involve dewatering and volume reduction of clay, or of a gel or colloidal suspension. Either or both of these processes can occur in sediments of varying grain size and sorting. Syneresis, unlike desiccation, can generate either tension or extension fractures. Syneresis fractures are referred to in this report as “chicken-wire fractures” because of the three-dimensional

polygonal network of fractures developed within the sediment (Figure 7). Because Syneresis fractures are initiated by internal body forces, they tend to be closely and regularly spaced, and are often isotropically distributed in three dimensions (equal spacing in all directions). Associated fracture permeability also tends, therefore, to be isotropically distributed. While desiccation fractures are restricted primarily to shaly or clay-rich sediments, syneresis fractures have been observed in shales, siltstones, limestones, dolomites, and fine- to coarse-grained sandstones. Desiccation and syneresis have been separated as distinct processes in this discussion. But in reality, a gradation between the two probably exists. What is important is that these two end-member processes produce fracture systems of distinctly different properties (Figure 3.8). Of these two, syneresis is far more important to hydrocarbon production because it occurs in greater volumes and types of rocks, and because the fracture system interconnects in three dimensions.



Figure 3.7: Contractional (chicken-wire) fractures in core sample

PROCESS	DESICCATION ←————→ SYNAERESIS	
	MECHANICAL	CHEMICAL
ENVIRONMENT	SUBAERIAL	SUBAERIAL, SUB-AQUEOUS OR SUBSURFACE
FRACTURE PATTERN	2-D POLYGONAL	3-D POLYGONAL
MATERIAL	CLAY-RICH SEDIMENTS	CLAY-RICH SEDIMENTS OR COLLOIDS (SILICA)

Figure 3.8: Contrasting characteristics of desiccation and syneresis.

3.5.3.3 Thermal contractional fractures

For the purposes of this project, macroscopic thermally induced fractures are those caused by contraction of hot rock as it cools. Depending on the depth of burial, these can be either extension or tension fractures and their generation is usually dependent on the existence of a thermal gradient across the material. In the subsurface, both overburden-derived and thermally-derived stresses are superimposed. In this way, tensile stresses derived from heating are often cancelled out by larger compressive stresses derived from overburden pressure. As such, true thermal fracturing at depth in the subsurface is probably rare relative to fracture patterns of other origin. In most cases, the effects of temperature are evidenced by an alteration of the mechanical properties and rheological behaviour of rocks rather than by true thermally induced fracturing. True thermal fracturing may be of use in hard-rock mining and wellbore fracturing, but is considered of minimal importance in petroleum production in all but igneous rocks, such as oil production from the tertiary basalt flows at West Rozel Field, Salt Lake, Utah. In this field, sustained flow of oil and water of up to 1,000 barrels per day (bbl/day) was achieved from this form of contractional fractures.

3.5.3.4 Mineral Phase Change Fractures

This fracture system is composed of extension or tension fractures of often-irregular geometry related to volume reduction due to mineral phase change in the carbonate and



clay constituents of sedimentary rocks. The chemical change from calcite to dolomite, for example, involves a change in molar volume of about 13 percent. Phase change from montmorillonite to illite involves a similar type of volumetric change. Under proper conditions, such phase change shrinkage could cause chicken-wire fracturing, especially if superimposed over other contractional processes. A possible fracture pattern of this type has been reported in a porous dolomitized reef.

3.5.4 Surface related Fractures

This diverse class includes fractures developed during unloading, release of stored stress and strain, creation of free surfaces or unsupported boundaries, and weathering in general. Surface-related fractures are often developed due to the application of body forces. They have not proven to be important in hydrocarbon production to date in other than weathering surfaces (Karst), but it is important to know their origin with respect to other fracture types present in core or outcrop. Unloading fractures are often found in quarrying operations. As rock material is removed from the quarry, rock bursts are common. This is due to the release of load or constraint in one direction. The rock relaxes and spalls, or fractures, on a plane parallel to the newly developed free surface. These fractures are often irregular in shape and follow topography in many eroded areas. Such fractures are often called sheeting in erosional terrains.

Another type of fracture in this group is derived from the creation of a free or unsupported surface. These fractures can be either extension or tension and are often observed paralleling high canyon walls. A planar loss of support and gravitational forces acting on the unsupported material cause failure or spalling parallel to the strike of the free surface. Such fractures are similar in morphology and orientation to unloading fractures, but are primarily generated by gravitational forces, and are often associated with and initiate large-scale slumping. The term "weathering fracture" describes fractures that *relate to the diverse processes* of mechanical and chemical weathering (e.g., freezethaw cycles, small-scale collapse and subsidence, mineral alteration, and diagenesis) and mass-wasting. A weathering fracture should not be confused with the control of weathering or erosion by pre-existing fractures and residual stresses in outcrop. In these cases, fractures preferentially erode, causing the parallelism between free surfaces and fracture planes. Weathering fractures are probably of minimal importance to direct hydrocarbon production except possibly for such production as from the Precambrian granite wash in Kansas and the buried granite hills in China, and various solution enlarged weathering fractures associated with karsting in carbonates. Such solution-related fracture porosity may be quite important in unconformity related carbonate reservoirs.



3.6 Fracture Properties affecting Reservoir Performance

Once the origin of a fracture system has been determined in a reservoir, the petrophysical properties of the rock-fracture system must be addressed next. This involves characterization of the fracture system in terms of physical morphology, distribution, and estimation of the reservoir properties (porosity, permeability, etc.) resulting from the fracture system characteristics. Fractures are present in all rock formations; subsurface or outcrop. The physical character of these fractures is dictated by their mode of origin, the mechanical properties of the host rock, and subsurface diagenesis. These factors combine to develop a feature that can either increase or decrease reservoir porosity and permeability. While always present in some large scale, it is only when fractures occur in sufficient spacing or length that their effect on fluid flow becomes important. To accurately assess this effect, either positive or negative, it is important to know the fluid flow properties of individual representative fractures and how many of these fractures of a given orientation exist in a given reservoir volume. Therefore, in addition to the normal petrophysical determinations made on the rock matrix (rock in which the fracture resides), it is also necessary to determine the reservoir properties of the fracture network (either advantageous or detrimental to fluid flow) and how it changes with depth and reservoir depletion, which tends to mechanically close the fractures. The four petrophysical determinations most useful in evaluation are, in order of increasing difficulty of calculation:

- Fracture permeability
- Fracture porosity
- Fluid saturations within the fractures
- The recovery factor expected from the fracture system

The data most useful in these determinations are derived either from analysis of whole-core samples or from single or multiple well testing. Data derived from various well logs are also often used but are not very accurate. Whole core samples are useful in fracture evaluation for two reasons:

- They sample a relatively large volume of rock and thus potentially sample more regularly-spaced reservoir fractures than plug analysis
- Standard permeability analyses can be performed in three dimensions on these samples (vertical, maximum horizontal and horizontal 90 degrees to maximum horizontal permeability).



Such permeability analyses not only allow for calculation of the absolute permeability of a fracture or fractures at surface conditions, but also adequately depict the permeability anisotropy developed due to the presence of the fractures. In addition, correlative fractured and unfractured plugs taken from the whole-core samples can be subjected to tests that measure the variation in fracture and matrix properties under simulated burial conditions. This is done in confining pressure tests or under a variety of mixed loading conditions to simulate subsurface conditions. Determinations of fracture permeability under confining pressure are very important because open fractures are generally higher in absolute permeability than the matrix, but the fractures are much more compressible and, therefore, reduce in permeability and porosity much more rapidly than the matrix with the application of force. Whole-core samples can also be used as material for selected mercury injection and fluid saturation or relative permeability tests, which sample both fractured and unfractured material. The difference between the two companion (fractured and unfractured) samples can be considered a crude measure of fracture width distribution in the mercury injection tests (fracture width analogous to pore throat size) and variations in fluid saturation and relative permeability between the matrix and fractures in the fluid saturation tests.

Core analysis is used to determine reservoir quality and performance by summing together the individual small-scale elements of the reservoir. Well testing, on the other hand, is used to determine the bulk response of a relatively large volume of the reservoir and is a summary of the relative contribution of all its individual parts. A complete, accurate evaluation includes both small-scale and large-scale determinations of porosity, 3-D permeability, etc. However, early in exploration, sophisticated well-test data, especially multiple well interference test data, may be unavailable and more emphasis must be placed on smaller-scale whole-core analyses. The useful well tests are pressure transient analysis, pressure pulse testing, and interference testing.

Log analysis has been used successfully to delineate fracture occurrence and distribution in the wellbore. The quantification of the subsurface reservoir properties such as porosity and permeability of fracture systems by well logs is, however, much more difficult. Quantitative measurement of subsurface fracture porosity and fracture permeability by well logs gives highly variable and inaccurate results, especially when not tied closely to core from the specific fractured zones of interest.

3.6.1 Fracture morphology

An important factor that dictates fracture porosity and permeability is the morphology of the fracture planes. This morphology can be observed in core and outcrop and inferred from some well logs. There are four basic types of natural fracture plane morphology:

- Open fractures
- Deformed fractures (a). Gouge-filled fractures (b). Slickensided fractures
- Mineral-filled fractures
- Vuggy fractures

3.6.1.1 Open fractures

Open fractures, as the name implies, possess no deformational or diagenetic material filling the width between the walls of the fracture. Such fractures are potentially open conduits to fluid flow. The permeability of open fractures is a function of the initial fracture width, the *in situ* effective stress component normal to the fracture plane, and the roughness and contact area of the fracture walls. Initial fracture width, roughness, and contact area are functions of the grain size distribution of the host material because the number and height of asperities along the surface dictating these parameters must be made up of multiples of the smallest basic rock units—grains. In general, open fractures greatly increase reservoir permeability parallel to the fracture plane. Because the fracture is only the width of one pore, it will have little or no effect on fluid flow perpendicular to the fracture plane (Figure 3.9).

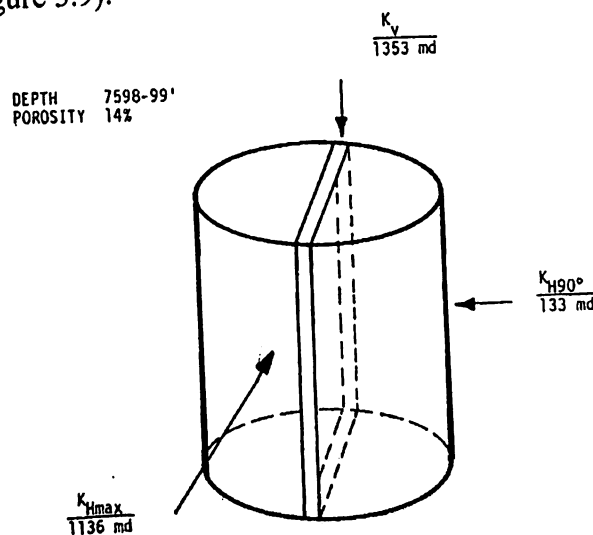


Figure 3.9: Example of 3-D whole-core permeability associated with an open fracture.

Fractures open to fluid flow are often evidenced in outcrop by an oxidation staining or liesegang banding parallel to the fractures. These features indicate groundwater motion along the fracture planes. Open fractures show little associated deformation in thin section and scanning electron microscope (SEM) photographs.



3.6.1.2 Deformed Fractures

Deformed fractures are ones that either formed as a relative ductile shear zone or were initially open and subsequently physically altered by later tectonic shear motions. This morphology creates strong anisotropy within the reservoir that is considered two end-member fracture morphologies within the deformed fracture category: gouge-filled (deformation bands) and slickensided. Intermediate mixtures of the two are possible and do occur in the subsurface.

Gouge Filled Fractures (Deformation Bands) - Gouge is defined as the finely abraded material occurring between the walls of a fracture as a result of grinding or frictional sliding motion. Displacement of rock masses along the fracture plane causes cataclasis or granulation of the grains in contact across the fracture. This granulation or cataclastic zone can be several grain diameters wide, and it reduces the porosity, grain size, sorting, and therefore, the permeability of the fracture zone. In some instances, secondary mineralization on the freshly broken mineral surfaces further reduces the porosity and intrinsic permeability. In addition, the fine-grained deformed material possesses high-water saturation that can drastically reduce the relative permeability to hydrocarbons. In controlled laboratory experiments, it appears that the width of the gouge zone within a rock increases with the amount of shear displacement. Because the fracture is long and narrow, reduction in permeability occurs primarily perpendicular to the fracture or gouge zone (Figure 3.10). Rock ductility and sliding friction developed across the fracture are of prime importance in the formation of gouge and, as will be discussed later, slickensides. The two vary with composition and texture of the rock. In general, sliding friction (not to be confused with *internal* friction) along a fracture plane is relatively low if we consider brittle rock in contact with brittle rock across the fracture plane and relatively high if we consider two ductile rocks in contact across the fracture plane. The lowest relative sliding friction is developed with unlike rocks in contact across the sliding surface. Gouge-filled fractures are often the easiest of the fracture morphologies to observe in core or outcrop, because gouge material is usually more resistant to weathering and abrasion than the unfractured rock. It usually shows up as light colored, raised linear features in sandstone.

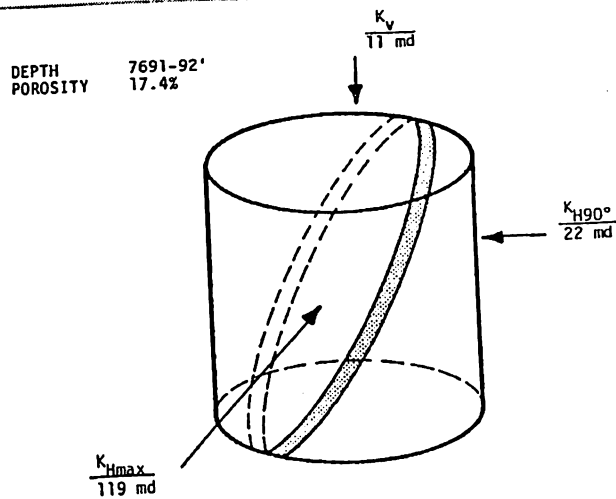


Figure 3.10: Example of 3-D whole-core permeability associated with a gouge-filled fracture.

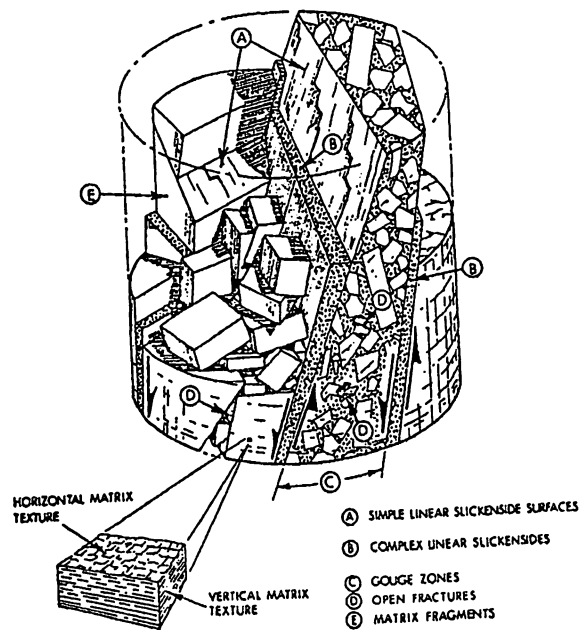


Figure 3.11: Gouge texture in shales and carbonates

Slickensided fractures-

A slickenside is a polished or striated surface that results from frictional sliding along a fracture or fault plane. Slickenside development involves either pulverization followed by cataclasis of the host rock, or the creation of glass by grain melting. The result of this deformation is a reduction in permeability, at least in the direction perpendicular to the slip surface. However, some permeability increase may occur parallel to the slip surface due to mismatch of the smooth fracture walls. In contrast to gouge, the deformation zone

in slickenside development is generally only one or two grain diameters away from the fracture plane (Figure 3.12).

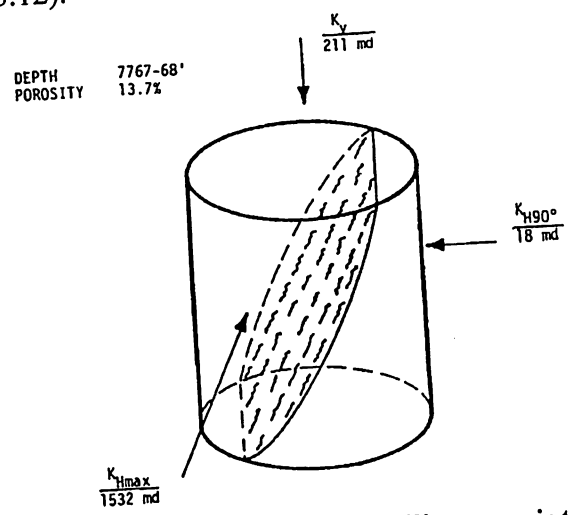


Figure 3.12: Example of 3-D whole-core permeability associated with a slickensided fracture.

In the literature, these fractures are most often described in sandstones and especially in limestones, but they have also been found with increasing regularity in shales as shales are being examined more often for reservoir and source potential. Slickensides are prominent in relatively low-porosity sandstones and carbonates of various properties. These rocks are usually somewhat stronger or more brittle than analogous rocks that develop gouge, environmental conditions being equal. Also, rocks that contain significant amounts of material not subject to granulation or cataclasis, such as clay, gypsum and calcite fill, will tend to form slickensides in preference to gouge even though they are not strong, brittle materials. Occasional glass development can be seen in thin sections along the sliding surface. This glass is the result of quartz grain melting during frictional sliding along the fracture surface. Laboratory experiments indicate at least 1200°C can be developed along sliding surfaces in sandstone. Such pools of glass are impervious to fluid flow. If sufficient glass is created by continued displacement, permeability perpendicular to the fracture plane will be drastically reduced. The slickenside morphology can either form as a primary feature of the fracture surface or as an effect of rejuvenation of slip at a later event.

3.6.1.3 Mineral filled Fractures

As the name implies, these fractures are those that have been filled or 'choked-off' by secondary or diagenetic mineralization. Quite often this secondary cementing material is quartz, carbonate, or both. Mineral filling may or may not be complete, of course. Its effect on permeability depends on the completeness of filling and diagenetic history of the



material. Usually, filled fractures are permeability barriers, but incomplete filling of a fracture in the form of either vug development or intergranular porosity can give some measurable increase in permeability to the reservoir (Figure 3.13). Mineral-filled fractures are extremely common. Mineral filling is the nemesis of flow prediction and quantification in fractured reservoirs. While the presence, width, and intensity of natural fracture systems can be predicted to some degree, mineral filling and the completeness of filling cannot. The presence of complete mineral filling can kill an otherwise scientifically sound exploration play. Fortunately, mineral filling is often incomplete or has undergone some degree of dissolution, making reservoir permeability acceptable for production. Mineralized fractures occur frequently in sandstone, shale, and limestone.

Completely filled fractures: Complete mineral filling in a fracture system imparts no positive reservoir attributes to the rock in which it resides. There are, however, some analyses that can be performed on these fractures that are relevant to an in-depth reservoir study. First, if the fractures are filled with a mineral phase significantly different in acoustic properties from the matrix, recognition on the acoustic televiewer may be easier and facilitate fracture recognition and orientation. This allows for better determination of and intensity of the fracture system. This may in turn allow for the prediction of a fractured reservoir nearby where the fractures are not completely filled. Other uses of completely filled fractures lie in documenting diagenesis. The fracture-fill often records deformation and cementation events that occurred after the fracture was formed. Evidence for these events can be found in the form of twinning and translation of the filling crystals, multiple cementation sequences, and fluid inclusions. These occurrences can be quite useful in unravelling the depth, alteration, and fluid migration history of the rock after fracturing took place.

Incompletely filled fractures: In incompletely filled fractures, some measurable pore space exists within the filling material. This pore space may be primary to the fracture or secondary in nature. Frequently, secondary porosity development in fracture fill is the result of calcite dissolution. Incomplete mineral fill in fractures can be very important and in some cases actually creates the *total* reservoir quality. The Tuscarora Sandstone is an example of such a reservoir. In this rock the matrix porosity is about 0.5 percent. The dissolution/fracture porosity is about 1 percent. This dissolution/fracture porosity is the result of a complex diagenetic history of the fracture fill. After fracturing, four periods of mineralization took place in fractures of one tectonic fracture set. The sequence was:

- Early chlorite coating the fracture walls
- Euhedral quartz mineralization
- Calcite mineralization
- Sulphide mineralization (mostly pyrite, chalcopyrite, and galena)

Subsequent to this, a period of calcite dissolution took place forming the present day secondary porosity along the fracture fill that represents the essential porosity and permeability within the reservoir. Initial flow rates from this discovery well were estimated at 48 million cubic feet per day (MMcfd).

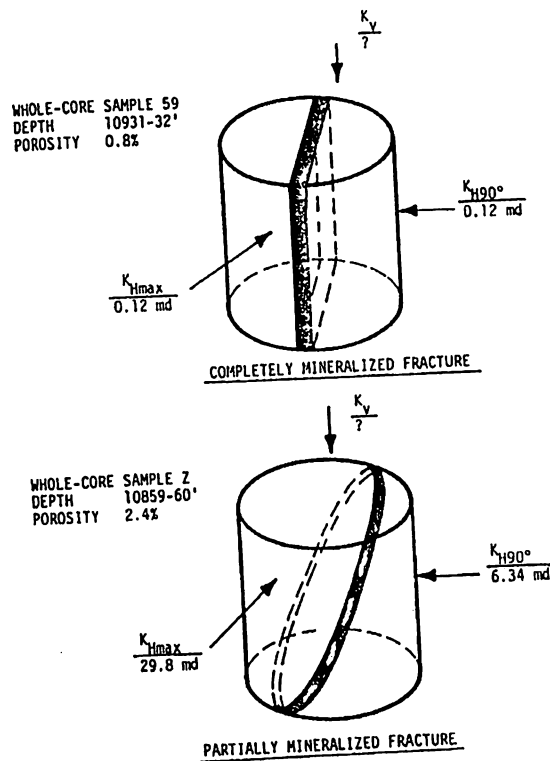


Figure 3.13: Example of 3-D whole-core permeability associated with mineralized fractures.

3.6.1.4 Vuggy Fractures

Vuggy fractures are not so much a true fracture morphology as they are a matrix alteration surrounding the fracture. Vuggy fractures form when fluids enter a low-permeability rock along fracture planes. If the fluid is in disequilibrium with the rock matrix, dissolution may occur. Vugs develop along and adjacent to the fractures and are more or less restricted to a narrow zone surrounding the fracture "channel." This produces vuggy porosity intimately associated with fractures. Such vuggy fractures are often associated with unconformities in carbonates and the development of karst. Similar morphologies have also been observed in fine-grained cherts, like the Caballos Novaculite and in the hydrothermally altered granites at Bach Ho Field in offshore Vietnam. Vuggy fractures are very important in many of the largest carbonate reservoirs in the world, such as the Middle Eastern Asmari fields. Secondary porosity associated with these fractures can be quite large compared to more normal fracture porosity values



(Weber and Bakker, 1981). In addition, due to the spherical to oblate shape of the vugs, this fracture-associated porosity will be relatively incompressible during reservoir drawdown.

3.6.1.5 Morphology/ Permeability summary

It can be seen from the preceding sections that the morphology of a fracture can influence the directional permeability of the rock mass around it. In general, an open fracture will dramatically increase reservoir permeability parallel to the fracture plane. However, because the fracture may be only one matrix pore or so wide, reservoir permeability across the open fracture will be identical to normal matrix permeability in that direction. A gouge filled fracture will drastically reduce reservoir permeability across the fracture. Due to the relatively small cross-sectional area of the fill, however, permeability will be close to (or slightly less than) normal matrix permeability parallel to the fracture fill. A slickensided fracture creates perhaps the largest permeability anisotropy of all the fracture morphologies because it increases permeability parallel to the fracture and decreases it across the fracture. The deformation along the walls of the fracture decreases reservoir permeability, as in gouge, across the fracture. However, due to the mismatch of smooth sliding surfaces, continuous interconnected pore space occurs along the fracture, which increases reservoir permeability parallel to the fracture. Vuggy fractures without diagenetic alteration of the vug walls should, as in open fractures, increase reservoir permeability parallel to the fracture and have little permeability effect across the fracture. Mixtures of the various morphologies can give unusual directional permeability effects and must be treated individually, often with 3-D whole-core data.

3.6.2 Fracture Width and Permeability

This section addresses the problem of quantifying the effect of natural fracture systems on reservoir quality and productivity. While exact quantification of a reservoir during exploration is very difficult, this section will discuss the determination of subsurface fracture width and permeability and the geologic parameters necessary for an early understanding of how fractures can affect reservoir performance.

3.6.2.1 Equations for Fluid Flow

The first quantitative description of fluid flow through porous media was by Darcy (1856). In his general equation, derived for laminar, incompressible, single-phase, Newtonian flow in a continuous, homogeneous, porous material, Q , the flow rate is:



$$Q = KA \frac{dh}{dl}$$

where K = hydraulic conductivity
 A = cross-sectional area
 dh/dl = head gradient

Hubbert (1940) showed that:

$$K = k(\rho g / \mu)$$

and

$$k = Nd^2$$

where k = intrinsic permeability
 ρ = fluid density
 g = acceleration of gravity
 μ = fluid viscosity
 N = a dimensionless coefficient characteristic of the medium
 d = average constitutive grain diameter of the rock.

The resultant dimensions of k are (length)². It was later realized that Nd^2 could not be defined for flow along a fracture. Therefore, in an attempt to model fractures, the parallel-plate theory of flow was developed. Flow in this theory is assumed to occur between two smooth parallel plates separated by a distance, e . The basic equation as used by Huitt (1955), Lamb (1957), Snow (1965, 1968a, 1968b), and Sharp and others (1972) is:

$$\frac{Q}{A} = \frac{e^3}{12D} \frac{dh}{dl} \cdot \frac{\rho g}{\mu}$$

Where D = fracture spacing, the average distance between parallel regularly spaced fractures

This equation is valid for single-phase, Newtonian, laminar flow in planar fractures with small overall changes in width e . Each of these two quantitative relations describes only a portion of the total flow through a fractured, porous rock; Darcy's equation for the intact-rock portion of the system, and the parallel plate theory for the fractures. The next logical approach to determine the total flow was to combine these equations (Parsons, 1966):



$$k_{fr} = k_r + \frac{e^3 \cos^2 \alpha}{12D}$$

and

$$k_f = \frac{e^2}{12} \cdot \frac{\rho g}{\mu}$$

where k_{fr} = permeability of the fracture plus intact-rock system
 k_f = permeability of a fracture
 k_r = permeability of the intact-rock

α is the angle between the axis of the pressure gradient and the fracture planes.

This equation assumes that flow is laminar between smooth, non moving, parallel plates, that fluid flow across any fracture/matrix surface does not alter the flow of either system, and that the fractures are homogeneous with respect to orientation, width, and spacing. The assumption of laminar flow in a subsurface reservoir is valid for low fluid-flow rates and low surface roughness relative to e . Increased subsurface flow velocities due to production may, however, cause turbulence. If so, much more complicated equations than those of Parsons (1966) are necessary to accurately calculate permeability. Such approaches, however, involved parameters often outside the realm of available geologic data. Parsons' relationship is simple but appears applicable for oil and gas movement in fractured rock.

A fractured reservoir is equivalent to a homogeneous porous medium if the dimensions of the matrix blocks are small (less than 1 m) and the matrix permeabilities are significant (greater than 0.01 milli-darcies [md]).

The concept of an equivalent porous media is an important one in modelling fractured reservoirs and deserves more discussion. As shown by the previous flow equations, fractured rock can be treated by various levels of complexity. In the simplest approach, the reservoir can be treated as a single porosity system with anisotropic Darcy flow (parallel plate flow if only fractures are present). More complex forms of modeling treat the fractured rock mass as a dual-porosity system, using Darcy flow for the porous matrix system and parallel plate flow for the porous fracture system. In both approaches, the continuity of the fracture system becomes important. If at a given scale the fracture system is continuous and interconnected, it can be treated as an equivalent porous medium using either a single- or dual-porosity model. However, if the fracture system is distinctly discontinuous and non-interconnected at a given scale, it cannot be treated as an



equivalent porous medium. If this is the case, the simplifying assumptions of the equivalent porous media approach, such as symmetry of the permeability tensor, do not hold and the reservoir cannot be treated using statistical abstractions for the fracture system. The reservoir must then be modelled using discrete fractures mimicking the real size, orientation and position of the fractures present, a different task. The question of continuous versus discrete modeling has been addressed by Long (Long and others, 1982; Long, 1983). This is an important distinction because in exploring for and engineering in subsurface fractured hydrocarbon reservoirs, we will never have sufficient fracture data to adequately apply discrete or discontinuous fracture modeling. At best, in subsurface reservoirs we can abstract the real or predicted properties of the natural fracture system for use in a continuous, dual-porosity approach. If this equivalent porous media approach is invalid for theoretical reasons, our best-case modeling will be in error. This is why there is substantial debate in the literature about the applicability of equivalent porous media concepts to fractured reservoir modeling.

For natural subsurface reservoirs prior to production, Parsons Equation presents a reasonable approximation of total reservoir flow. As has been stated previously, this equation assumes that flow across the fracture/ matrix surface does not alter the flow of either system. This is true for rocks of either high or near nonexistent matrix permeability. Stated another way, high matrix permeability would allow the matrix to respond individually to the overall pressure gradient rather than to the relative pressure sink of the fracture. If, on the other hand, the matrix permeability is so low as to become nonexistent, cross-flow once again becomes unimportant. In a rock of relatively low or intermediate matrix permeability, cross-flow becomes more important and Parson's Equation becomes a poorer approximation of the total flow. If a more accurate approximation is needed in a rock, more complex cross-flow equations such as those of Barenblatt and others (1960), Duguid (1973), Duguid and Lee (1977) and Evans (1982) should be used. Such equations are extremely complicated and difficult to work with. Most petroleum exploration geologists would either lack the expertise or the interest to pursue them. This, coupled with the fact that Jones (1975) has had good success with Parson's (1966) equations in laboratory experiments on low-permeability carbonates, leads to the conclusion that Parson's Equation is an apt semi-quantitative representation of fractured reservoir flow for use in exploration where data are often scarce.



**Fluid Flow In Fractured Porous Rock After
Barnblat, Zheltov, and Kochina (1960)**

$$\frac{K_m}{\mu_w} \nabla^2 P_m = (C_m + \phi_m C_m) \frac{dP_m}{dt} + \frac{\alpha}{\mu_w} (P_m - P_f)$$

$$\frac{K_f}{\mu_w} \nabla^2 P_f = (C_f + \phi_f C_w) \frac{dP_m}{dt} + \frac{-\alpha}{\mu_w} (P_m - P_f)$$

Where: K = Permeability
 P = Pressure
 t = Time
 φ = Porosity
 C = Compressibility
 μ = Viscosity
 α = Cross-Flow Coefficient
 (φ_m to φ_f)

Subscript m is Matrix
 f is Fracture
 w is Water

After Duguld (1973)

Continuity Eq. for Fluid In Pores

$$(1 - \phi_f) \phi_m C_w \frac{dP_m}{dt} + (1 - \phi_f) \phi_f C_w \frac{dP_f}{dt} + \frac{r}{\rho_w} + \nabla \cdot \langle \bar{v}_m \rangle = 0$$

Continuity Eq. For Fluid In Fractures

$$(1 - \phi_m) \phi_m C_w \frac{dP_m}{dt} + (1 - \phi_m) \phi_f C_w \frac{dP_f}{dt} - \frac{r}{\rho_w} + \nabla \cdot \langle v_{fm} \rangle = 0$$

Where:

$$\langle v_{fm} \rangle = \frac{K_f}{\mu_w} \left[\rho_w \frac{d \langle v_{fm} \rangle}{dt} + \nabla P_f \right], \langle \bar{v}_m \rangle = - \frac{K_m}{M_w} \nabla^2 P_m$$

Written in Terms of
 3 Components of
 Fluid Velocity in Fractures
 Pressure in Matrix
 Pressure in Fractures

Dilation of the Medium
 r = Cross-flow Term
 φ_m to φ_f



After Parsons (1966)

$$K_{fm} = K_m + \frac{e_1^3 \cos A_1}{12 D_1} + \dots + \frac{e_n^3 \cos A_n}{12 D_n}$$

$$K_f = \frac{e^2}{12} \cdot \frac{\rho_w g}{\mu_w}$$

For 1 → n
Fracture Sets

Where K = Permeability
e = Fracture Width
D = Fracture Spacing
A = Angle Between Axis of Pressure Gradient and Fracture Planes
ρ = Density
μ = Viscosity
g = Acc. Gravity

Subscripts:

m is Matrix
f is Fracture
fm is Matrix and Fracture Combined
w is Water (Fluid)

Parsons (1966) also showed that his equation could be expanded to incorporate multiple fracture sets:

$$k_{fr} = k_r + a \cos^2 \alpha + b \cos^2 \beta$$

where

$$a = \frac{e_1^3}{12 D_1} \text{ for Fracture Set 1}$$

and

$$b = \frac{e_2^3}{12 D_2} \text{ Fracture Set 2}$$

Each of these additional terms refers to a separate parallel fracture set of constant spacing (D_n) and opening (e_n). As in Parson's equation, $\cos 2\alpha$, $\cos 2\beta$, etc., refers to the angle between each parallel fracture set and the pressure gradient. Modified Parson's equation,



then, can deal with a number of intersecting fracture sets, a geologically prevalent situation. In fact, this ability to deal with multiple fracture sets in a permeable matrix overshadows any imprecision that may result from using such a simple and direct equation.

3.6.2.2 The Direct Effect of Fractures on Fluid Flow

Contrary to popular belief, reservoir fractures are not always high-permeability channels, but often they act to impede or as barriers to fluid flow. The effect of individual fractures on permeability is dependent on the character and morphology of the fracture plane itself. It is often difficult to determine if natural fractures play an important role in fluid production in a given well. There are, however, several clues that can give the geologist or engineer suspicion of fracture control. All include core data. Several indicators are:

- Direct observation of oil-stained or “bleeding” fracture planes in core samples can indicate fracture control. Often, evidence of oil movement along fracture planes is prevalent.
- High flow test permeability from zones of relatively low core-derived plug permeability can indicate flow control by natural fractures. An example of this is found in Amoco Norway 2/8-10 well, Valhall Field, Norwegian North Sea. Here, a flow test permeability of greater than 100 md was recovered from a zone with corresponding atmospheric pressure plug permeability of less than 1 md, indicating fracture control of reservoir flow.
- Fluid flow control can also be revealed by three-directional whole-core permeability analysis (K_{hmax} , K_{h90° , K_v).

In a vertical versus horizontal permeability plot, most well-bedded rocks will plot below the line of equal permeability (isotropy) emphasizing preferential flow parallel to bedding. However, if substantial scatter of points exists both below and above the line of isotropy (Figure 3.13), fracture control within the reservoir should be suspected.

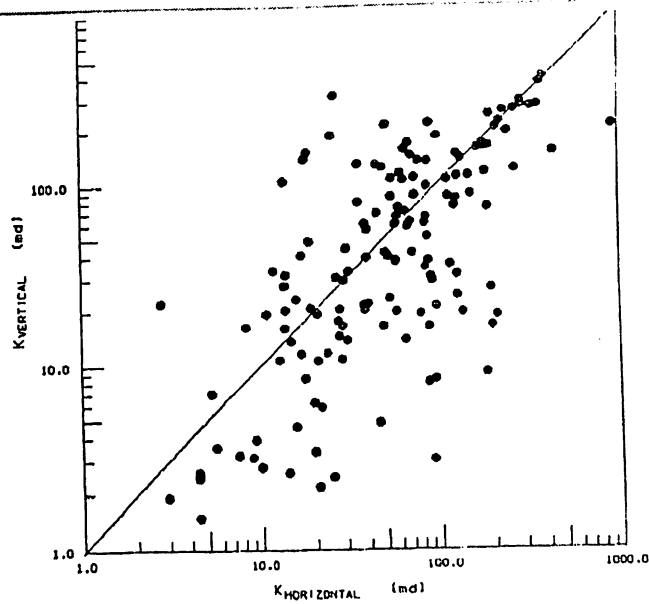


Figure 3.14: vertical vs. horizontal permeability

3.6.2.3 Fracture Permeability versus Confining Pressure

In order for Parson's equation to simulate subsurface reservoir flow, estimation of K_r and K_f or e at depth must be made. These estimations are generally made by subjecting a nonporous, fractured laboratory rock sample to external loads (simulating depth of burial) as permeability is being measured (Summers and others, 1978; and Engelder and Scholz, 1981). For porous rocks, these tests can be run on unfractured rock (k_r) and fractured rock (k_{fr}). Fracture permeability (k_f) can then be calculated using Parson's equations. Once k_f and k_r are known as a function of depth, the total reservoir permeability (k_t) can be calculated for any combination of reservoir fracture systems in that rock. Usually in such tests a hydrostatic confining pressure is applied to the outside of a jacketed sample. This does not, however, simulate natural subsurface conditions where the vertical and horizontal components of burial stress are not equal ($\sigma_v \neq \sigma_h$).

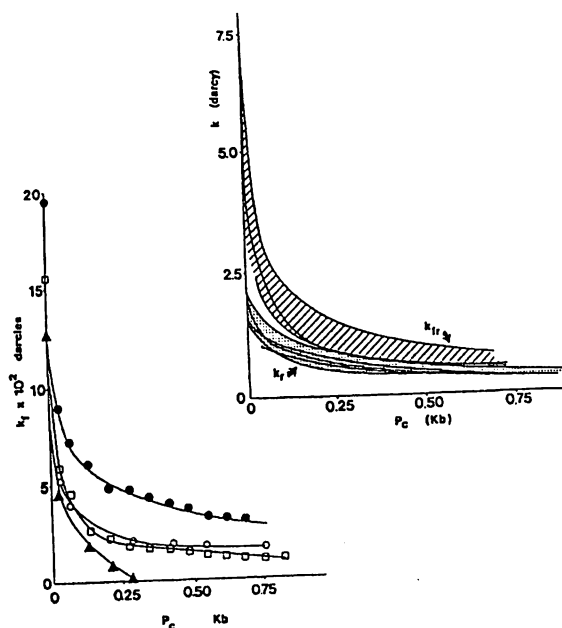


Figure 3.15: Matrix (k_r) and fracture (k_f) and total (k_{fr}) permeability versus hydrostatic confining

3.6.2.4 Fracture Width versus Confining Pressure

Subsurface fracture permeability can be approximated from laboratory data in a manner discussed in the last section or by complex testing of large in situ fractured blocks (Swolfs and others, 1981). Using the data documenting fracture permeability as a function of stress state or simulated depth from laboratory or in situ measurements, we can calculate an average effective fracture width necessary to give each permeability value from Parsons' equation. The appropriate permeability value is input to this equation along with the angle (α) between the real or artificial fracture plane and the pressure gradient, and the value for fracture spacing in the sample (D). If multiple parallel fractures are used, the average distance between fractures is input for D . If one fracture parallel to the cylinder axis is used, the assumption of an image well source from hydrology is applied (Walton, 1970), and one sample diameter is input for D . With these input values and Parson's equation, average effective fracture width or hydraulic aperture (e) can be approximated (Figure 3.16). The hydraulic aperture is somewhat different from the mechanical width, which is highly variable along the fractures. This distribution of mechanical width is difficult to measure on natural fractures and has been investigated as a function of stress by Sharp and others (1972). Other investigations have looked at changes in total area of contact along the fracture as a function of stress (Gale, 1982). The number derived from the fracture permeability measurement mentioned above does not directly address the mechanical width distribution or contact area, but better represents

the overall hydraulic effect of its distribution in fluid flow. In this manner, one can derive a suite of hydraulic fracture width versus stress curves representative of various lithologies or grain sizes and from them simplify prediction of fracture permeability and fracture porosity in the subsurface.

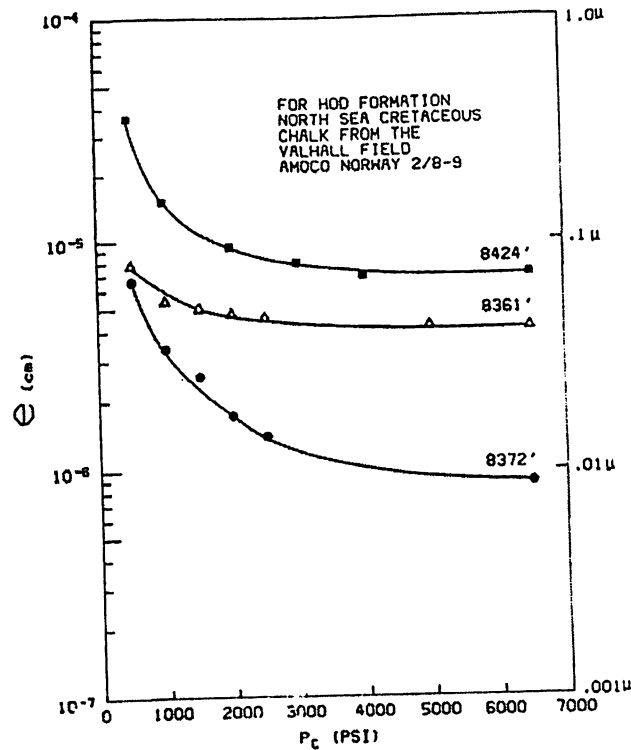


Figure 3.16: Calculated fracture width (e) versus hydrostatic confining pressure (P_c) plot for several North Sea chalk samples.

3.6.2.5 Fracture Spacing

Along with fracture width, fracture spacing is the other important quantitative fracture system parameter necessary to predict fracture porosity and permeability in a reservoir. Unlike subsurface fracture width, which is difficult to observe directly, fracture spacing can be directly quantified and also does not change when the reservoir is perturbed. However, while fracture spacing can be directly observed in outcrop and mines, difficulties in quantification often arise due to the small size of our subsurface sampling methods (core and wellbore observations) with respect to the fracture spacing or matrix block size. In addition, natural fracture systems are often of such a complicated cross-cutting fabric as to make determination of an average spacing difficult if not ill-defined. Many parameters have been used in the literature in an attempt to quantify the abundance of fractures in a reservoir. Terms such as fracture intensity, fracture density, fracture index, fracture surface area, fracture intersection density, and fracture spacing have all been used with the exact definitions of each varying from author to author. Several

usages involve volumetric terms while most are in actuality vector terms. In this text, fracture spacing is defined as the average distance between regularly spaced fractures measured perpendicular to a parallel set of fractures of a given orientation (Parsons, 1966). The terms can be applied to numerous parallel fracture sets of various orientations within the reservoir. Each spacing term will therefore, be a vector (direction and magnitude) representing an average distance along the direction normal to the fracture planes. This definition of fracture spacing is used here primarily because it is the format most frequently used in theoretical fracture permeability equations (e.g., Lamb, 1957).

Effect of variation in fracture spacing: Variation in fracture spacing can have a dramatic effect on both fracture porosity and permeability (Figures 3.17 and 3.18). A good qualitative feeling for the effect of outcrop or core observations of fracture spacing at an assumed fracture width, or vice versa, can be derived from these diagrams.

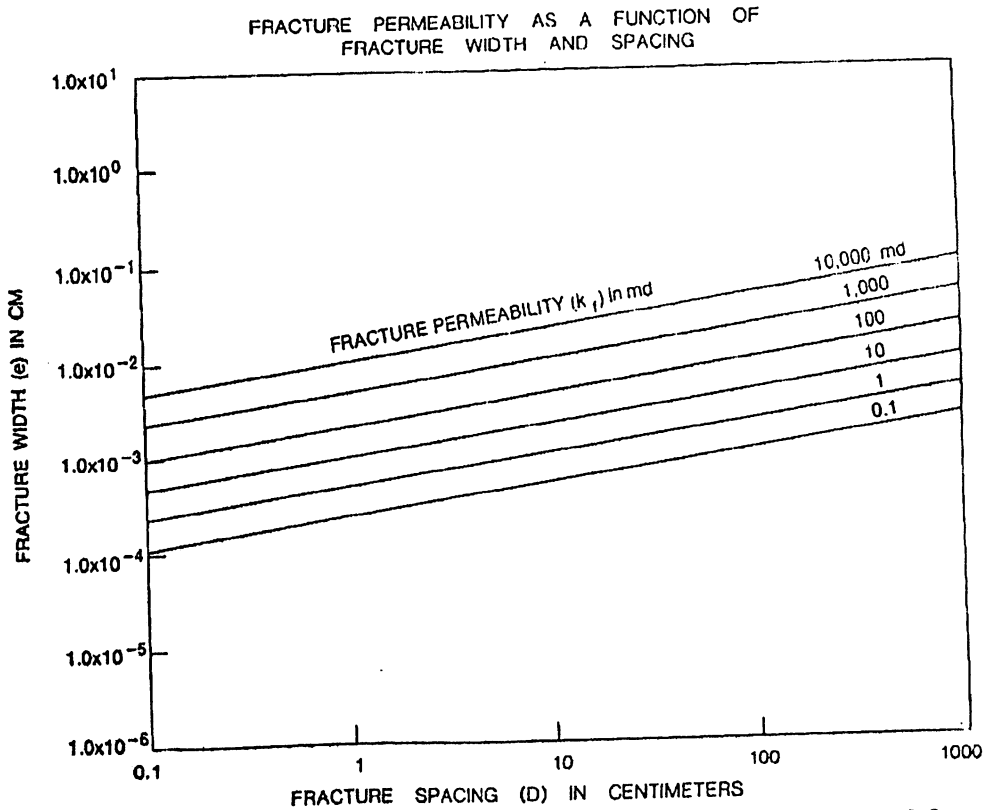


Figure 3.17: Fracture permeability as a function of fracture width and fracture spacing

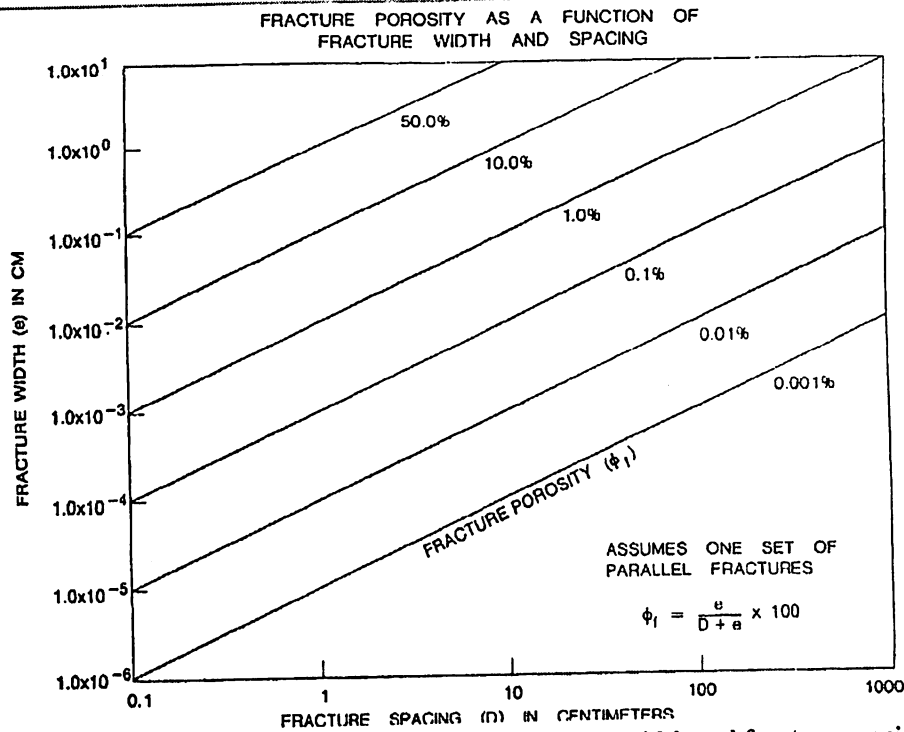


Figure 3.18: Fracture porosity as a function of fracture width and fracture spacing.

3.6.3 Fracture and Matrix Porosity Communication

Once fracture origin and the reservoir properties of the fracture and matrix systems have been determined, fracture and matrix porosity interaction should be addressed. Any reservoir in which fractures play a significant role in production and storage of reserves must be treated as a two-porosity system—one system in the matrix and one in the fractures. Reservoir interpretation that does not recognize the potential for reduced recovery because of an adverse interaction between the two porosity systems will lead to an incorrect estimation of reserves and recovery factors. These complexities in fractured reservoirs make reliable early estimations of reserves or recovery factors more complex than in conventional reservoirs. Early warning of fracture/matrix interaction problems can be gained by thin-section observation of fracture planes and by analysis of whole-core directional permeabilities selected to illustrate in a relative sense the interaction and flow rates between matrix and fractures. In many cases, flow communication or interaction between these two systems may be good. However, in other reservoirs such communication may be inhibited by mineralization within or deformation along the fracture plane surfaces. For example, in a fractured reservoir where: (1) deformation is accomplished primarily by extension fracturing and (2) diagenetic mineralization is minimal; fracture/matrix interaction or cross-flow is probably good. In such a system, both porosity systems can respond to the overall fluid pressure gradient as well as directly to each other. Poor fracture/matrix porosity interaction may occur either because of

deformation along, or mineralization within, the fracture. Such lack of communication may or may not be a problem in production, depending on the petrophysical properties of the two systems. For instance, poor communication between a moderately porous, permeable fracture system and a low-porosity, high-water saturation matrix would not be a problem. Such a prospect would be judged on the reservoir properties of the fracture system alone. On the other hand, poor communication between a highly permeable fracture system and a matrix system with a large volume of potentially flowable hydrocarbons presents a significant production and evaluation problem. If the presence of an impervious lining to the fractures is not recognized, it will result in an erroneous estimate of the matrix contribution into the fracture system and then to the wellbore. The properties of a two porosity system and some misconceptions and non-parallelisms are discussed next.

3.6.3.1 Basics

Fracture porosity, like matrix porosity, is the percentage of a particular void volume in a rock mass compared to its total volume. It accounts for only those voids occurring between the walls of fractures. Matrix porosity, on the other hand, accounts for all voids within a rock other than those within fractures. Thus, matrix porosity includes voids of various origin— vuggy porosity, intergranular porosity, dissolution porosity, etc. The two basic relationships used to calculate fracture porosity and matrix porosity are presented as following:

$$\varphi = \left(\frac{V_p}{V_b} \right) \times 100$$

$$\varphi_f = \left(\frac{e}{D+e} \right) \times 100$$

where φ_r = matrix porosity
 φ_f = fracture porosity
 V_p = volume of pores (other than fractures)
 V_b = bulk volume
 D = average spacing between parallel fractures
 e = average effective width of fractures

In the calculation of Φ_f , by having a spacing term built into its calculation, it is scale-dependent and as such presents a more severe sampling problem in its calculation than does matrix porosity. In fracture porosity calculations, we must use a large enough sampling element to encounter several regularly spaced fractures to get an accurate

measurement. It appears that we need an area encompassing four to five regularly spaced fractures to accurately assess fracture porosity.

3.6.3.2 Porosity- Permeability Relationships

A second way that fracture porosity and matrix porosity are different is in their effect on permeability. While fracture porosity is usually slight, it is highly interconnected and does, therefore, have a much more dramatic effect on permeability than does matrix porosity. Relatively small increases in fracture porosity cause immense changes in permeability parallel to the fracture (Figure 3.18). Fracture porosity and matrix porosity thus should not be given equal significance in reservoir flow predictions.

3.6.3.3 Compressibility Differences

A third way that Φ_f and Φ_r , differ is in their compressibility. In general, fractures are much lower in porosity and much higher in permeability than the matrix in which they reside. However, as external stress increases (below the yield point) due to either increasing depth of burial or reservoir depletion, fractures compress or reduce in porosity and permeability much more readily than the matrix (Figure 3.19 a and b). This difference in behavior is most dramatic in relatively brittle rocks and less dramatic in rocks with a ductile matrix, where the compressibilities of the two phases are more nearly the same.

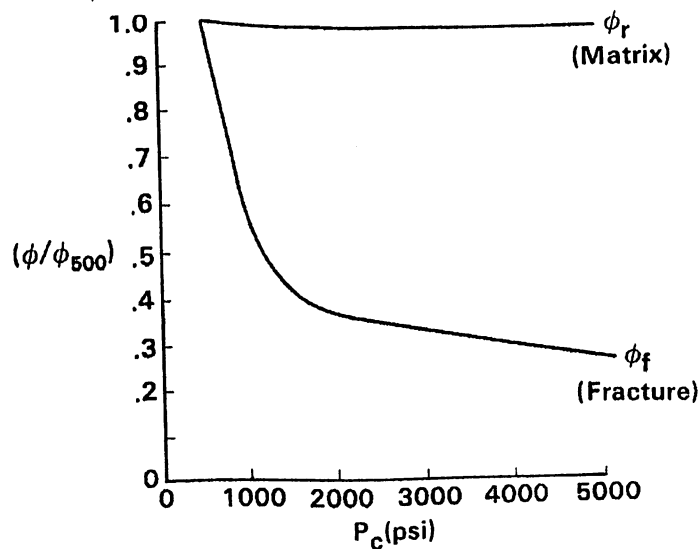


Figure 3.19 a and b (below): Normalized porosity (ϕ/ϕ_{500}) and permeability (k/k_{500}) are shown as a function of P_c

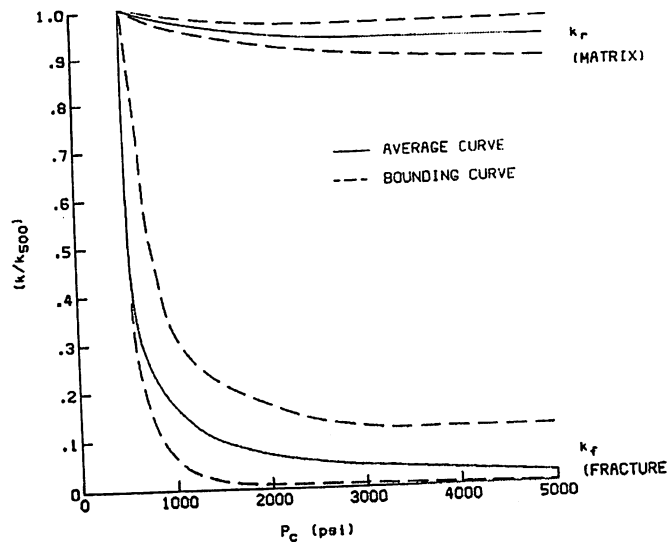


Figure 3.19 b

3.6.3.4 Magnitude Differences

Fracture porosity is generally a small number compared to “normal” matrix porosity. Most good fractured reservoirs possess less than 1 percent fracture porosity. Any large-scale subsurface fracture system of around 2 percent or greater fracture porosity has undergone dissolution along the fracture planes as in many limestones to attain sufficient void space or has unusually close fracture spacing as in some cherts. These numbers do not include grain-scale cracking, which can give larger porosities, but are usually ineffective to large-scale fluid flow. As was pointed out earlier, fracture porosity is a difficult number to calculate. Once it is calculated, however, its significance to production is still not always immediately clear.

Guidelines for Fracture Porosity

Always Less Than	2%
Excluding Small Zones Less Than	1%
General Less Than	0.5%
Vuggy Fractures	0-Large

Fracture porosity is usually low but can be important in specific reservoirs with large vertical and areal extent.

3.6.3.5 Significance of Fracture Porosity



The significance or importance of Φ_f values in reservoir evaluation and potential production problems depends on the type of fractured reservoir encountered. In a fractured reservoir, where the fracture system provides the essential porosity and permeability to the reservoir, an early calculation of Φ_f or fracture volume attainable per well is of paramount importance. We must have an accurate knowledge of this volume as early as possible to evaluate the reservoir properly, and this estimation must be updated continuously through the early production history with as many methods of calculation as the data permit. The significance of a Φ_f calculation in fractured reservoirs, where the fracture system provides only permeability of various amounts to the reservoir and the matrix supplies the porosity or storage volume, is much less if not negligible. In those reservoir types, the Φ_r , which is usually several orders of magnitude greater than Φ_f , so overshadows the volume in the fractures as to make an accurate, early calculation of Φ_f unimportant. What is important is to determine the reservoir type as early as possible.

3.6.3.6 Fracture Porosity Estimations

Fracture porosity is a very difficult number to calculate. Estimates can be made by:

- Core analysis
- k_f/α_f relationship
- Field determinations
- Logs
- Multiple well tests

These methods usually give slightly different values of Φ_f because they are based on slightly different data. It is, therefore, important to use as many different methods to calculate Φ_f as possible with the data available in order to determine the range of possible values in the reservoir.

3.6.3.6.1 Core Analysis

Whole core analysis samples a relatively large rock volume (3- to 5-in. Diameter sample) compared to plug analysis (3/4-in. diameter sample) and, therefore, often depicts a measure of fracture porosity unattainable by standard plug analysis. Using a Tuscarora sandstone example (table given below) the fracture porosity exists as incompletely mineralized, partly dissolved fractures. By subtracting the consistently low matrix porosity (taken from the average of the unfractured samples) from the whole core samples containing fractures, an estimate of fracture porosity is made. This method of



calculating Φ_f is, of course, fraught with scale and sampling problems. The fractures in this core are vertical (parallel to the core axis). The core diameter is 4 in. At any spacing of parallel fractures greater than 4 in., the sampling becomes a “hit-or-miss” problem. If fractures were spaced more than 4 in. apart, hitting one with the 4-in. core would give an anomalously high Φ_f compared to that portion of the reservoir. Conversely, not intersecting fractures with the core would give an anomalously low fracture porosity ($\Phi_f = 0$ percent). Because of these and other sampling problems, core analysis—though the most direct procedure—can often give the most misleading value for fracture porosity. However, this is often the first method available for the analysis of Φ_f and should be performed as soon in evaluation as possible.

Average Porosity from Whole-Core Analysis (Arithmetic Average)

Tuscarora-Amoco #1 Texas-Gulf

Assumes < 0.5% = 0.0%

All Core	= 0.9%
Best Zone	= 1.4%
Unfractured Rock	= 0.6%
All Core ϕ_f	= 0.4%
Best Zone ϕ_f	= 0.9%
Highest ϕ_f	= 2.9%

3.6.3.6.2 Fracture Porosity- Fracture Permeability Relations

Another method used in fracture porosity calculations involves the relationship between fracture porosity and fracture permeability (Figure 3.20). In the Valhall Field in the Norwegian sector of the North Sea, a reservoir permeability of 66 md was calculated from a flow test in the same zone from which a core was taken. By standard analysis of the core, the matrix permeability was so low (much less than 1 md) that all flow measured in the test must have been from the natural fracture system. Observation of the core material indicated fracture spacing from this same zone of about 0.5 cm (a very intense fracture system). Therefore, by knowing the spacing of the fracture system and the total permeability of the same fracture system, fracture porosity (Φ_f) could be approximated (Jones, 1975). By this method, a Φ_f of 0.3 to 0.4 % was calculated for that particular portion of the reservoir. This method of calculating fracture porosity from fracture permeability is quite elegant and should give fairly accurate values. However, the possible situations where this can be used are relatively few. Three conditions must be met:

- Flow test permeability must have been calculated for the same zone from which a core was pulled.

- Core analysis must show that the rock matrix (Φ_r) contributed negligible flow to the flow test.
 - A good estimate of fracture spacing must be obtainable from the core.
- If these conditions are met, the $\Phi_f - k_f$ method of Φ_f calculation can be used.

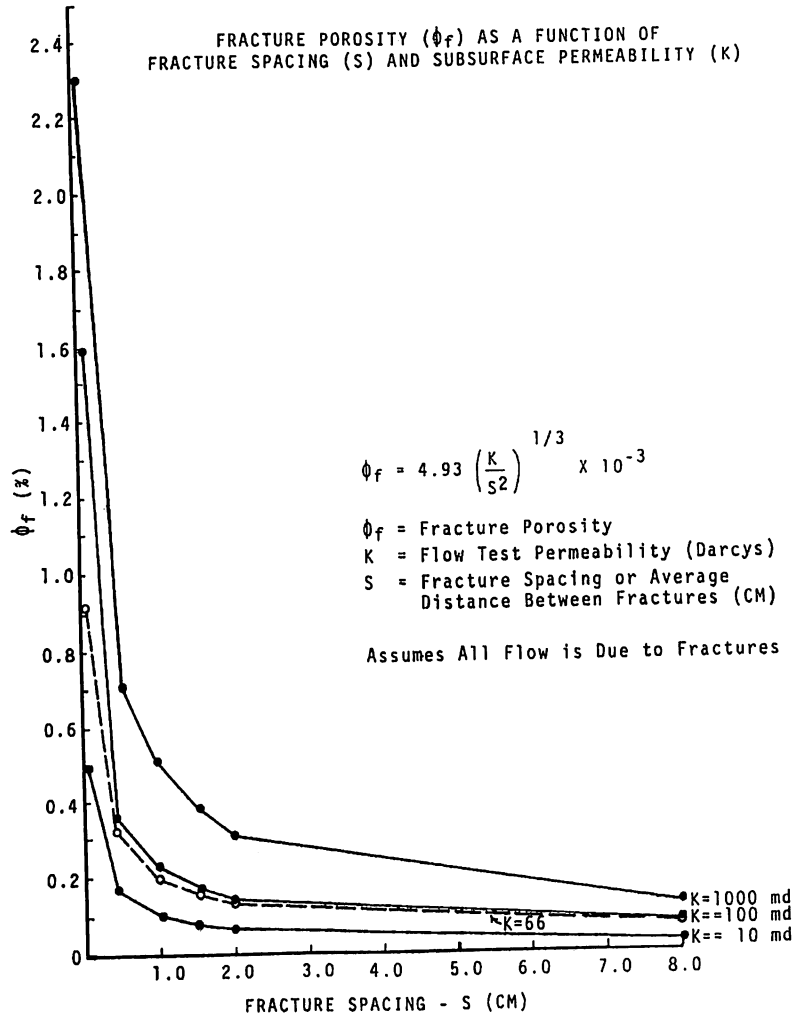


Figure 3.20: Fracture porosity as a function of fracture spacing and flow test permeability.

Field- lab determination: Because fractures are planar entities, both Φ_f and k_f are directly dependent on the width and spacing of the fractures (e).

$$\phi_f = \left(\frac{e}{D+e} \right) \times 100$$

$$k_f = \left(\frac{e^3}{12D} \right)$$



Where D = average fracture spacing and where the fracture plane is parallel to the fluid pressure gradient

In the laboratory, we can measure the permeability of fractured and unfractured companion samples of reservoir rock under confining pressure. The permeability difference between those two curves (k versus confining pressure) at any confining pressure can be considered the effect of the fracture on flow in the samples, or fracture permeability (k_f). Once k_f is measured and an estimate of D made, these variables can be applied to equation given above and the effective width of the fractures (e) at any confining pressure can be calculated. Once e is known for any confining pressure or simulated depth, subsurface fracture spacing data can be applied to the previous equation and Φ_f calculated. This method of Φ_f calculation involves both field and laboratory measurements and is, therefore, quite time-consuming. Its advantage lies in the fact that structural and stratigraphic discontinuities in Φ_f can be modeled and predicted.

3.6.3.6.3 Log- log Suites

There is no direct method of calculating fracture porosity from well logs. Several log suites have been developed to detect natural fracture systems but none can calculate Φ_f directly. Most early methods used (such as the borehole gravimeter) relied on measuring matrix porosity on one tool and total porosity on another. The difference between the two is taken to be the fracture porosity. However, because Φ_f is so small, calibration errors often overshadowed the true value of Φ_f . Calculations of Φ_f by logging methods are and should be routinely made in reservoirs where this is a relevant term; however, these values tend to overestimate fracture porosity.

3.6.3.6.4 Multiple Well Tests

Both single- and multiple-well testing can be used to effectively calculate Φ_f . Pulse testing and pressure transient analyses are good methods for doing this. These methods probably give the most accurate estimates of subsurface Φ_f . However, they require close-spaced wells for testing and are usually only applicable in well-developed areas where production can be ceased in several wells long enough to perform the tests.

3.7 Estimation of Porosity Interaction

Direct determination of fracture/matrix communication is very difficult. It is as important at this point to recognize that poor communication in a reservoir exists as it is to accurately quantify it. Early recognition of poor fracture/matrix interaction allows us to



be more cautious in economic evaluation of a reservoir. The importance of thin-section observation of fracture/matrix interfaces in fractured reservoir analysis cannot be overemphasized. Such observations give direct evidence of major interaction problems as well as a chance to document the geometry of the interface itself. Porosity, grain size and shape, and sorting of the interfacing material can all be quantified and applied in estimations of fracture/matrix interaction. In addition to thin-section measurements, estimates of communication between the two systems can sometimes be made by analyzing directional permeability data. Open or partially open fractures will generally have permeabilities much greater than the matrix rock in which they are found. Such fractures will have higher permeability parallel to the plane and "normal" matrix permeability across the fracture. In cases where poor fracture/matrix interaction exists, however, permeability perpendicular to the fracture plane is lower than that of normal or average matrix permeability, reflecting the reduced porosity and permeability of the interface or deformation zone. The reduced permeability of the zone or interface can then be used in modeling the flow distribution in the reservoir in a manner possibly similar to that of skin effects in wellbore damage.

Chapter 4

Basics of Well Test Analysis

4.1 Introduction

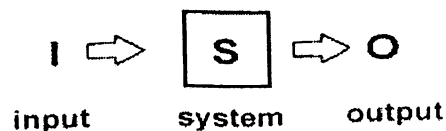
Well Testing is a means of accessing reservoir performance by monitoring the transient pressure response created by a temporary change in the production rate. This pressure response is analyzed versus the elapsed time Δt since the start of the period. From pressure curve analysis, it is possible to determine the following reservoir properties:

- Permeability
- Reservoir heterogeneity
- Boundaries
- Pressure

Well test analysis has been used for many years to assess well condition and obtain reservoir parameters. Early interpretation methods (using straight-lines or log-log pressure plots) were limited to the estimation of well performance. Modern Well Testing analysis has been greatly enhanced by the use of the Derivative Plots (Log-Log Diagnostic Plot). With the introduction of pressure derivative analysis and the development of complex interpretation models that are able to account for detailed geological features, well test analysis has become a very powerful tool for reservoir characterization. The interpretation model of a well with wellbore storage and skin in an infinite reservoir with homogenous behavior is probably the most widely used for pressure transient testing.

4.2 Methodology: *The Inverse Problem*

The objective of well test analysis is to describe an unknown system S (well reservoir) by indirect measurements (O is the pressure response to change in rate I). Solving $S=O/I$ is a typical inverse problem.



The solution of the inverse problem is usually not unique.



4.3 Plots used in Well Testing

- **History Plots:** Linear plot of pressure vs. time used basically to identify pressure drawdown and build-up periods.
- **Semi-log Plots:** Plot of the pressure versus the log of time. There are typically four different semi-log plots used in pressure transient which are
 - Miller Dyes Hutchinson (MDH) Plot
 - Horner Plot
 - Agarwal Equivalent Time Plot
 - Superposition Time Plot

Each plot uses a different time function, therefore, use of the appropriate plot with the correct time function is critical for the analysis. In the current project, the semi-log plots which are used include Superposition Plot and Horner's Plot.

After plotting the appropriate semi-log plot, a straight line should be drawn through the points located within the equivalent radial flow portion of the plot identified from the log-log plot.

- **Log-Log Diagnostic Plots (Derivative Plots):** Plot the pressure and semi-log pressure derivative versus time on a log-log diagnostic plot. With the derivative approach, the time rate of change of pressure during a test period is considered for analysis. In order to emphasize the radial flow regime, the derivative is taken with respect to logarithm of time. By using the natural logarithm, the derivative can be expressed as the time derivative, multiplied by the elapsed time Δt since the beginning of the period.

$$\Delta p' = \frac{dp}{d \ln \Delta t} = \Delta t \frac{dp}{dt}$$

As pressure analysis, the derivative is plotted on log-log coordinates versus Δt .

The use of this pressure derivative type curve offers the following advantages:

- Heterogeneities hardly visible on the conventional plot of well testing data are amplified on the derivative plot.
- Flow regimes have clear characteristic shapes on the derivative plot.



- The derivative plot is able to display in a single graph many separate characteristics that would otherwise require different plots.
- The derivative approach improves the definition of the analysis plots and therefore the quality of the interpretation.

4.4 Types of flow behavior

The different flow behaviors are usually classified in terms of rate of change of pressure with respect to time.

Steady state

During steady-state flow, the pressure does *not change* with time. This is observed for example when a constant pressure effect, such as resulting from a gas cap or some types of water drive, ensures a pressure maintenance in the producing formation.

$$\frac{\partial p}{\partial t} = 0$$

Pseudo steady state

The pseudo steady state regime characterizes a closed system response. With a constant rate production, the drop of pressure becomes *constant* for each unit of time.

$$\frac{\partial p}{\partial t} = \text{constant}$$

Transient state

Transient responses are observed before constant pressure or closed boundary effects are reached. The *pressure variation* with time is a function of the well geometry and the reservoir properties, such as permeability and heterogeneity.

$$\frac{\partial p}{\partial t} = f(x, y, z, t)$$

Usually, well test interpretation focuses on the transient pressure response. Near wellbore conditions are seen first and later, when the drainage area expands, the pressure response is characteristic of the reservoir properties until boundary effects are seen at late time (then the flow regime changes to pseudo steady or steady state). In the following, several characteristic examples of well behavior are introduced, for illustration of typical well test responses.

Chapter 5

Pressure Behavior in Naturally Fractured Formations

5.1 Fissured Reservoir

Among the different heterogeneous interpretation models, the double porosity solutions have been the most frequently discussed in the technical literature. They assume the existence of two porous regions within the formation. One region, of *high conductivity*, is called the *fissures* whereas the other, of *low conductivity*, is called the *matrix blocks*. As described in Figure 5.1, the concept of double porosity is representative of the behavior of fissured and multiple-layer formations, when the permeability contrast between layers is high (the "fissure system" describes the high permeability layers, and the "matrix blocks" the tight zones).

The double-porosity model was first introduced by Barenblatt et al. in 1960: a low permeability porous system, the matrix blocks, is surrounded by a fissure network of high permeability. The matrix blocks are not producing to the well, but only to the fissures. The fissure network provides the *mobility*, and the matrix blocks supply most of the *storage capacity*. A double porosity response depends upon the storativity contrast between the two reservoir components, and the quality of the communication between them.

Two types of flow from matrix to fissures are considered, depending upon the presence of minerals in the fissure network that reduce the flow from matrix to the fissures. The *restricted interporosity flow* hypothesis, also called the Warren and Root model, or pseudo-steady state interporosity flow model, was first available for transient test analysis. This model is discussed in Section 5.2.1 for a well with wellbore storage and skin. The *unrestricted interporosity* hypothesis is then presented in Section 5.2.2.

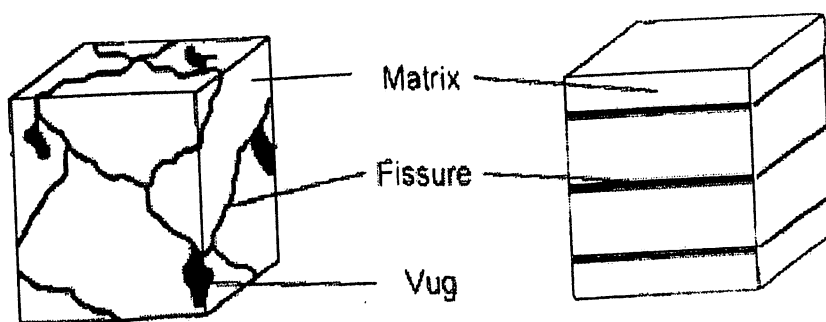


Figure 5.1: Example of double porosity reservoir, fissured and multiple-layer formations.



5.2 Double Porosity Models

Fissured reservoirs are complex. The density of the fissure network can vary with position in the reservoir, as a function of the rock stresses due to curvature of the formation. The orientation of the fissures can induce permeability anisotropy. The mathematical models for fissured reservoirs use a simplified description of the heterogeneous system. The parameters resulting from the interpretation define the idealized model, but they do not describe the geological configuration in detail. In the following, we summarize the different assumptions used in the equations for the models.

Basic assumptions

- 1 - The dimensions of the matrix blocks are *small* compared to the reservoir volume involved in the test. Each point in the reservoir is associated with two pressures, namely p_r , the pressure of the fluid in the fissures, and p_m , the pressure of the fluid in the matrix pore volume.
- 2 - The fluid flows to the well through the fissure system only; the matrix blocks are *not connected* (or the radial permeability of the matrix system is negligible, $k_{m,rad} = 0$). The isolated matrix blocks are described as source terms in the fissure element, and the mobility measured during the test corresponds to the fissure system alone.
- 3 - Most of the reservoir fluid is *stored* in the matrix blocks porosity, the storage of the fissure network is only a small fraction of the reservoir storage.
- 4 - Three matrix block *geometries* are usually considered, depending upon the number n of fissure plane directions.

For $n = 3$, the matrix blocks are cubes (spheres are also described with three directions of fissure planes) but $n = 2$ (cylinder matrix blocks) and $n = 1$ (slab matrix blocks) can also be envisaged.
- 5 - Two different types of *matrix to fissure flow* have been considered:

In the first solution, as described by Barenblatt et al. in 1960, it is assumed that the flow of fluid from blocks to fissures occurs under *pseudo-steady state* conditions. The model was extended in the present form by Warren and Root (1963). Moench (1984) and Cinco-Ley et al. (1985) demonstrated later that it describes a *restricted* interporosity flow condition, when there is a skin effect between the matrix and the fissures, making the pressure gradient in the matrix blocks negligible.



The second type of interporosity flow described by several authors (Kazemi, 1969 a; de Swaan, 1976; Najurieta, 1980; Streltsova, 1983), considers *transient flow* in the matrix blocks. There is *no flow restriction* at the matrix - fissure interface, and the matrix blocks response starts earlier.

- 6 - In the double porosity models, all matrix blocks are *homogeneous*, and they have the same size. Other multiple porosity solutions consider different matrix block sizes, either uniformly distributed in the reservoir, or organized according to several possible geometries.

Behavior

When a well is opened in a fissured reservoir, a rapid pressure response occurs in the fissure network due to its high diffusivity. A *pressure difference* is created between matrix and fissure, and the matrix blocks start to produce into the fissures. The pressure of the matrix blocks p_m decreases as flow progresses and, finally, tends to equalize with the pressure of the surrounding fissures p_f .

Definitions

In the permeability thickness product kh , an equivalent permeability is used. The fissure system is assumed to be uniformly distributed in all the reservoir thickness but, in practice, the fissures involve only a fraction of the pay zone thickness h . The equivalent distributed permeability (*bulk fissure permeability*) k_f is a function not only of the actual fissures thickness and intrinsic permeability, but also of the fissure network characteristics (such as tortuosity and fissure connectivity when material separates individual fractures).

$$kh = k_f h_f \dots\dots\dots \text{Eq 5.1}$$

Two porosities are defined in double porosity systems. We call Φ_f and Φ_m , the ratio of pore volume in the fissures (or in the matrix), to the total volume of the fissures (or the matrix). V_f is the ratio of the total volume of the fissures to the reservoir volume, and V_m , that of the total volume of the blocks to the reservoir volume ($V_f + V_m = 1$). The average reservoir porosity Φ is given by:

$$\phi = \phi_f V_f + \phi_m V_m \dots\dots\dots \text{Eq 5.2}$$



In fissured formations, both Φ_f and V_m , are close to 1. The average porosity as given above can be simplified as:

$$\phi = V_f + \phi_m \dots\dots\dots\text{Eq 5.3}$$

Frequently, V_f is called the fissure porosity.

The storativity ratio ω expresses the contrast between the two porous systems:

$$\omega = \frac{(\phi V c_t)_f}{(\phi V c_t)_f + (\phi V c_t)_m} = \frac{(\phi V c_t)_f}{(\phi V c_t)_{f+m}} \dots\dots\dots\text{Eq 5.4}$$

ω defines the contribution of *the fissure system to the total storativity*. Usual values for ω are in the order of 10^{-1} for multiple-layer systems down to 10^{-2} or 10^{-3} for fissured formations: the fissures provide only a fraction of the total storativity.

In case of multiple-layer systems, matrix blocks and fissures are represented by horizontal slabs, h_m and h_f being the cumulative thickness of the "matrix" and the "fissure" layers, the volume ratios now are $V_f = h_f / (h_f + h_m)$ and $V_m = h_m / (h_f + h_m)$. The equivalent permeability thus is expressed as $k = k_f V_f$.

A second heterogeneous parameter, called interporosity flow coefficient λ , is used to describe the ability of the matrix blocks to *flow* into the fissures. λ , as expressed by Warren and Root (1963), is a function of the matrix blocks geometry and permeability k_m .

$$\lambda = \alpha r_w^2 \frac{k_m}{k} \dots\dots\dots\text{Eq 5.5}$$

where α is related to the geometry of the fissure network. It is a function of the number n of families of fissure planes:

$$\alpha = \frac{n(n+2)}{r_m^2} \dots\dots\dots\text{Eq 5.6}$$



r_m is the characteristic size of the matrix blocks. It is defined as the ratio of the volume V of the matrix blocks, to the surface area A of the blocks with:

$$r_m = n \frac{V}{A} \dots \dots \dots \text{Eq 5.7}$$

λ defines the *communication* between the matrix blocks and the fissures. When λ is small, the fluid transfer from matrix to fissure is difficult, and it takes a long time before the double porosity model behaves like the equivalent homogeneous total system. Such behavior is obtained for example, when the matrix is tight, and the permeability k_m is small. Low density of fissures is another example of poor matrix communication: the characteristic block size r_m is large, and α is small. Usual values for λ are in the range of 10^{-4} to 10^{-10} .

In the expression for λ , matrix skin is not considered. In case of restricted interporosity flow, λ does not describe completely the matrix flow condition and an effective interporosity flow parameter λ_{eff} should be used.

5.2.1 Restricted interporosity flow model (Wellbore storage and skin)

In 1963, Warren and Root presented the double porosity solution described in this section. The flow from matrix blocks to the fissures is assumed to be *pseudo-steady state* regime.

Moench demonstrated in 1984 that the apparent pseudo-steady state flow regime in the matrix blocks is the result of damage at the surface of the blocks. The fissures are partially plugged by mineral deposition or by chemical precipitation, but they include some channels allowing the fluid to flow towards the well. The matrix feed the channels, but the flow first has to cross the thin low permeability deposit layer on the walls of the fissures.

The *matrix skin* theory (also called interporosity skin) provides a link between the pseudo-steady state matrix flow condition discussed here and the transient interporosity solution presented in Section 5.2.2: the different mathematical approaches describe two limiting cases of the same reservoir configuration. The influence of the matrix skin S_m is further discussed in Section 5.3 of this chapter. It is shown that, for large interporosity skin S_m the pseudo-steady state hypothesis of Warren and Root's (1963) is a realistic approximation of the matrix flow condition.



Behavior

With restricted interporosity flow, three different regimes can be observed on a producing well response:

1. First a *fissure flow*, when the matrix contribution is negligible. This corresponds to a homogeneous behavior, where only the fissure system is producing.
2. At intermediate times, during a *transition* regime, the response deviates from the fissure homogeneous behavior as the matrix blocks start to produce into the fissures. The pressure tends to stabilize to a constant value.
3. Later, the pressure of the matrix blocks equalizes with the pressure of the surrounding fissures. A new homogeneous behavior is reached, called the *total system flow* regime.

All the fluid flows to the wellbore through the fissures alone: the two homogeneous behaviors are characterized by the permeability thickness product kh of the fissure system. The first homogeneous regime corresponds to the fissure storativity, whereas the second involves the total storativity. The transition between the two homogeneous behaviors describes an increase of storativity, the pore volume of the fissures being a small fraction of the total.

During the two homogeneous regimes, the pressure response can exhibit a straight-line behavior on semi-log scale. The first straight line corresponding to fissure flow, the second to the total system regime. The permeability thickness kh being the same during the two homogeneous regimes, the lines are parallel.

More frequently, tests in fissured reservoirs do not show the characteristic "two *parallel semi-log straight lines*": either the first line is masked by wellbore storage effect, or the test period is too short to show the second. Many examples of analysis with double porosity type curves show that the occurrence of parallel semi-log straight lines is in fact exceptional. Furthermore, the characteristic features of double porosity responses can be identified in other regimes than the infinite acting radial flow.

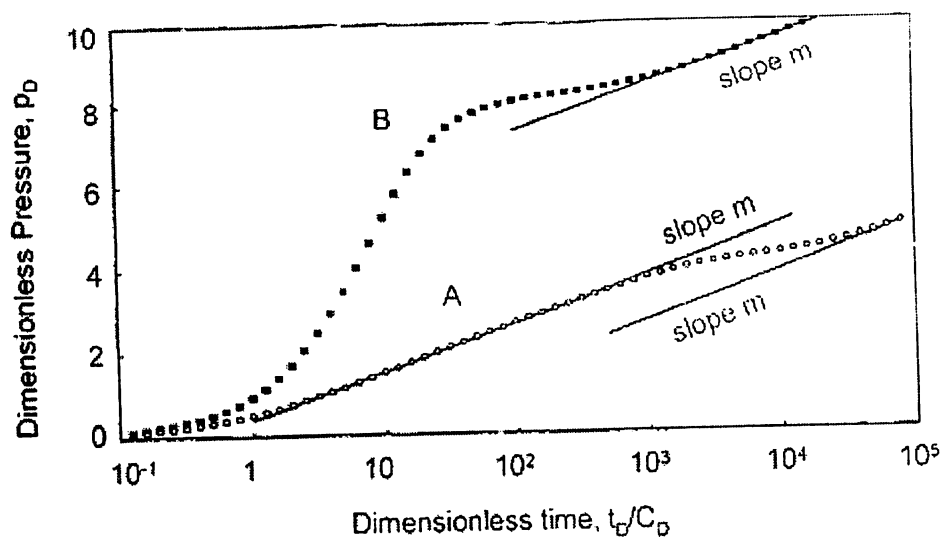


Figure 5.2: Semi-Log Plot of a well in double porosity reservoir

Derivative type-curve

The two double porosity examples A and B are presented on Figure below with the pressure and derivative. During the fissure flow, this homogeneous regime is described on the derivative response by a $C_D e^{2S}$ curve and, when semi-log radial flow is reached, the derivative stabilizes on 0.5 in dimensionless terms. At transition time, the flattening of the pressure curve is changed into an obvious *valley* on the derivative response. Later, the derivative returns to the 0.5 stabilization during the total system equivalent homogeneous behavior.

- With example A, the wellbore storage effect ends during fissure regime, and a first radial flow is seen before the start of transition. Two parallel semi-log straight lines are present on the semi-log plot Figure 5.2. On Figure 5.3, the derivative reaches the 0.5 line, both before and after the transition valley.
- With example B, storage is still present when the transition starts: the semi-log curve of shows only one straight line, during total system flow. On Figure 5.3, the derivative response goes directly from the wellbore storage hump to the transition valley, and the first 0.5 plateau is not seen.

The two examples of the following figure illustrate that, as opposed to the log-log pressure curves, the derivative emphasizes the small variations of behavior characterizing double porosity responses.

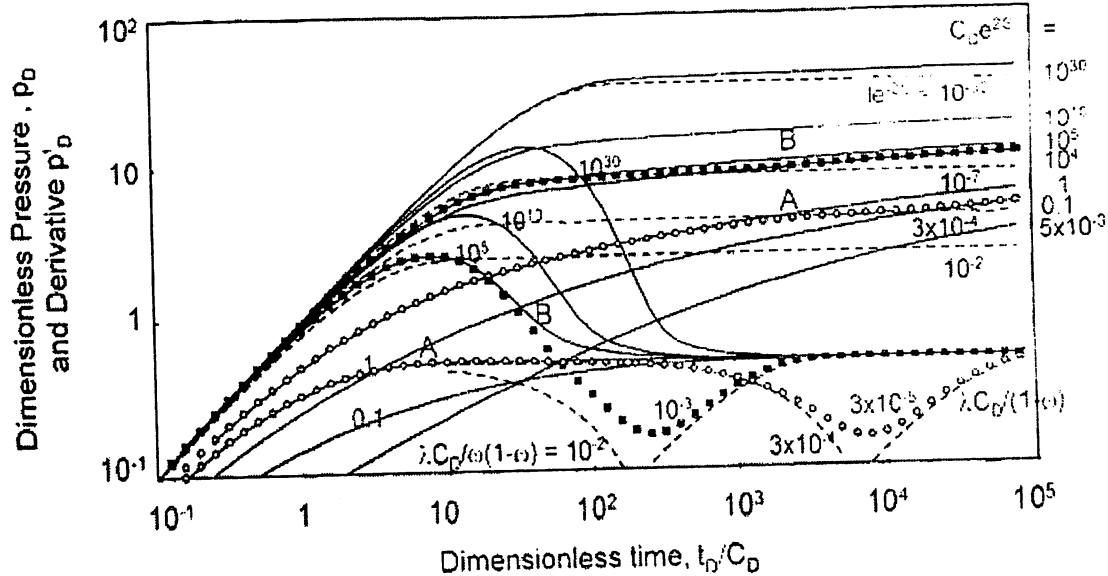


Figure 5.3: Pressure and derivative plot of a well in double porosity reservoir, pseudo steady state interporosity flow.

5.2.2 Unrestricted interporosity flow model (Wellbore storage and skin)

In this section, the effect of transient flow from blocks to fissures is considered. As opposed to the pseudo steady state interporosity flow model presented in Section 5.2.1, there is no skin effect at the surface of the blocks. The transient interporosity flow solution is also called unrestricted matrix flow. Transient matrix flow has been studied by several authors, and two matrix blocks geometries, slab or sphere, are usually considered. Following the theory developed by de Swaan in 1976, Bourdet and Gringarten (1980) presented a pressure type-curve for a well with wellbore storage and skin in a double porosity reservoir with unrestricted interporosity flow. The type curve was later extended to describe derivative responses (Bourdet et al., 1984).

Behavior

In the case of unrestricted interporosity flow, the matrix blocks react almost immediately to any change of pressure in the fissures: the transition starts earlier than in case of restricted flow, and the fissure flow regime is generally not seen.

Only two flow regimes are observed with this double porosity solution:

1. At early time, both fissure and matrix are producing, but the rate of change of pressure is faster in the fissure system than in the matrix blocks. The first response observed is in *transition* regime.
2. Later, the *homogeneous* behavior corresponding to the *total system* is reached.

Derivative type-curve

The derivative response of examples A and B are presented below.

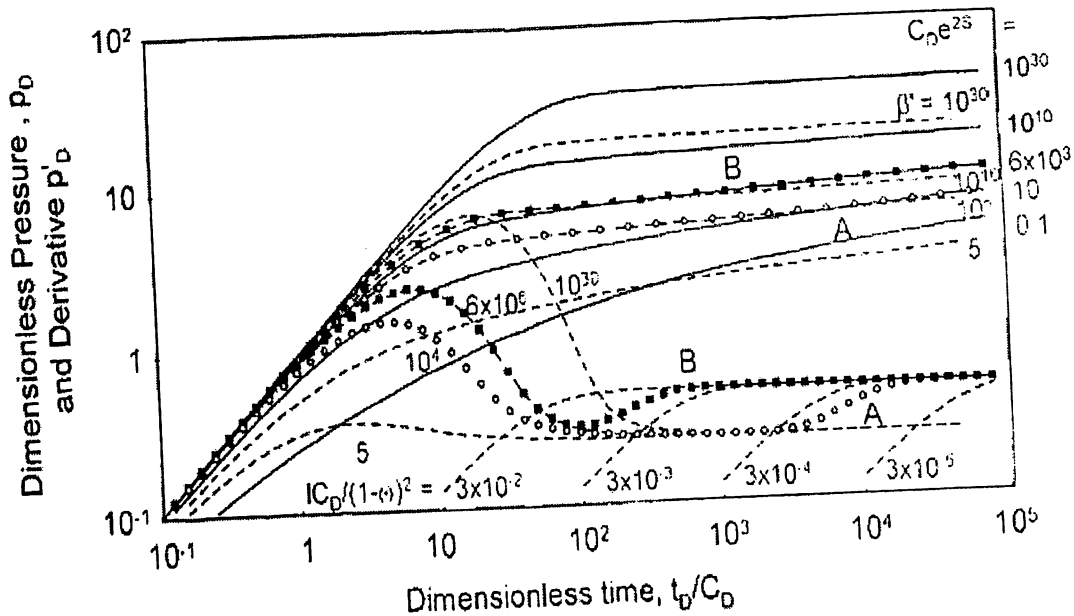


Figure 5.4: Pressure and derivative plot of a well in double porosity reservoir, transient interporosity flow.

With example A, two *derivative plateaus* are evident: the first during transition is at 0.25 and the second, during the total system homogeneous behavior, is on the usual 0.5 line. With example B, the transition is described by a short derivative valley before the stabilization at 0.5. On drawdown responses, the main difference with the restricted matrix flow solution is in the transition regime: with the examples such as in the Figure above, the derivative does *not drop below* 0.25 but tends to stabilize. It is a flat bottomed valley rather than a deep rounded valley.

5.3 Matrix skin

When the surface of the matrix blocks is damaged, the interporosity skin S_m , is defined, in dimensionless terms, as (Moench, 1984)

$$S_m = \frac{k_m h_d}{r_m k_d}$$

where h_d and k_d are respectively the damaged zone thickness and permeability. As already mentioned, the matrix skin term is not present in the Warren and Root's (1963) definition of λ . For high S_m (>10), several authors have proposed a correction to the interporosity flow parameter.

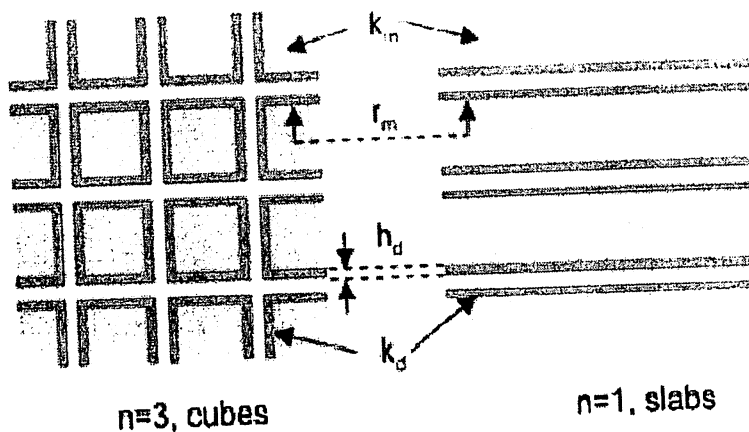


Figure 5.5: Matrix Skin. Slab and sphere matrix blocks.

For slab matrix blocks of thickness $2r_m$, Cinco et al. (1985) define the effective interporosity flow parameter, λ_{eff} as:

$$\lambda_{eff} = \frac{\lambda}{3(1-\omega)S_m}$$



Chapter 6

Pressure Behavior in Layered Reservoir

6.1 Introduction

The most common type of heterogeneity results from various cycles of sedimentation- a set of heterogeneous layers. In reservoirs composed of stratified layers, the most important question is whether there is sufficient interlayer pressure and fluid communication or lack of it. If unrestricted interlayer crossflow can occur, the reservoir behavior will be analogous to that of a single layer reservoir having the average properties of the layered system. If the discrete reservoir layers communicate only by means of common wellbore, then they will perform in a much different way.

The performance of a bounded reservoir composed of stratified layers was investigated theoretically for a no-crossflow case by Lefkowitz et al. The idealized reservoir system that they studied is shown in the figure below. Each layer is assumed to be homogeneous and isotropic with different porosity and permeability. Together with other usual single fluid study assumptions, a mathematical solution was also found for pressure behavior which results when the well is producing at a constant rate. It is important to realize that a constant producing rate from each layer is not assumed. This means, then, that differential depletion between the layers can cause their respective producing rates to vary until semi-steady state conditions are reached.

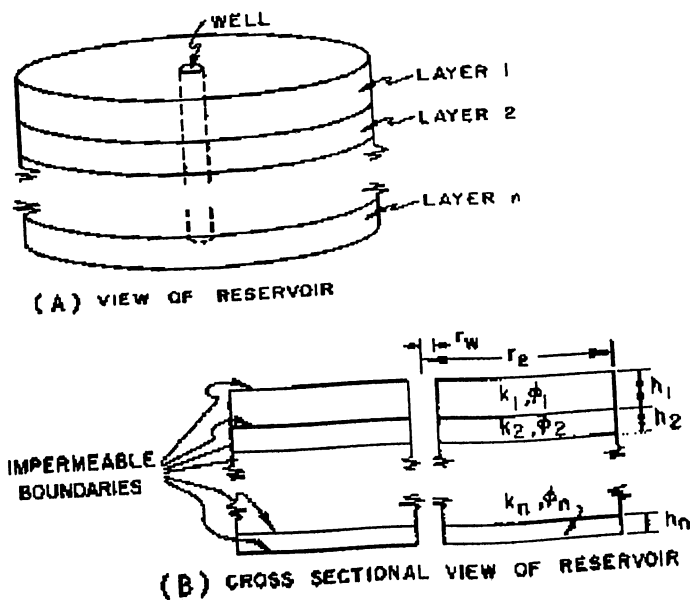


Figure 6.1: Layered Reservoir System

6.2 Pressure Decline Curves

Some theoretical pressure decline curves from the subject study are showing the figure 6.2 During early times at which drainage boundary effects have not been felt, the pressure behavior at the well in the two layer case is given by:

$$\frac{p_i - p_{wf}}{q_i \mu} = \ln t - \ln \gamma$$

$$\frac{q_i \mu}{4\pi (kh)_t}$$

$$\frac{k_1 h_1 \ln \frac{\phi_1 \mu c r_w^2}{4k_1} + k_2 h_2 \ln \frac{\phi_2 \mu c r_w^2}{4k_2}}{(kh)_t} \dots \dots \dots \text{Eq 6.1}$$

Where $(kh)_t = k_1 h_1 + k_2 h_2$. From equation 6.1 and the pressure decline curves, we see that prior to boundary effects the pressure behavior is that of a single layer reservoir with $kh = (kh)_t$. The pressure drop is proportional to $\ln t$ plus a constant, and the rate of depletion of a layer is proportional to the kh product of that layer.

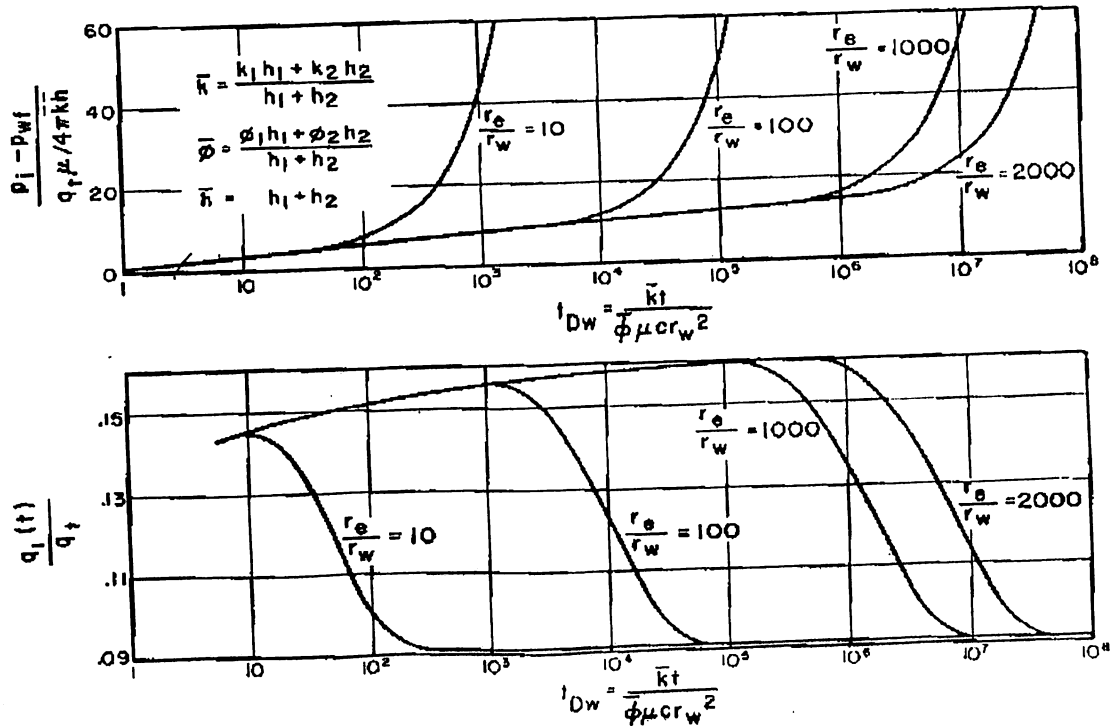


Figure 6.2: Well pressure decline and fractional flow rate from one layer for a two-layer reservoir.

In the figure 6.2, $k_1/k_2=4$, $h_1/h_2=0.05$, and $\Phi_1/\Phi_2=2$. initially the fraction of total flow which comes from layer 1, $q_1(t)=q_t$ is approximately equal to $k_1 h_1/(kh)_t=0.166$. After boundary effects are felt and semi steady state is reached, the fractional flow rate from Layer 1 is proportional to pore volume of Layer 1.

Because of the rate adjustment which can occur between the layers, there may be a long transition between the early transient behavior and the onset of the semi steady state. For the two layer cases studied by Lefkovits et al., the average value of time for occurrence of semi steady state was 50 times as great as that for single layer case with the same drainage radius.

6.3 Pressure Build-up

Lefkovits et al. also considered pressure build up performance. The figure 6.3 is the pressure build up curve for two layer reservoir. As in single layer case, there is an initial straight line section AB.

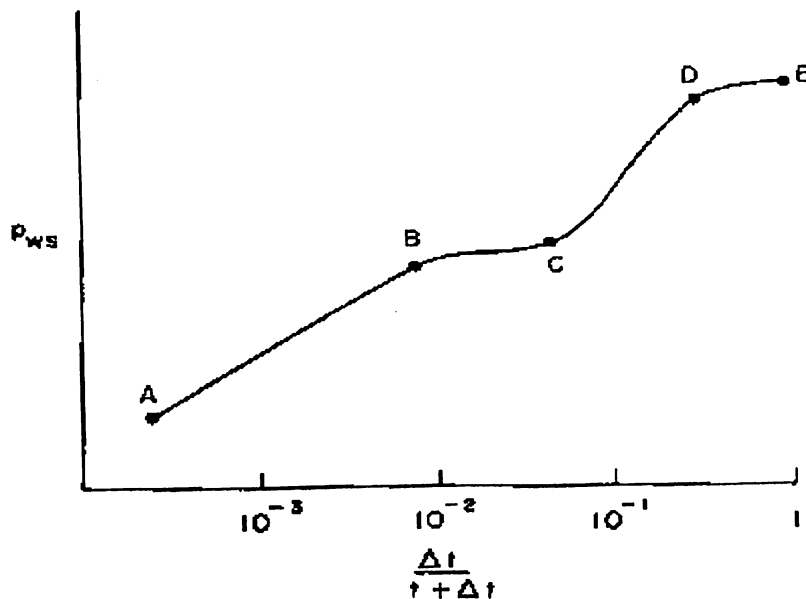


Figure 6.3: Theoretical pressure build up curve for two-layer reservoir.

After the straight line portion, the pressure build up curve levels off (BC). This leveling off corresponds in a single layer reservoir to pressure's having almost reached its average value. However, in a two layer reservoir the pressure again rises (CD). And finally levels off to the average pressure (DE). The rise in portion CD is due to the repressuring of the more depleted, more permeable layer by the less depleted and less permeable layer.

In the case where no barrier to vertical flow of fluids between the layers is present, the pressure behavior of the well will be considerably different from the one which we have just discussed. A schematic cross section of the reservoir situation of interest is shown in the figure 6.5. In case of constant producing rate, it has been found that the flowing bottom-hole pressure performance of a two layer crossflow system can be represented almost exactly by an equivalent homogenous system of identical radial dimensions, and with $(kh)_t$ and $(\Phi h)_t$ substituted for kh and Φh , respectively in the homogeneous-case formulas. Thus the transient bottom-hole pressure performance of a well in a reservoir with crossflow is given by

$$p_{wf} = p_i - \frac{162.6q\mu B}{(kh)_t} \left[\log \frac{(kh)_t t}{(\phi h)_t \mu c r_w^2} - 3.23 \right] \dots\dots\dots \text{Eq 6.2}$$

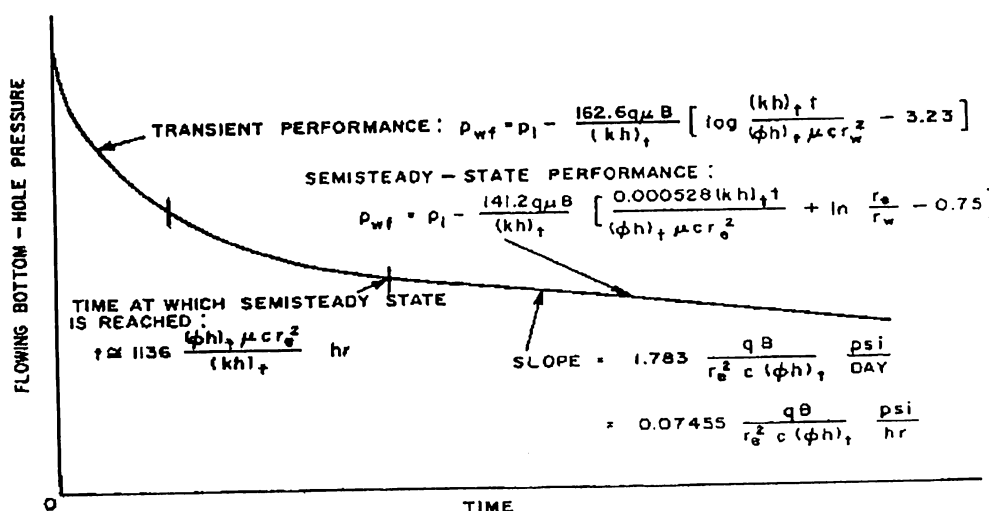


Figure 6.4: Build up in two-layer reservoir.

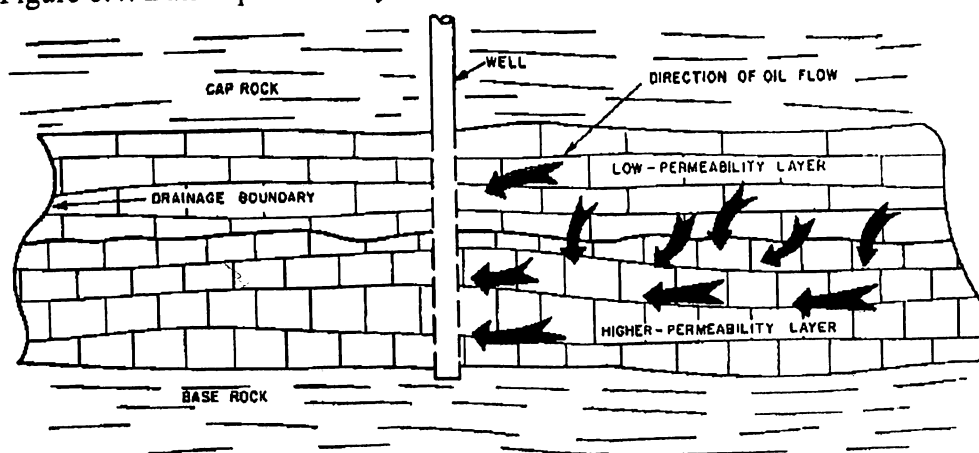


Figure 6.5: Schematic cross section of a portion of a two-layer reservoir with inter-layer crossflow

From the differences between pressure behavior with and without crossflow, it is sometimes possible to infer the presence or absence of crossflow. If the well flows, one should be able to detect crossflow either from pressure drawdown or from pressure build up tests. In case of drawdown test with the well adjusted to produce at a constant rate, the linear coordinate plot of flowing bottom-hole pressure plot vs. time should be linear after semi steady state is reached. The drawdown curve at semi steady state will have the same slope whether crossflow occurs or not. The figure 6.6 shows the pressure performance at constant production rate with and without crossflow.

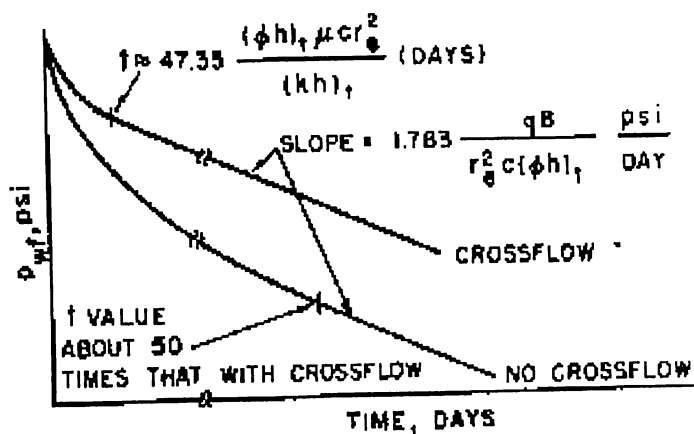


Figure 6.6: Pressure performance at constant production rate with and without crossflow.

Chapter 7

Pressure Behavior in Hydraulically Fractured Wells

7.1. Hydro-fractured Wellbore Models

The hydraulic fracturing technique has been used from the 1950's to improve the productivity of damaged wells, or wells producing from low-permeability reservoirs. By injecting fluid into the formation, a vertical plane fracture is created and filled with propping agents to prevent closure. The fracture is symmetrical on both sides of the well and it intercepts the complete formation thickness, X_f is the half fracture length.

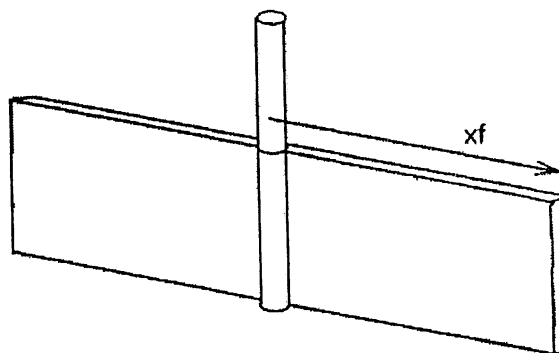


Figure 7.1: Fracture Geometry

7.2 Infinite Conductivity Fractured Well

In the infinite conductivity fracture model, it is assumed that the fluid flows along the fracture without any pressure drop. At early time, the flow-lines are perpendicular to the fracture plane. This is called a linear flow regime. Later, the reservoir regions at the two ends of the fracture starts to contribute significantly to the flow, the linear flow regime ends, to change into an elliptical flow geometry. Ultimately, the well response shows the characteristic radial flow regime behavior.

During linear flow, the pressure change is proportional to the square root of the elapsed time since the well was opened

$$\Delta p = 4.06 \frac{qB}{hx_f} \sqrt{\frac{\mu}{\phi c_i k}} \sqrt{\Delta t}$$

.....Eq 7.1

Specialized analysis

The linear flow regime can be analyzed with a plot of the pressure change Δp versus the square root of elapsed time $\sqrt{\Delta t}$: the response follows a straight line of slope m_{LF} , intercepting the origin. When the reservoir permeability is known from the analysis of the subsequent radial flow regime, the slope m_{LF} of the linear flow straight line is used to estimate the half fracture length X_f .

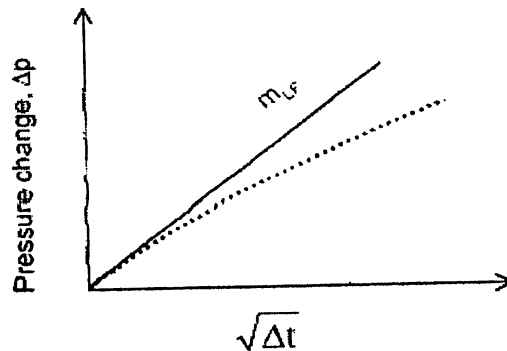


Figure 7.2: Infinite Conductivity Fracture

$$x_f = 4.06 \sqrt{\frac{\mu}{\phi c_f k} \frac{qB}{hm_{LF}}} \dots\dots\dots \text{Eq 7.2}$$

Model description

The well intercepts a symmetrical vertical plane fracture of half-length X_f . The well and the fracture penetrate totally the reservoir thickness and there is no pressure loss along the fracture plane. Wellbore storage effects can be present in the well, and the fracture can be affected by a skin damage.

Characteristic flow regimes

Two characteristic regimes can be observed after the wellbore storage early time effect:

1. Linear flow, with Δp proportional to $\sqrt{\Delta t}$ and a half unit slope straight line on pressure and derivative log-log curves. The linear flow regime defines the $k(X_f)^2$ product, and therefore the fracture half-length X_f .

2. Pseudo-radial flow regime when the flow lines converge from all reservoir directions. During the pseudo-radial flow regime, the pressure follows a semi-log straight-line behavior, as during the usual radial flow regime towards a cylindrical vertical well. The fracture influence is then described by a geometrical negative skin and the pseudo-radial flow analysis provides the permeability thickness product kh and S_G .

Skin Discussion

This geometrical skin S_G is related to the fracture half-length X_f . For the uniform flux solution, the geometrical skin S_{UFF} is:

$$x_f = 2.718r_w e^{-S_{UFF}} \dots\dots\dots \text{Eq 7.3}$$

For the infinite conductivity solution, S_{HKF} is expressed:

$$x_f = 2r_w e^{S_{HKF}} \dots\dots\dots \text{Eq 7.4}$$

Values of skin for fractured wells can be as low as -6 or -7.

Matching procedure on pressure and derivative responses: Infinite conductivity and uniform flux models

In practice, wellbore storage is short lived in fractured wells, and frequently is not observed on the recorded data. The two high conductivity fracture models are slightly different at intermediate times, between linear flow and radial flow. With the uniform flux model, the transition from the half unit slope straight line to the 0.5 line is shorter, and the angle between the two regimes is more pronounced. The pressure curve is slightly higher.

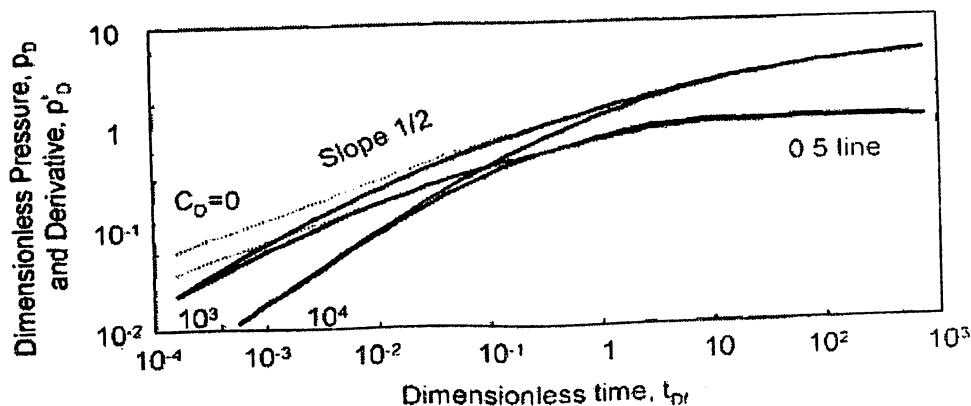


Figure 7.3: Responses of well intercepting a high conductivity fracture. Infinite Conductivity and Uniform Flux Model

When matching test data against a high conductivity fracture model such as on Fig.7.3, the derivative stabilization during the pseudo radial flow regime is used to determine the pressure match (giving the permeability thickness product kh). The location of the half unit slope pressure and derivative straight lines provides the half fracture length X_f . The longer the fracture, the later the start of the pseudo radial flow regime.

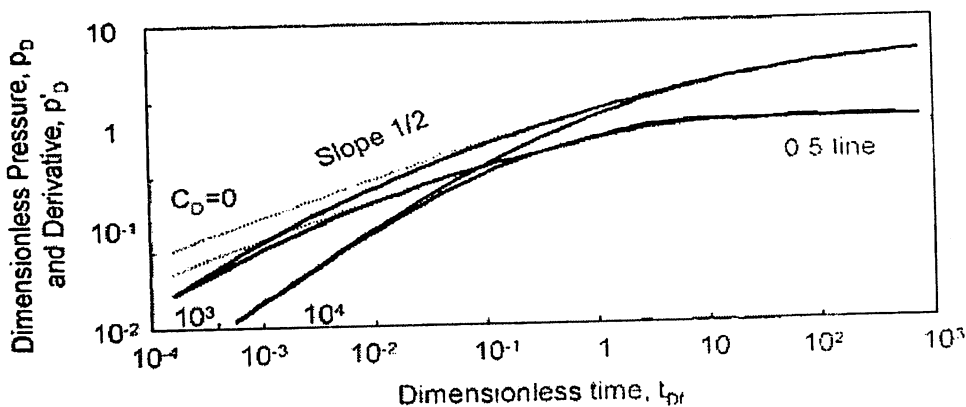


Figure 7.4 Responses for a fractured well with wellbore storage. Infinite Conductivity Fracture

Effect of wellbore storage

On Figure 7.4, wellbore storage effect is introduced on infinite conductivity fracture responses. For C_D values of 10^3 or above, the wellbore storage effect is indicated by a deviation below the half unit slope lines, before linear flow becomes evident. In case of high C_D , the wellbore storage effect masks the half unit slope pressure and derivative straight lines, the choice between a high or a low conductivity model is difficult, and X_f is not uniquely defined from early time data analysis.

Damaged fracture

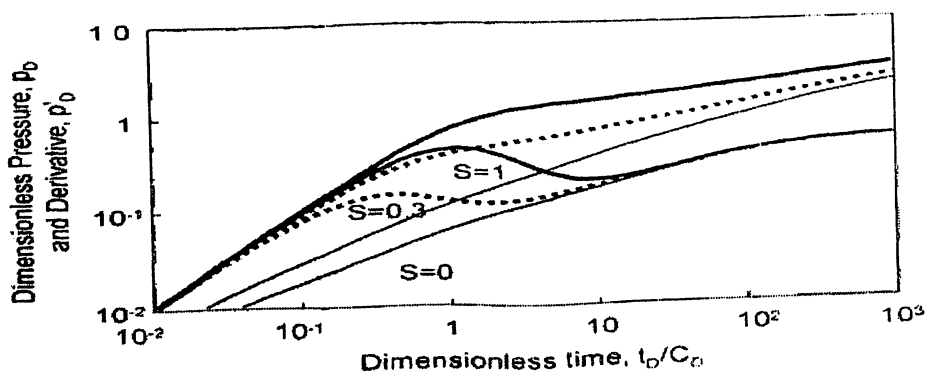


Figure 7.5: Responses of a well intercepting a high conductivity damaged fracture.

Two types of damaged fracture have been considered. Either an infinitesimal skin is located around the fracture (when a zone of reduced permeability has been created around the fracture by fracturing fluid loss), or the damaged region is located within the fracture near the wellbore (this configuration is called choked fracture).

With damaged fractures, the duration of the wellbore storage effect is extended and the response follows a unit slope straight line at early time, as illustrated in Figure 7.5. Later, the derivative describes a hump until the sand face rate is fully established. Then, the reservoir response shows the linear, followed by the pseudo radial flow, characteristic derivative behaviors.

7.3 Finite Conductivity Fractured Well

When the pressure gradient along the fracture length is not negligible, the low conductivity fracture model has to be used for the analysis of hydraulically fractured wells. This may happen for example when the permeability of the fracture is not very high compared to the permeability of the formation, especially when the fracture is long. In case of finite conductivity fracture, a second linear flow regime is established along the fracture extension. Before the two ends of the fracture are reached, this well configuration produces the so-called bi-linear flow regime.

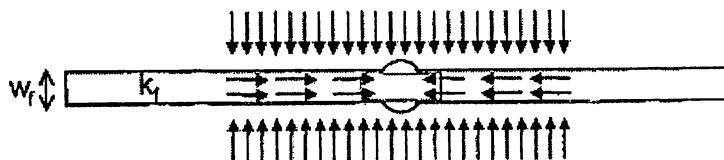


Figure 7.6 Finite Conductivity Fracture

During bilinear flow, the pressure change is proportional to the fourth root of the elapsed time since the well was opened. With w_f the width of the finite conductivity fracture and k_f the permeability in the fracture:

$$\Delta p = 44.11 \frac{qB\mu}{h\sqrt{k_f w_f} \sqrt[4]{\phi\mu c_i k}} \sqrt[4]{\Delta t} \dots\dots\dots \text{Eq 7.5}$$

Specialized analysis

On a plot of the pressure change Δp versus the fourth root of elapsed time $\sqrt[4]{\Delta t}$, pressure response follows a straight line of slope m_{BLF} , intercepting the origin, during the bilinear flow regime.

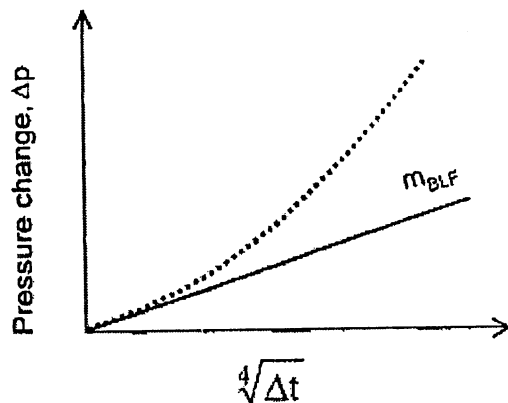


Figure 7.7: Finite Conductivity Fracture. Pressure vs. fourth root of time

As for the linear flow analysis, provided the reservoir permeability can be estimated from semi-log analysis of the late time response, the slope m_{BLF} of the bilinear flow straight line is used to estimate the controlling parameter, namely the fracture conductivity $k_f w_f$

$$k_f w_f = 1944.8 \sqrt{\frac{1}{\phi \mu c_f k} \left(\frac{q B \mu}{h m_{BLF}} \right)^2} \dots\dots\dots \text{Eq 7.6}$$

Model description

With the finite conductivity fracture model, linear flow is produced within the fracture, in addition to the linear flow regime from the pay zone into the fracture plane. The fracture geometry is defined on Figure 7.6: the well intercepts a symmetrical vertical plane fracture of half length X_f , w_f is the width, k_f is the fracture permeability and $k_f w_f$ is the fracture conductivity.

Characteristic flow regimes

Three characteristic regimes can be observed after the wellbore storage effect:

1. At early times, as long as the fracture tips have not been reached, the combination of fracture linear flow and reservoir linear flow produce the so-called bi-linear flow

regime. The pressure change is then proportional to the fourth root of the elapsed time $4 \sqrt[4]{\Delta t}$ and, on the log-log plot, both the pressure and derivative responses follow a quarter unit slope straight line. When present, the bi-linear flow regime gives access to the fracture conductivity k_{fwf} (the wellbore pressure is independent of the fracture half-length X_f during bi-linear flow).

Later, the pressure behavior becomes equivalent to that of an infinite conductivity fractured well. A linear flow regime can be observed, characterized by the usual pressure and derivative half unit slope log-log straight lines. The fracture half-length X_f can be estimated.

2. Pseudo-radial flow regime, with the derivative stabilization is observed next, to give the permeability thickness product kh and the geometrical skin S_G

Skin discussion

For a finite conductivity fracture, the skin is defined by two terms: the geometrical/ skin S_{HFK} assuming an infinite conductivity fracture, and a correction parameter G to account for the pressure losses resulting from the low fracture conductivity.

$$S_{LKF} = G \left(\frac{k_f w_f}{k x_f} \right) + \ln \frac{2r_w}{x_f}$$

.....Eq 7.7

Matching procedure on pressure and derivative responses

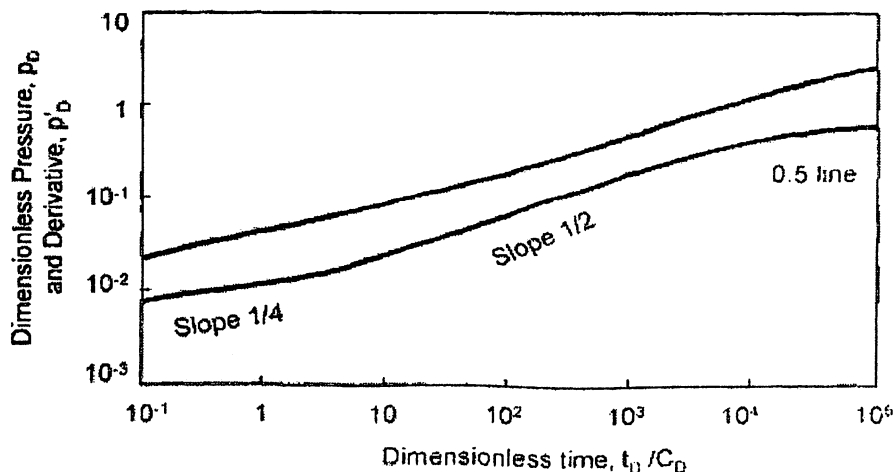


Figure 7.8: Response of a well intercepting a Finite Conductivity Fracture (No Fracture Skin, $k_{fD} w_{fD} = 25$)



The wellbore storage effect is not visible in Fig. 7.8, and three subsequent flow regimes can be identified:

1. At early times, during bilinear flow, pressure and derivative curves follow two parallel straight lines of slope $1/4$.
2. During the linear flow regime, two other parallel straight lines of slope $1/2$ are evident.
3. When radial flow is reached, the derivative stabilizes on 0.5 (in dimensionless scales).

The distance between the two quarter-unit slope straight lines is $\log(4)$, and the distance between two half-unit slope lines is $\log(2)$. For large fracture conductivity $k_{fD} w_{fD}$, the bilinear flow regime is short lived and the $1/4$ slope pressure and derivative straight lines are moved downwards. The behavior tends to a high conductivity fracture response.

Conversely, when the dimensionless fracture conductivity is low (curve $k_{fD} w_{fD} = 1$ on Fig. 7.8), the linear flow regime is not present and the response changes directly from bilinear flow to the pseudo radial flow regime, through a transition that never describes the half unit slope line. In such configuration, the pressure loss in the fracture is large, and two segments of the fracture near the tips are not participating to the flow.

With real test data ($\Delta p, \Delta p'$ vs. Δt), when all flow regimes are clearly defined, the match against a low conductivity fracture model such as on Fig. 7.8 provides the kh product from the pressure match, the fracture half-length X_f and the fracture conductivity $k_f w_f$ from the location of the half unit and quarter unit slope derivative straight lines respectively.

The example response of Fig. 7.8 is displayed over 6 time log-cycles. Frequently, log-log plots of actual build-up data describe the response during a smaller time range, and the match is performed only on a fraction of the complete model response. Matching is then difficult and the solution non-unique:

With some fractured well responses, it may take several months to reach the start of the pseudo radial flow regime but in practice the data do not go beyond the bilinear or linear flow period.

Depending upon the wellbore storage and fracture parameters, the different regimes can overlap, and some of them are not shown clearly. When the response is similar to the infinite fracture example with wellbore storage, the choice of the type of fracture response, and the resulting fracture parameters, are not uniquely defined.



When a long fracture is planned, it is recommended to test the well before fracturing, in order to obtain an estimate of the permeability thickness product. After fracturing, this parameter may not be defined by transient pressure analysis.



Chapter 8

Case Study: Well Test Interpretation of Hydro-Fractured Well

8.1 Introduction

Well PQR # 1 drilled ABC in exploratory block XYZ is situated in Cambay sedimentary basin. The well has been drilled to a depth of 2250m. Subsequent to the perforation well couldn't come on self flow. The well fluid was knocked out by application of compressor for activation and measurement of influx. Gauges were lowered and parked for measuring 24 hrs of influx. The next 24-hour showed a good inflow of oil of Sp. Gravity 0.71 and Influx rate of $9.7 \text{ m}^3/\text{day}$. Stimulation by Hydro-fracturing was done on 22.11.06 to enhance the productivity of the well. After HF well came on self flow and pressure transient testing was carried out to evaluate the fracture parameter and reservoir quality.

8.2 Input Data for Interpretation

Item	Value	Unit
Test Type	Standard	
Well Radius	4.25	In
Pay Zone	8	M
Porosity	0.12	
GOR	83.005	M^3/M^3
Fluid Type	Oil	
Reference Fluid	Oil	
Available Rates	Oil and Gas	
Reservoir temperature	109	$^{\circ}\text{C}$
Reservoir Pressure	197.827	kg/cm^2
PVT Data		
B	1.28337	B/STB
μ	0.380236	Cp
c_t	1.91266E-5	psi^{-1}

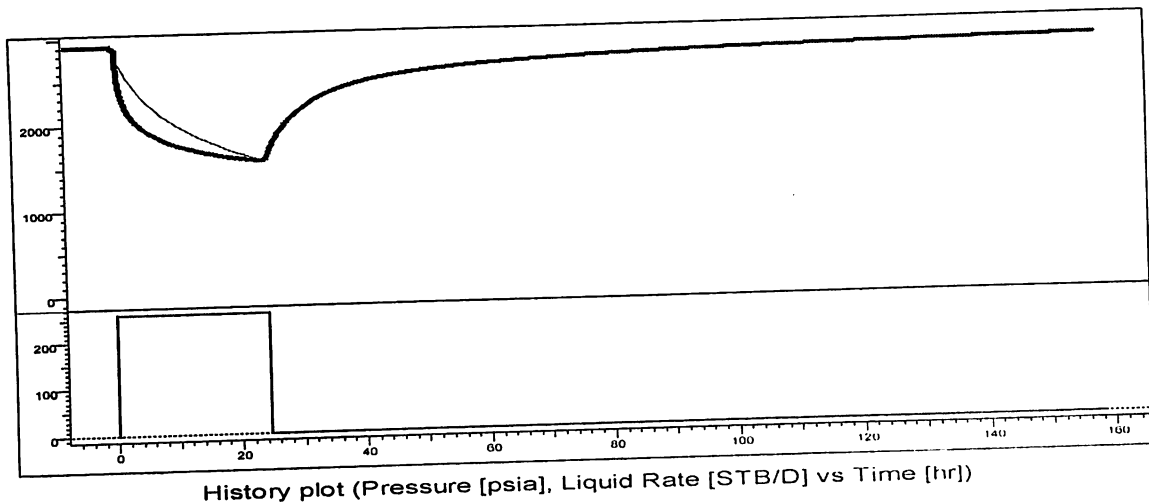
Flow Sequence:

Duration	q_o	q_g	q_t	Remark
hr	STB/D	MMscf/D	STB/D	
24.4722	259.643	0.12101	259.65	Main Flow
133.325	0	0	0	Final B-UP

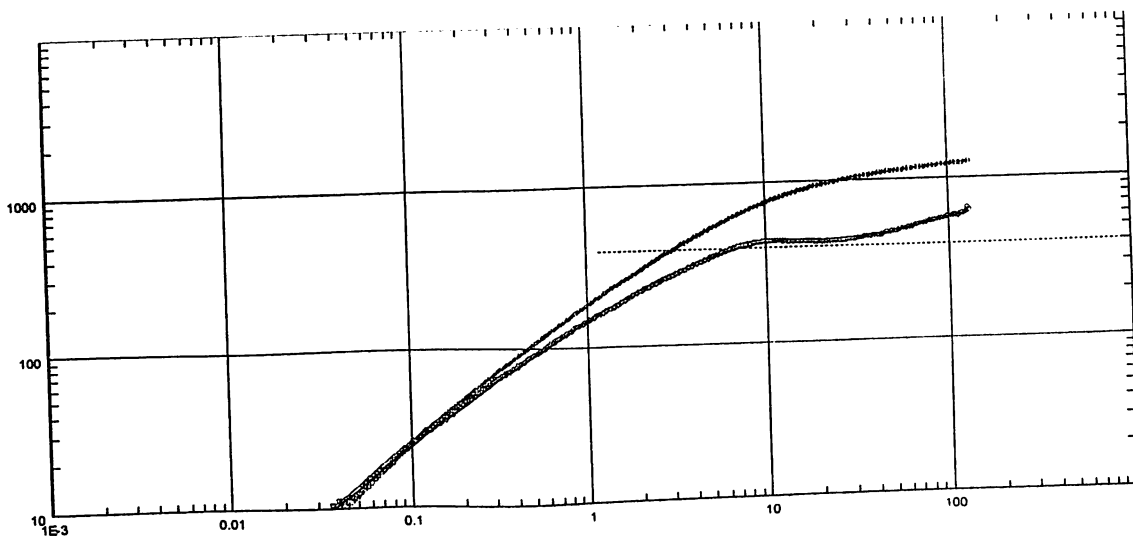
8.3 Plots

After pulling out of gauge, raw data was extracted successfully and the data was interpreted using above input data with the help of saphir. Following are the main plots generated for detailed interpretation.

- **History Plot:** A history plot is basically used to identify the pressure drawdown and build-up periods.



- **Derivative Plot:** A Derivative Plot is plotted to identify the different flow regimes that would have prevailed during the well test.



Log-Log plot: dp and dp' [psi] vs dt [hr]



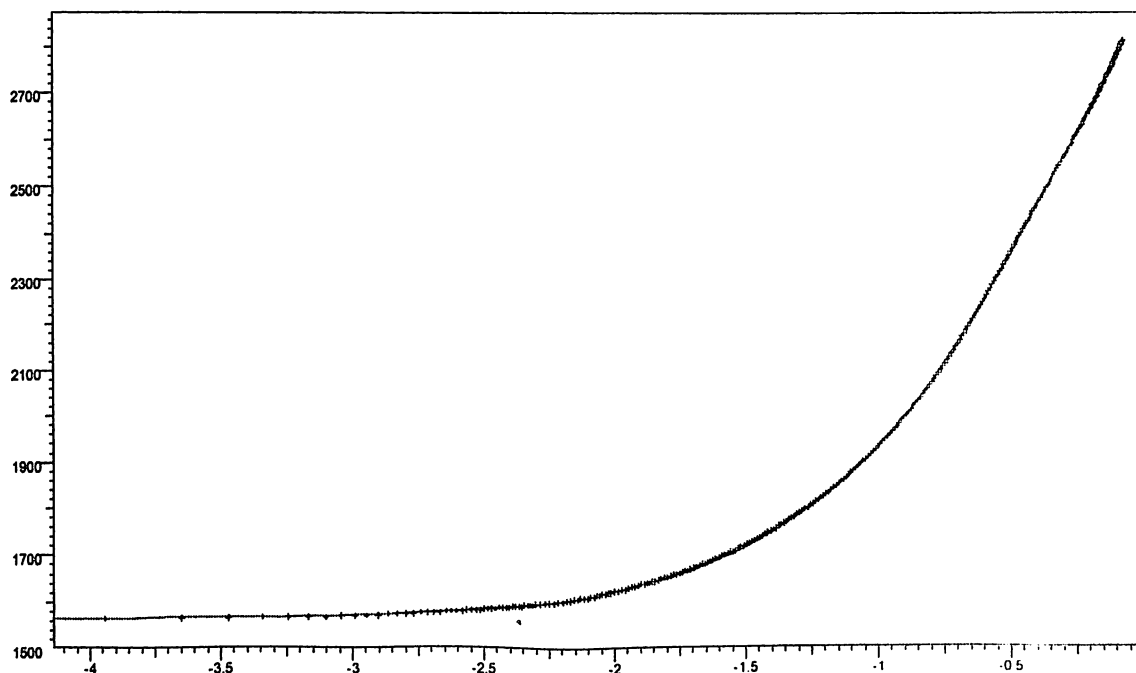
On careful analysis of the derivative pattern, the following series of flow regimes were observed:

The initial unit slope indicates wellbore storage. And the subsequent faint half unit slope points towards linear flow. This is due to masking of the linear slope by the wellbore storage. Linear flow is a sign of infinite conducting fracture.

Following the linear flow, a zero slope pattern which signifies Infinite Acting Radial Flow (IARF) is observed. The successive quarter slope does not yield anything crucial. But if the transient test would have been performed over a prolonged period, the derivative may have again stabilized at zero slope indicating IARF.

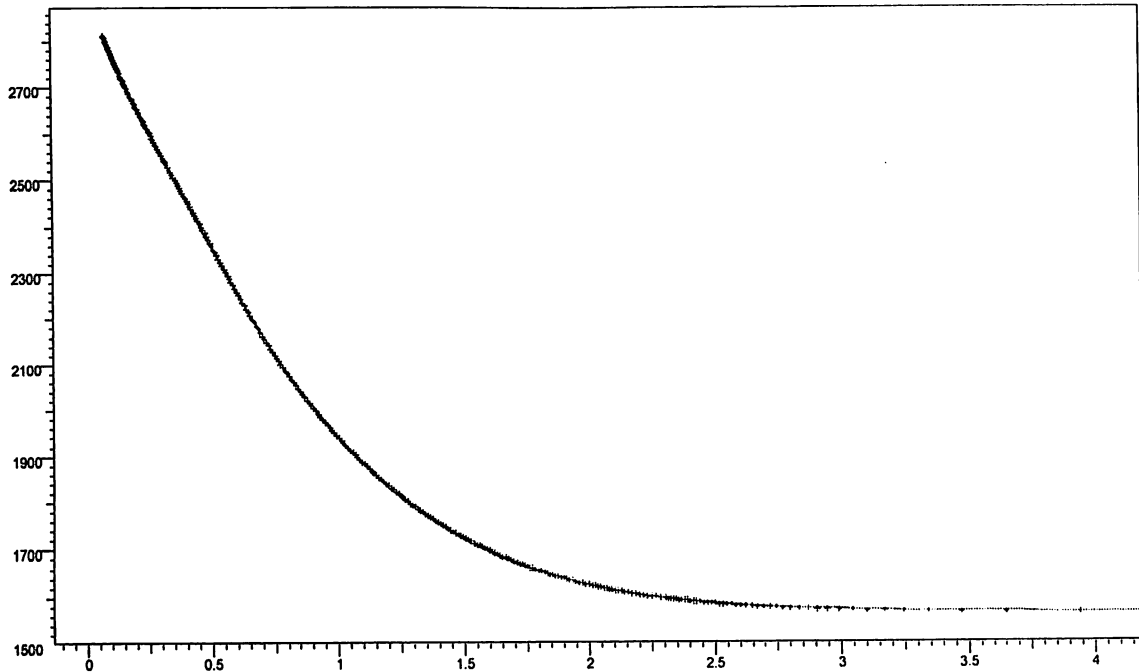
Considering the overall derivative response, the sharp transition from linear flow to radial flow demarcates the hair-line difference between Infinite Conducting Fractures and Fracture-Uniform Flux. Thus the further calculations were done considering the well as Fracture-Uniform Flux..

- **Semi-Log Plot:** After plotting the appropriate semi-log plot, a straight line is drawn through the points located within the equivalent radial flow portion of the plot identified from the above log-log plot.

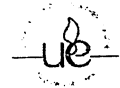


Semi-Log plot: p [psia] vs Superposition Time

- **Horner Plot:** this plot is plotted between the Pressure and the Elapsed Time to finally yield initial reservoir pressure after the identification of the radial flow equivalent straight line portion.



Horner plot: p [psi] vs $\log(tp+dt) - \log(dt)$



8.4 Results and Discussion

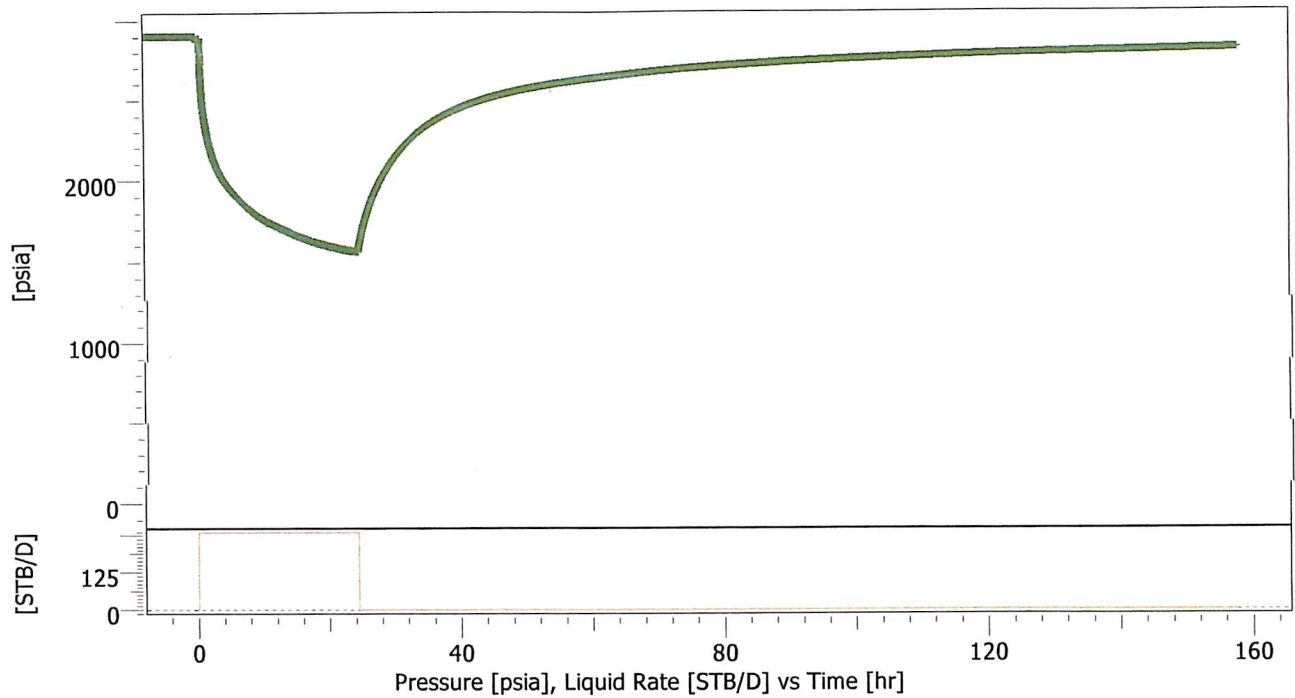
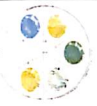
- The reservoir pressure is 2933 psia and the reservoir temperature is 108°C.
- From the Derivative response and the study of the different flow regimes, it can be concluded that the wellbore model is Uniform Flux Fracture. And the other derived results have been tabulated below.

Selected Model		
Model Option	Standard Model	
Well	Fracture - Uniform flux	
Reservoir	Homogeneous	
Boundary	One fault	
Main Model Parameters		
TMatch	0.103	[hr]-1
PMatch	0.00125	[psia]-1
C	0.0408	bbl/psi
Total Skin	-3.95	--
k.h, total	22.4	md.ft
k, average	0.853	Md
Pi	2933.02	Psia
Model Parameters		
Well & Wellbore parameters (Tested well)		
C	0.0408	bbl/psi
Skin	0	--
Geometrical Skin	-3.95	--
Xf	50.1	Ft
Theta	90	°
Reservoir & Boundary parameters		
Pi	2933.02	Psia
ko_eq.h	22.4	md.ft
ko_eq	0.853	Md
kro	0.5	--
L - No flow	116	Ft



The negative value of the Geometrical skin -3.95 substantiates the manually calculated value of skin and thereby confirms that the well has been stimulated by Hydro-fracturing.

The weak indication of the half slope is due to the small value of fracture half length X_f (50.1 ft). due to this the linear flow has been partially masked by the wellbore storage.

Company
Well Tested wellField
Test Name / #**Pressure build-up #1**

Rate 0 STB/D
 Rate change 259.643 STB/D
 P@dt=0 1565.55 psia
 Pi 2933.02 psia
 Smoothing 0.1

Selected Model

Model Option Standard Model
 Well Fracture - Uniform flux
 Reservoir Homogeneous
 Boundary One fault

Main Model Parameters

TMatch 0.103 [hr]⁻¹
 PMatch 0.00125 [psia]⁻¹
 C 0.0408 bbl/psi
 Total Skin -3.95
 k.h, total 22.4 md.ft
 k, average 0.853 md
 Pi 2933.02 psia

Model Parameters**Well & Wellbore parameters (Tested well)**

C 0.0408 bbl/psi
 Skin 0
 Geometrical Skin -3.95
 Xf 50.1 ft
 Theta 90 °

Reservoir & Boundary parameters

Pi 2933.02 psia
 k_{o eq}.h 22.4 md.ft
 k_{o eq} 0.853 md
 k_{ro} 0.5
 L - No flow 116 ft

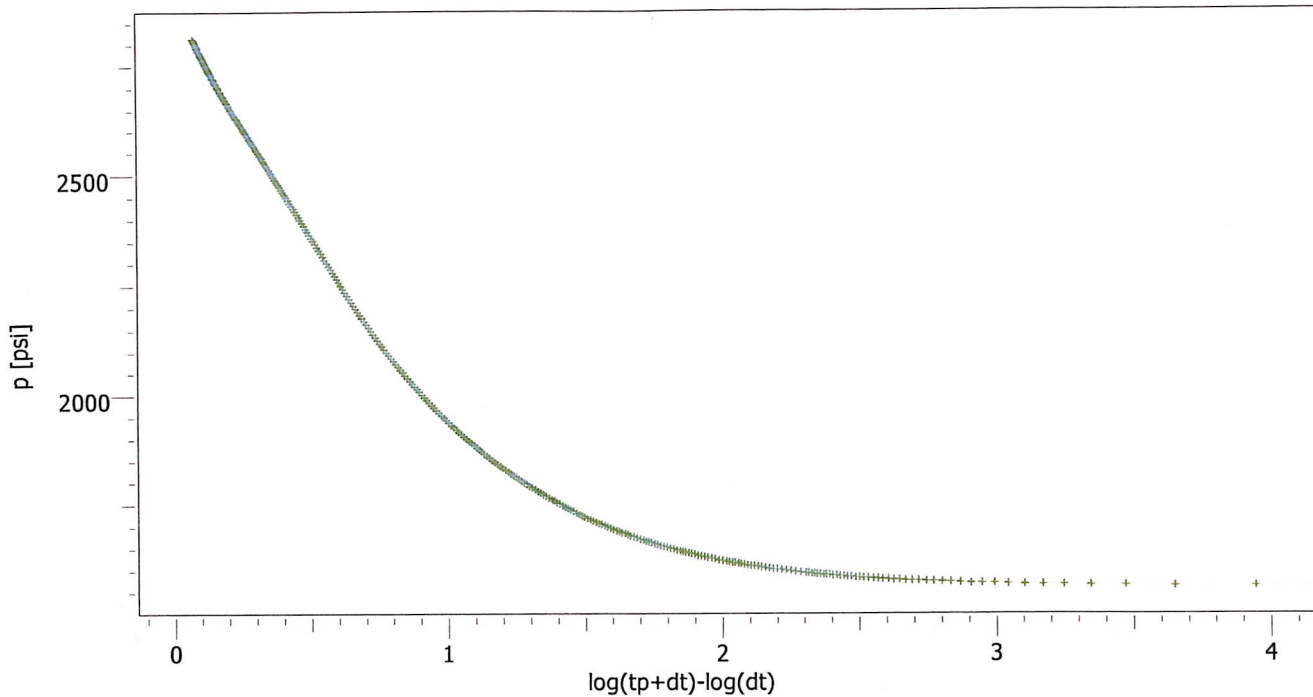
Derived & Secondary Parameters

k_o (Perrine) 0.853 md
 k_g (Perrine) 2.94E-9 md
 Delta P (Total Skin) -3159.96 psi
 Delta P Ratio (Total Skin) -2.53245 Fraction



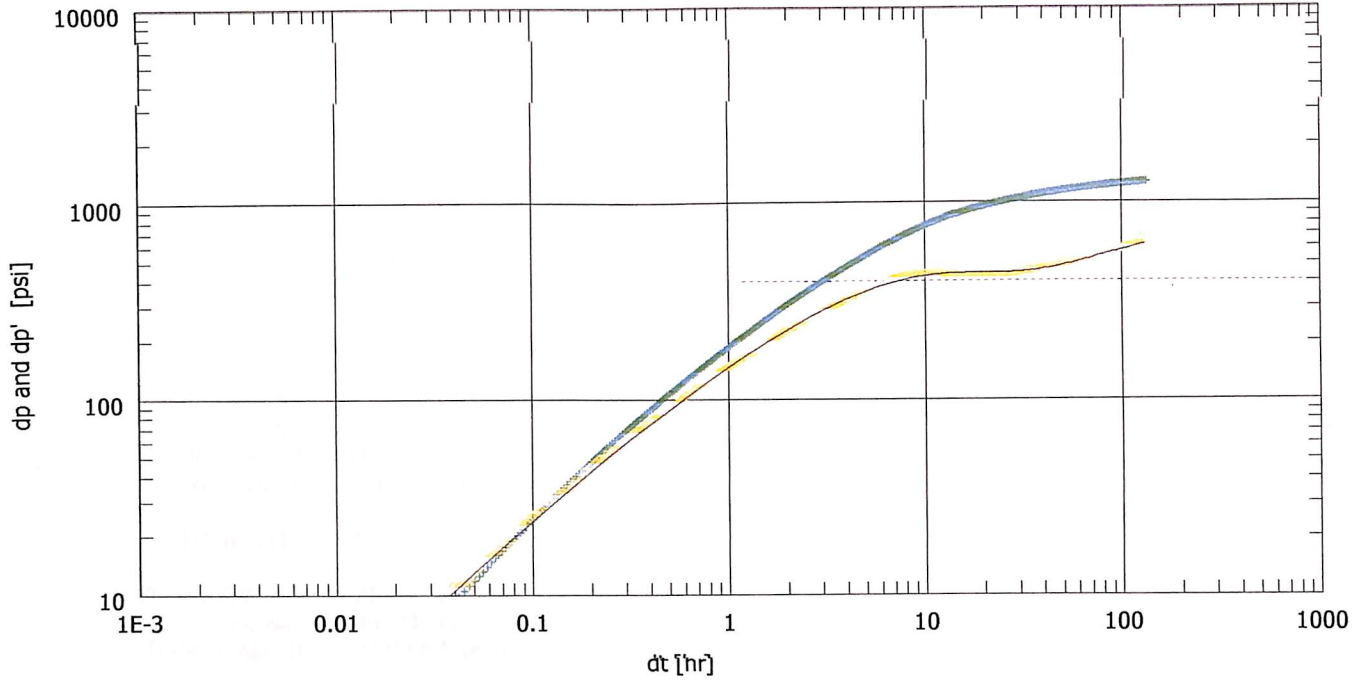
Company
Well Tested well

Field
Test Name / #



Pressure build-up #1

Rate 0 STB/D
Rate change 259.643 STB/D
P@dt=0 1565.55 psia
Pi 2933.02 psia
Smoothing 0.1



Pressure build-up #1

Rate 0 STB/D
 Rate change 259.643 STB/D
 P@dt=0 1565.55 psia
 Pi 2933.02 psia
 Smoothing 0.1

Selected Model

Model Option Standard Model
 Well Fracture - Uniform flux
 Reservoir Homogeneous
 Boundary One fault

Main Model Parameters

TMatch 0.103 [hr]⁻¹
 PMatch 0.00125 [psia]⁻¹
 C 0.0408 bbl/psi
 Total Skin -3.95
 k.h, total 22.4 md.ft
 k, average 0.853 md
 Pi 2933.02 psia

Model Parameters

Well & Wellbore parameters (Tested well)

C 0.0408 bbl/psi
 Skin 0
 Geometrical Skin -3.95
 Xf 50.1 ft
 Theta 90 °

Reservoir & Boundary parameters

Pi 2933.02 psia
 k_{o,eq,h} 22.4 md.ft
 k_{o,eq} 0.853 md
 k_{ro} 0.5
 L - No flow 116 ft

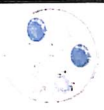
Derived & Secondary Parameters

k_o (Perrine) 0.853 md
 k_g (Perrine) 2.94E-9 md
 Delta P (Total Skin) -3159.96 psi
 Delta P Ratio (Total Skin) -2.53245 Fraction



Company
Well Tested well

Field
Test Name / #



Test date / time
Formation interval
Perforated interval
Gauge type / #
Gauge depth

TEST TYPE Standard

Porosity Phi (%) 12
Well Radius rw 0.354167 ft
Pay Zone h 26.2467 ft

Water Salt (ppm) 10000
Form. compr. 3E-6 psi-1
So 1
Sg 0
Sw 0
Reservoir T 226.4 °F
Reservoir P 2813.76 psia

FLUID TYPE Oil

Volume Factor B 1.28337 B/STB
Viscosity 0.380236 cp
Total Compr. ct 1.91266E-5 psi-1

Selected Model
Model Option Standard Model
Well Fracture - Uniform flux
Reservoir Homogeneous
Boundary One fault

Main Model Parameters
TMatch 0.103 [hr]-1
PMatch 0.00125 [psia]-1
C 0.0408 bbl/psi
Total Skin -3.95
k.h, total 22.4 md.ft
k, average 0.853 md
Pi 2933.02 psia

Model Parameters
Well & Wellbore parameters (Tested well)

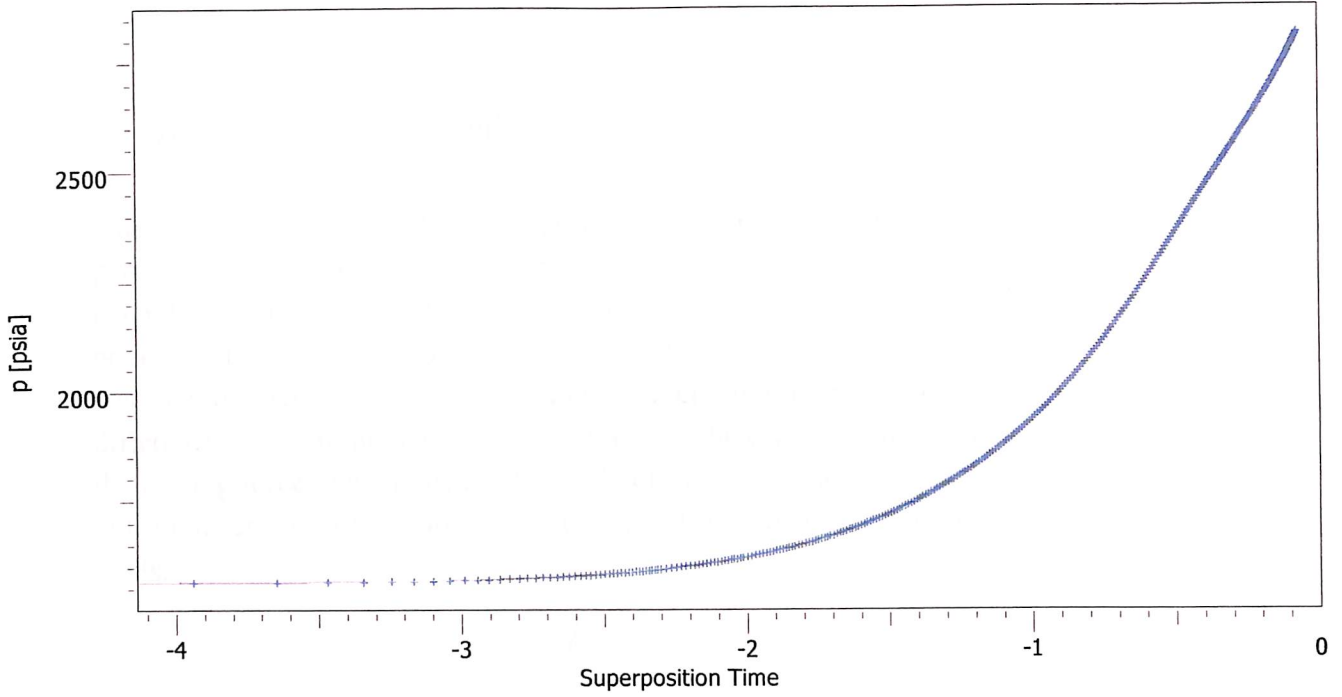
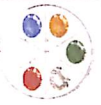
C 0.0408 bbl/psi
Skin 0
Geometrical Skin -3.95
Xf 50.1 ft
Theta 90 °

Reservoir & Boundary parameters

Pi 2933.02 psia
ko_eq.h 22.4 md.ft
ko_eq 0.853 md
kro 0.5
L - No flow 116 ft

Derived & Secondary Parameters

ko (Perrine) 0.853 md
kg (Perrine) 2.94E-9 md
Delta P (Total Skin) -3159.96 psi
Delta P Ratio (Total Skin) -2.53245 Fraction



Pressure build-up #1
 Rate 0 STB/D
 Rate change 259.643 STB/D
 P@dt=0 1565.55 psia
 Pi 2933.02 psia
 Smoothing 0.1

Selected Model
 Model Option Standard Model
 Well Fracture - Uniform flux
 Reservoir Homogeneous
 Boundary One fault

Main Model Parameters
 TMatch 0.103 [hr]⁻¹
 PMatch 0.00125 [psia]⁻¹
 C 0.0408 bbl/psi
 Total Skin -3.95
 k.h, total 22.4 md.ft
 k, average 0.853 md
 Pi 2933.02 psia

Model Parameters
Well & Wellbore parameters (Tested well)
 C 0.0408 bbl/psi
 Skin 0
 Geometrical Skin -3.95
 Xf 50.1 ft
 Theta 90 °

Reservoir & Boundary parameters
 Pi 2933.02 psia
 $k_{0_eq,h}$ 22.4 md.ft
 k_{0_eq} 0.853 md
 k_{r0} 0.5
 L - No flow 116 ft

Derived & Secondary Parameters
 k_o (Perrine) 0.853 md
 k_g (Perrine) 2.94E-9 md
 Delta P (Total Skin) -3159.96 psi
 Delta P Ratio (Total Skin) -2.53245 Fraction

Chapter 9

Recovery and material balance equations of double porosity reservoirs

Many of the crude oil- and natural gas reservoirs are dual porosity: i.e. they are fractured-porous. The fractures have low porosity (1-2 %) and high permeability (in the order of magnitude Darcy); the rock matrix, on the contrary, has high porosity (15-25 %) and low permeability (0.1-100 mD). The irregular fracture system crossing the rock renders possible the recovery of the accumulated crude oil and natural gas. The pressure difference between the matrix and the fracture, the capillary and the density difference is the driving force, which pushes the crude oil from the matrix to the fracture system. The latter collects the crude oil and natural gas leads to the perforation of the production wells.

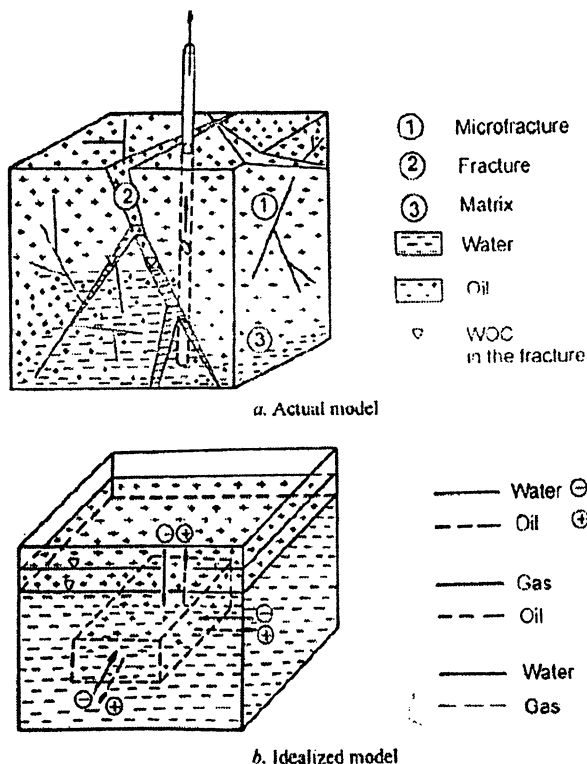


Figure 9.1 - Model of double porosity reservoir

If the reservoir is recovered by water flooding or gas injection, the displacing agent progressing in the fracture system surrounds the matrix and, by capillary and/or gravitational forces, displaces the crude oil and the natural gas in counterflow from the matrix. Because of the rock structure, the hydrocarbon cannot be displaced frontally from the matrix. The wellstream composition (fraction of oil, gas, water) is determined by the rate of the phase exchange between the fracture and the matrix system, the permeability



of the fracture system and the injection and production rate. The hydrocarbon displacement caused by capillarity and/or gravitational force is called spontaneous imbibition. This is a very complex process so it is investigated with the help of idealized models; the functions are deduced from this idealized model and are generalized for the whole reservoir. The matrix is represented in *Figure 9.1* by a parallelepiped, which is surrounded by the displacing phase, the water. The water imbibes into the matrix and the crude oil flows in counterflow into a vessel representing the fracture system.

9.1 Determination of Imbibition using empirical correlations: Aronofsky J. S., Masse L. and Natanson S. G. developed a model in 1958. The assumption is that the velocity of change for any naturally occurring process e.g. oil recovery can be approximated by an exponential function:

$$V(t) = V_i R (1 - e^{-\lambda t})$$

Where:

- | | | |
|-----------|---|--------------------|
| $V(t)$ | - the volume of crude oil (natural gas) recovered from an elementary flooded rock during the period "t" | [m ³]. |
| V_i | - initial volume of crude oil (natural gas) in the matrix | [m ³]. |
| R | - ultimate recovery factor after infinite immersion time | [-]. |
| λ | - constant, determining the convergence rate of the process bound for R, depending on the rock parameters, fluid properties, etc. | [1/day] |
| t | - time of immersion | [day]. |

Equation given above shows that the cumulative volume of crude oil (natural gas) is increasing as a function of the time, but the rate of growth is decreasing.

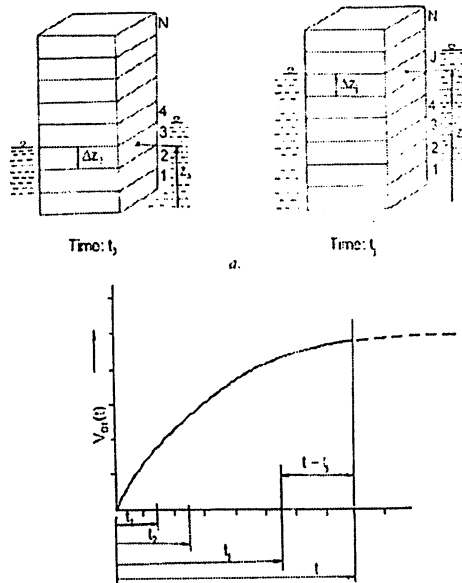


Figure 9.2 - Reservoir being considered as a series of blocks

The reservoir can be considered as the series of elementary blocks, which are immersed in the water at a different time – *Figure 9.2*. Total production is the sum of the production of individual blocks:

$$V_o(t) = \sum_{j=1}^n n^* \Delta z_j R [1 - e^{-\lambda(t-t_j)}]$$

Where:

$$n^* = \frac{\phi A S_{oi}}{B_o}$$

And,

$$V_{ij} = \frac{\phi A S_{oi} \Delta z_j}{B_o}$$

n= number of blocks

t_j	- time from the beginning until the flooding of the j^{th} block	[day]
$t - t_j$	- duration of immersion of block j	[day]
$V_o(t)$	- the volume of cumulative recovered crude oil (natural gas) during the period "t" (end of production or for example 10 years after the start of production)	[m ³].
V_{ij}	- the initial volume of crude oil in the j^{th} block	[m ³].
ϕ	- porosity	[-].
A	- cross section (base) of the reservoir parallelepiped	[m ²].
S_{oi}	- initial oil saturation	[-].
B_o	- formation volume factor	[-].
Δz_j	- thickness of the j^{th} block	[m].

If the reservoir or a vertical section of it is modeled as a series of infinite elementary units, equation for determination of imbibition will have the following form:

$$V_o(t) = n^* R \int_{z=0}^{z_j} [1 - e^{-\lambda(t-t_j)}] dz_j .$$

Let us assume that in the period $t = 0, Z = 0$ and in the period $t = t, Z = z$, the process lasts until $t = t$ and the velocity "a" of water raise is constant in the fracture system, i.e.:

$$Z_j = at_j \quad \& \quad dz_j = adt_j$$

Then the above equation can be written as following:

$$V_o(t) = n^* R a \int_{t_j=0}^{t_j} (1 - e^{-\lambda(t-t_j)}) dt_j .$$

Integrating the above equation we get:

$$V_o(t) = n^* R a \left[t + \frac{e^{-\lambda t}}{\lambda} - \frac{1}{\lambda} \right] .$$

As $V_j(t) = an^*t$ i.e. $an^* = V_j(t)/t$ - therefore the equation given above has another form:

$$r(t) = R \left[1 + \frac{1}{\lambda t} (e^{-\lambda t} - 1) \right]$$

If the exploitation process of the reservoir is followed by a monitoring system and so the actual water-oil contact, the initial oil resource (O.O.I.P.) and the actual recovery factor r

$= r(t)$ are known in the rock volume under the actual water level, then the unknown R and λ can be determined.

The determination of the unknown R and λ is as follows:

- The actual recovery factor ' $r(t)$ ' is determined as a function of the actual water-oil contact and is plotted as a function of $(1/\lambda t)(1 - e^{-\lambda t})$, where a value of λ is estimated.
- If this estimated value λ is not equal to λ_{optimum} , the measured points do not fall on a straight line, so another value has to be estimated, etc. The axial section of the straight line gives the value of R

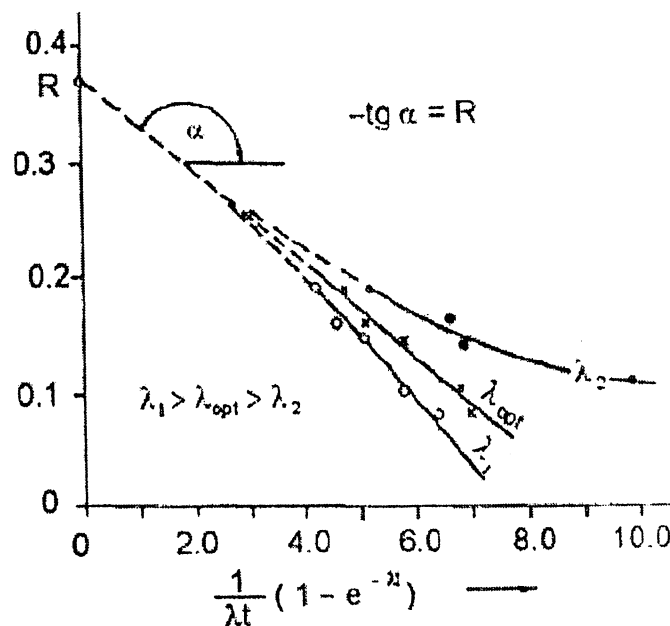


Figure 9.3- Determination of recovery parameters

If the velocity of water level is not constant, then the actual recovery factor is determined by the numerical integration of the following equation:

$$r(t) = \frac{R}{z(t)} \int_{t_j=0}^{t_j=t} [1 - e^{-\lambda(t-t_j)}] z'(t_j) dt_j.$$

Where z = height of water oil contact in the t moment.

The flow velocity may change due to the change of the production rate and/or even due to the geometry of the reservoir. If the reservoir is composed of different rocks, then different R and λ belong to each rock type. It is advisable to divide the rock into blocks in both cases and the equation given must be solved for each block. The R and λ value are determined for the lowermost block, which is flooded first by the displacing phase. Using

these parameters, the production of the block can be forecast even then, when the second block is flooded. In this period the total production will be the sum of the production of both blocks. The production of the second block can be determined as the difference of the total production and production of the first block; R_2 and λ_2 can be calculated from this and so forth.

As the observation of the actual location of the phase contact in the fracture takes place with some error, it is advisable to calculate R_i and λ_i , in such a complex case, by linear programming combined with minimizing of the square sum of the deviations. This method can be applied only when the pressure is constant during recovery. If the reservoir pressure is changing, the shrinkage of pore volume, the change of formation volume factor and the change of saturation due to gas liberation may also contribute to the production.

9.2 Flow between fracture and matrix: analytical analysis:

9.2.1 Unidirectional one dimensional displacement: This is the case when a matrix saturated with oil or gas, submerges into a displacing fluid at a given pressure and the displacement takes place by gravity and/or capillary forces and the displacing fluid moves in the same direction (e.g. vertically). This process is modeled very clearly by the procedure worked out by BIRKS J. in 1955. His method considers all the factors influencing the recovery process: block size, the properties of the displacing and the displaced fluid (density, viscosity) and the relative permeability functions. He assumes that the flow in the matrix is stationary.

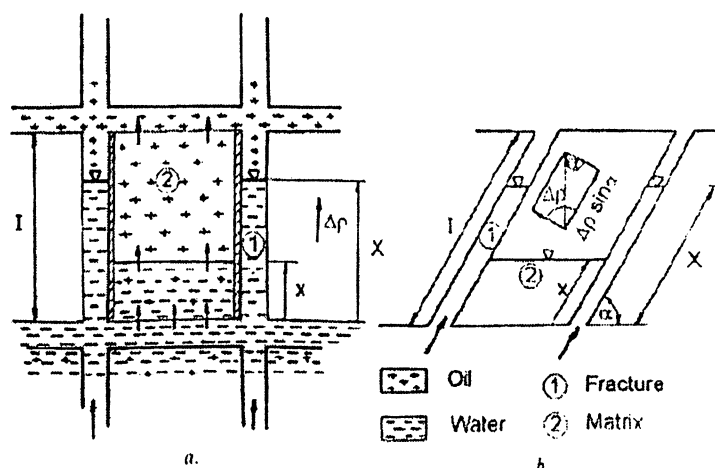


Figure 9.4- Birk's model

According to *Figure 9.4* the water enters the matrix through its bottom from the fracture and the displaced oil leaves the matrix at its top. The matrix is a prism (or cylinder) and



the vertical surfaces of matrix are impermeable, while its bottom and top surfaces are permeable. This means that the model is approximate one. In the case of gas displacement the process is analogous: the gas enters the matrix at the top of the prism, while the oil is produced through the bottom surface also. The equations deduced for water displacement are valid for gas displacement. If the capillary pressure in the fracture is neglected, the pressure in the fracture at the bottom surface of the prism is:

$$c^*g[X\rho_w + (I - X)\rho_o] = P_f$$

Where:

C^* = conversion factor 0.987×10^{-4}

g = acceleration due to gravity 9.81 m/s^2

X = height of water level in the fracture (cm)

ρ_w = density of water (gm/cm^3)

ρ_o = density of oil (gm/cm^3)

P_f = fracture pressure at the bottom of the block (atm)

I = height of the block (cm)

If the capillary pressure is also considered in the matrix, then the pressure in the matrix at the bottom surface is:

$$c^*g[x\rho_w + (I - x)\rho_o] - P_c = P_m$$

Where:

X = height of the water in the matrix

P_m = pressure in the matrix at the bottom of the matrix

P_c = difference between pressures of oil and water phase, capillary pressure

The pressure drop at the bottom surface is:

$$\Delta P = P_f - P_m = (X - x)(\rho_w - \rho_o)c^*g + P_c$$

If the displacement is not a vertical one, the gravity component being in the displacement direction must be taken. If the pressure drop ($\Delta P = \Delta P_w + \Delta P_o$) is expressed with the help of Darcy's law and it is assumed that the flow is stationary and the surface area is unit:

$$\Delta P = q \left[\frac{\mu_w}{k_w} x + \frac{\mu_o}{k_o} (1 - x) \right]$$

Where:

q = displacement velocity

μ_w = viscosity of water

μ_o = viscosity of oil

k_w = effective permeability of water

k_o = effective permeability of oil

Since,

$$q = (1 - S_{wc} - S_{or}) \phi_m \frac{dx}{dt}$$

And let it be that $X = 1$ i.e. the matrix block is completely submerged in the displacing fluid; therefore-

$$c * g(1 - x)(\rho_w - \rho_o) + P_c = (1 - S_{wc} - S_{or}) \phi_m \frac{dx}{dt} \left[\frac{\mu_w}{K_w} x + \frac{\mu_o}{K_o} (1 - x) \right]$$

Where:

S_{wc} = connate water saturation

S_{or} = residual oil saturation

t = time in seconds

ϕ_m = matrix porosity

Rearranging the equation:

$$\left[X \left(\frac{\mu_w}{K_w} - \frac{\mu_o}{K_o} \right) + \frac{\mu_o}{K_o} I \right] \frac{dx}{dt} + \frac{c * g(\rho_w - \rho_o)}{(1 - S_{wc} - S_{or}) \phi_m} = \frac{c * g I (\rho_w - \rho_o) + P_c}{(1 - S_{wc} - S_{or}) \phi_m}$$

This equation is solved utilizing Birk's hypothesis by assuming constant capillary pressure.

Until now we have studied the case in which the matrix instantaneously submerges in the displacing fluids that surrounds it. In the case in which the matrix block gradually sinks into the displacing fluid, i.e. $X = X(t)$, the following differential equation describes the advancement velocity of the displacing front in the matrix:

$$\frac{dx}{dt} \left[X \left(\frac{\mu_w}{K_w} - \frac{\mu_o}{K_o} \right) + \frac{\mu_o}{K_o} I \right] + \frac{c * g(\rho_w - \rho_o)}{(1 - S_{wc} - S_{or})} x = \frac{c * g(\rho_w - \rho_o) + P_c(x)}{(1 - S_{wc} - S_{or}) \phi_m}$$

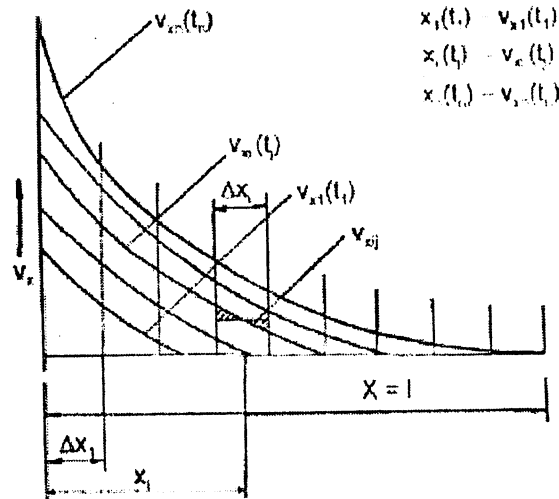


Figure 9.5- Displacement if matrix is gradually submerged in water

The equation is solved numerically in the following steps:

- The matrix is divided into elementary blocks which should be of identical length (ΔX_i).
- The height of the displacing phase in the fracture is assumed to be known $X_j = X_j(t_j)$ as a function of time (t_j).
- The V_{xi} values are determined for each X_j value by the equation proposed in this section so that $P_{ci} = P_c(X_i)$ - *Figure 9.5*.
- The flooding time of the matrix (until the block is submerged) is calculated by the help of the $V_{xi}(t_j) - X_i$ functions; and the following condition should be fulfilled:

$$\sum \Delta t_{ij} = \sum \frac{\Delta x_j}{V_{xij}} \equiv t_j.$$

The time (interval) necessary to flood an elementary block (t_{xi}) in the matrix at a given time (t_j) is always calculated with that velocity vs. height function $V_{xj} = V_{xj}f[X_j(t_j)]$ - belongs to the same (point of) time (t_j).

Continuing from that point of time when the matrix submerges in the water, the process of the displacement are determined by function $V_{xn} = V_{xn}(t_n, x)$.

9.2.2 Counterflow in 3D:

Single phase filtration between fracture and matrix: The applicability of the Birk's model is limited, since it presumes that the flow in the matrix is stationary and



unidirectional and displacement only takes place due to the effect of gravity and/or capillary forces when the filtration is two phase flow. On the contrary, the surfaces of the matrix are permeable in each direction, the flowing fluid may have single or multi-phase, the flow may be stationary, quasi-stationary or transient and production may also be influenced by depletion besides gravity and capillary forces.

Warren and Root determined the pressure as a function of production in the case of single phase flow and double porosity reservoir. They presume that the pressure is the same in the fracture surrounding the matrix block, the driving force of the fluid interchange between the block and the fracture is the matrix-fracture pressure difference only and surface all around of the matrix block is permeable. The rate of the fluid filtrates in the fracture from the matrix is as follows:

$$q = V \frac{\alpha}{\mu} k_m (P_m - P_f)$$

Where:

q= rate of fluid at reservoir condition	(cm ³ /sec)
V= volume of matrix	(cm ³)
α= shape or transmission factor	(1/cm ²)
μ= fluid viscosity	(cp)
K _m = matrix permeability	(Darcy)
P _m , P _f = matrix and fracture pressure	(atm)

Shape factor means that quantity of fluid, which flows out from unit matrix volume, during unit time, when matrix permeability, fluid viscosity and the pressure drop is also unit. The following equation can be used to determine the shape factor:

$$\alpha = 4 \left[\frac{1}{l_x^2} + \frac{1}{l_y^2} + \frac{1}{l_z^2} \right]$$

Where:

l _{x,y,z} = edges of the matrix block	(cm)
--	------

The quantity of fluid (oil and/or gas) flowing out of the matrix can be calculated by another equation also:

$$Q = V \phi_m (1 - S_{wc}) c (P_{mi} - P_m),$$

where:

Q	- cumulative quantity of fluid, at reservoir condition	[cm ³],
ϕ_m	- matrix porosity	[-],
S_{wc}	- connate water saturation	[-],
c	- effective compressibility	[1/atm],
P_{mi}	- initial pressure of the matrix	[atm],
P_m	- actual pressure of the matrix	[atm].

Since $q = dQ/dt$, therefore it can be written:

$$V \frac{\alpha}{\mu} K_m (P_m - P_f) = -V \phi (1 - S_{wc}) c \frac{dP_m}{dt}$$

At $t = 0$ of time the pressure in the fracture $P_{fi} = P_{mi} = P_i$, instantaneously drops to a value of $P_f = \text{const}$. We will determine the cumulative quantity of the fluid flowing out of the matrix $[Q(t)]$ by the effect of $\Delta P_f = P_i - P_f$ pressure drop as a function of time (t). If variables are separated and integrated and $P_{mi} = P_{fi}$ is taken into consideration, the matrix block pressure is a function of time:

$$P_m = P_f + (P_i - P_f) e^{-\frac{\alpha k_m}{\phi_m (1 - S_{wc}) c \mu} t}$$

Where:

$$P_m = P_m(t) \text{ and } P_f = \text{constant}$$

Since

$$Q = V \phi_m (1 - S_{wc}) c (P_{mi} - P_m)$$

It follows that:

$$\frac{Q(t)}{V \phi (1 - S_{wc}) c (P_i - P_f)} = 1 - e^{-\frac{\alpha k_m}{\phi_m (1 - S_{wc}) c \mu} t}$$

This is called the FLOW EQUATION. The right side of the equation is the dimensionless cumulative production $Q(t_D)$, where:

$$t_D = \frac{\alpha k_m}{\phi_m (1 - S_{wc}) c \mu} t.$$

The actual cumulative flow is:

$$Q(t) = V \Phi (1 - S_{wc}) c (p_i - p_f) Q(t_D); \text{ Where } Q(t_D) = 1 - e^{-t_D}$$

If the pressure changes in the fracture, superposition is applied and the quantity of the fluid as a function of time in the pore volume is as follows:

$$Q(t) = V \Phi (1 - S_{wc}) c \sum_{j=0}^{n-1} \Delta p_{fj} Q(t_D - t_{Dj})$$

In the fracture the pressure is $P_i, P_{f1}, P_{f2}, P_{f3}$ etc at $0, t_1, t_2, t_3$ etc points of time and is recommended that $\Delta t = t_i - t_{i-1}$ be constant.

The average pressure in the fracture is as follows in the particular time steps:

$$\overline{p_{f1}} = \frac{p_i + p_{f1}}{2}$$

$$\overline{p_{f2}} = \frac{p_1 + p_{f2}}{2}$$

$$\overline{p_{f3}} = \frac{p_2 + p_{f3}}{2}$$

.....

$$\overline{p_{fj}} = \frac{p_{j-1} + p_{fj}}{2}$$

The pressure drop in the fracture is calculated as following:

$$\Delta p_{fo} = p_i - \overline{p_{f1}} = \frac{p_i - p_{f1}}{2}$$

$$\Delta p_{f1} = \overline{p_{f1}} - \overline{p_{f2}} = \frac{p_i - p_{f1}}{2}$$

$$\Delta p_{f2} = \overline{p_{f2}} - \overline{p_{f3}} = \frac{p_{f1} - p_{f2}}{2}$$

.....

$$\Delta p_{fj} = \overline{p_{fj}} - \overline{p_{fj+1}} = \frac{p_{fj-1} - p_{fj+1}}{2}$$

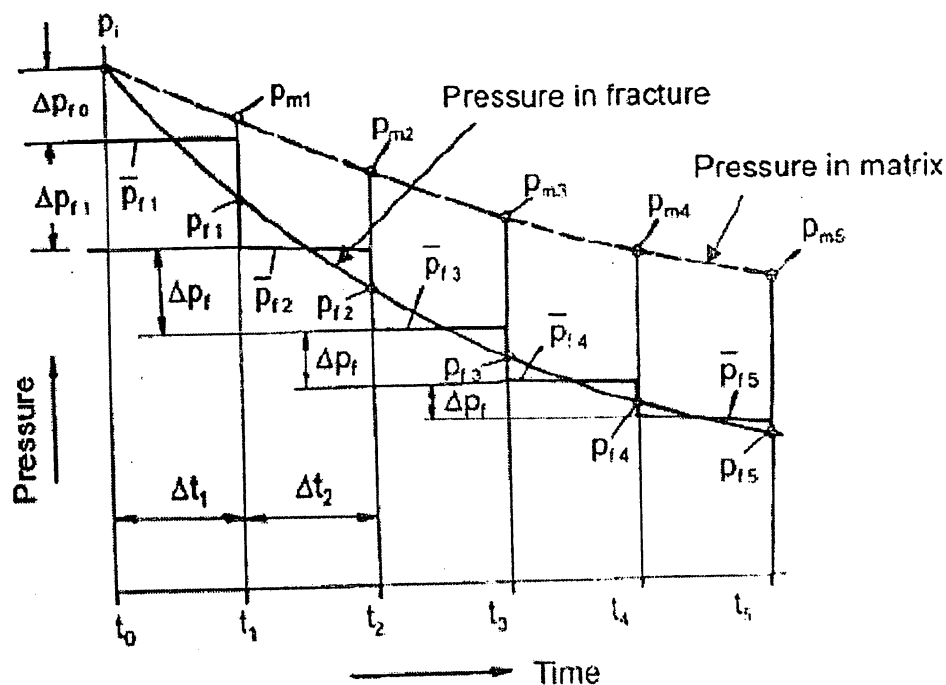


Figure 9.6- Pressure of fracture and matrix

We can modify the previously discussed flow equation with the help of the following designations:

$$J = V \frac{\alpha}{\mu} k_m$$

where:

- J - is the quantity of the fluid that can be recovered from the matrix block by 1 atm pressure drop, in pore volume [cm³/s].
- Q_i - is the initial quantity of oil in pore volume [cm³],
Q_i = V φ_m (1 - S_{wc}).
- Q_{ci} - is the quantity of oil that can be maximum recovered from the matrix at p_{fr} = 0 in pore volume [cm³],
Q_{ci} = c Q_i p_i.
- p_i - is the initial pressure [atm].

The flow equation has another form:

$$Q(t) = \frac{Q_{ei}}{P_i} (p_i - p_f) \left(1 - e^{-\frac{J p_i t}{Q_{ei}}} \right).$$

This is nothing but the Fetkovitch relation that was introduced to determine the quantity of water flowing into a reservoir from an aquifer of finite volume. In the cases of gas or saturated oil, both compressibility and viscosity are the function of pressure, therefore in these cases the precursors to the flow equation are solved by time steps, assuming that both compressibility and viscosity are constant during a given time step.

At the end of t_1 time step the pressure of the matrix block is:

$$p_{m1}(\Delta t_1) = \bar{p}_{f1} + (p_{mi} - \bar{p}_{f1}) e^{-\frac{\alpha k_m}{\phi_m (1-S_{wc}) \bar{c}_1 \bar{\mu}_1} \Delta t_1}.$$

At the end of t_1 time step the quantity of the fluid flown out of the matrix in pore volume is:

$$\Delta Q_1 = V \phi_m (1-S_{wc}) \bar{c}_1 (p_{mi} - p_{m1}).$$

At the end of t_2 time step the pressure of the matrix block is:

$$p_{m2}(\Delta t_2) = \bar{p}_{f2} + (p_{m1} - \bar{p}_{f2}) e^{-\frac{\alpha k_m}{\phi_m (1-S_{wc}) \bar{c}_2 \bar{\mu}_2} \Delta t_2}.$$

At the end of t_2 time step the quantity of the fluid flown out of the matrix in pore volume is:

$$\Delta Q_2 = V \phi_m (1-S_{wc}) \bar{c}_2 (p_{m1} - p_{m2}).$$

Hence generalizing, at the end of t_j time step the quantity of the fluid flown out of the matrix in pore volume is:

$$p_{mj}(\Delta t_j) = \bar{p}_{fj} + (p_{mj-1} - \bar{p}_{fj}) e^{-\frac{\alpha k_m}{\phi_m (1-S_{wc}) \bar{c}_j \bar{\mu}_j} \Delta t_j}.$$

At the end of t_j time step the quantity of the fluid flown out of the matrix in pore volume is:

$$\Delta Q_j = V \phi_m (1-S_{wc}) \bar{c}_j (p_{mj-1} - p_{mj}).$$

Multiphase flow between fracture and matrix: Two cases are studied. The first case is: the driving force of the fluid transmission between the matrix and the fracture is the gravitational and the capillary force (two-phase case of spontaneous imbibition). The second case is: the driving force is the pressure difference between the matrix and the fracture (caused by production flow from fracture) and the gravitational and the capillary force, filtration is three-phase flow.

Spontaneous imbibition: The equation corresponding to "j" point of time is as follows:

$$q_j = V\alpha \frac{k_r}{\mu} k_m [\Delta P_c(S_w) + \Delta P_g(S_w)]_j.$$

where:

$$k_r = k_{ro} \quad \text{or} \quad k_r = k_{rg},$$

$$\mu = \mu_o \quad \text{or} \quad \mu = \mu_g,$$

$$q_j = q_{wj} \quad \text{or} \quad q_j = q_{oj},$$

ΔP_c - capillarity force,

ΔP_g - gravitational force,

$$S_{wj} = S_{wr} + \sum_{j=1}^j \Delta S_{wj},$$

$$\Delta Q_{wj} = (V\phi)_m \Delta S_{wj},$$

$$\Delta t_j = \frac{\Delta Q_{wj}}{q_j}.$$

ΔS_{wj} - change of water saturation in the matrix
(is recommended as constant, e.g.: = 0.01) [-]

Cumulative parameters:

$$Q_w = \sum_{j=1}^j Q_{wj},$$

where:

$$Q_w = Q_o,$$

$$t = \sum_{j=1}^j \Delta t_j.$$

Fluid transmission caused by capillary, gravity force and pressure drop between the fracture and matrix: In case of spontaneous imbibition the production is the same as the pore volume quantity of the oil or natural gas displaced from the matrix by the effect of gravity and capillary force at the initial formation pressure, because there is no pressure

drop in the fracture due to water injection and/or water influx in the case of water flooding. In the case of a production rate realized in practice, the recovery from the matrix is influenced by the capillary force (ΔP_c), by the gravity (ΔP_g) and the pressure difference between the fracture and the matrix ($\Delta P_{f, m}$). Let us use the FLOW EQUATION for three phases at arbitrary time interval. In the i^{th} time step the oil, gas and water volume flown into the fracture from the matrix at normal condition are:

$$\Delta Q_o(\Delta t_i) = V_{pim} (1 - c_p \Delta P) \frac{S_o c_o}{B_o} (\tau_m - \tau_f)_o \left(1 - e^{-\frac{\alpha k_m k_{ro}}{\phi_i (1 - c_p \Delta P) S_o c_o \mu_o} \Delta t_i} \right)$$

$$\Delta Q_g(\Delta t_i) = V_{pim} (1 - c_p \Delta P) \frac{S_g c_g}{B_g} (\tau_m - \tau_f)_g \left(1 - e^{-\frac{\alpha k_m k_{rg}}{\phi_i (1 - c_p \Delta P) S_g c_g \mu_g} \Delta t_i} \right) + \Delta Q_o R_{sm}$$

$$\Delta Q_w(\Delta t_i) = V_{pim} (1 - c_p \Delta P) \frac{S_w c_w}{B_w} (\tau_m - \tau_f)_w \left(1 - e^{-\frac{\alpha k_m k_{rw}}{\phi_i (1 - c_p \Delta P) S_w c_w \mu_w} \Delta t_i} \right)$$

Where;

- ΔQ_o = the quantity of oil flowing out of or in the matrix [cm³]
- ΔQ_g = the quantity of gas flowing out of or into the matrix [cm³]
- ΔQ_w = the quantity of water flowing in or out of the matrix [cm³]
- V_{pim} = initial pore volume of the matrix [cm³]
- C_p = effective compressibility of the matrix [1/atm]
- S_o = average oil saturation
- S_g = average gas saturation
- S_w = average water saturation
- C_o = oil compressibility [1/atm]
- C_g = gas compressibility [1/atm]
- C_w = water compressibility [1/atm]
- B_o = reservoir volume factor of oil at average matrix pressure [m³/m³]
- B_g = reservoir volume factor of gas at average matrix pressure [m³/m³]
- B_w = reservoir volume factor of water at average matrix pressure [m³/m³]
- ΔP = difference between initial and final matrix pressure [atm]
- Φ_i = initial porosity of the matrix
- K_{ro} = relative permeability of oil depending on saturation
- K_{rg} = relative permeability of gas depending on saturation
- K_{rw} = relative permeability of water depending on saturation
- ΔT = time step [sec]
- τ = fluid potential [atm]

If Δt is small, parameters depending on pressure and saturation can be taken explicitly. In the case of fluid potential, the capillary and the gravity force must also be taken into consideration. It was recommended by Papay and Gundel in 1981 that gravity must be taken into consideration in numerical modeling. This concept is used here also. It is assumed that both in the matrix and the fracture the fluids distribute according to the density of phases, as shown in figure. The pressure differences of a phase are determined by the help of density gradient. For the sake of simplicity it is presumed that density of a fluid is identical both in the matrix and the fracture. This type of determination of the gravitational force is an approximation. In the first case the fluid distribution is homogenous. Consequently, gravitational force is not active in the fluid transport between fracture and matrix. In the second case the effect of gravitational force is maximum one. In the material balance calculation presented, the second assumption is accepted and explained.

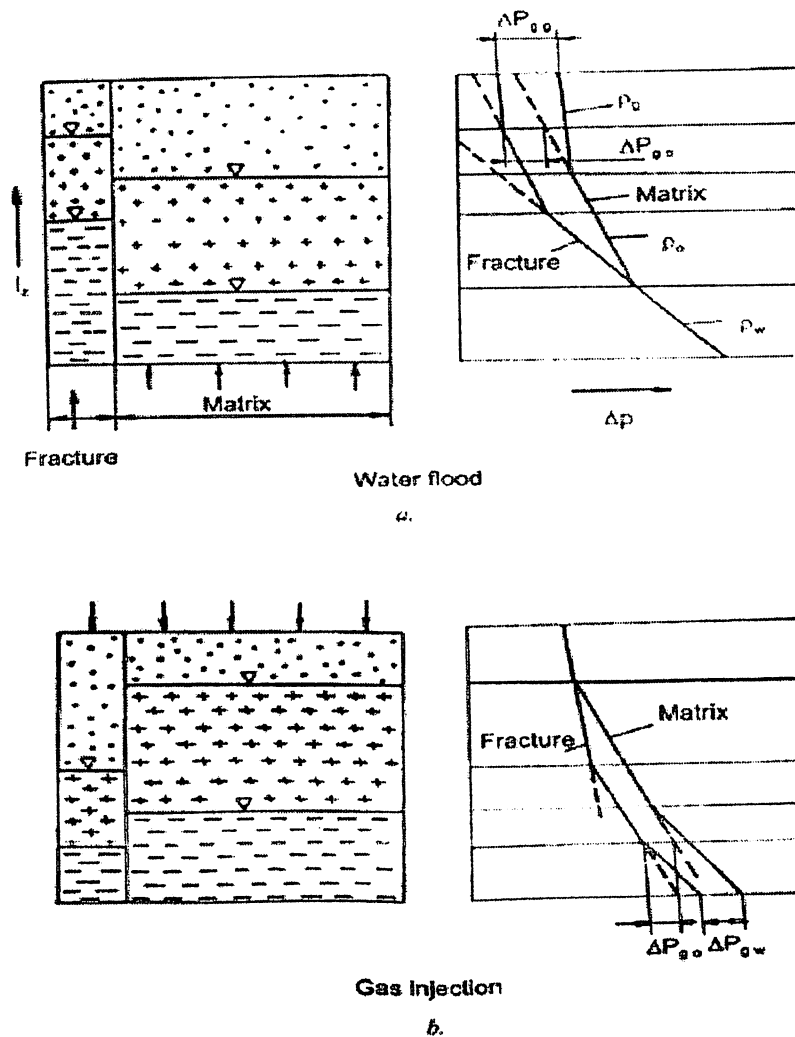


Figure 9.7- Approximation of gravitational force

The gravity force per phase is the following:

- In the case of water flood

$$\Delta P_{gg} = -c l_z g [(S_w \rho_w + S_o \rho_o + S_g \rho_g)_m - (S_w \rho_w + S_o \rho_o + S_g \rho_g)_f]$$

$$\Delta P_{go} = -c l_z g \{ (S_w \rho_w)_m + [(S_w + S_o)_f - S_{wm}] \rho_{om} - (S_w \rho_w + S_o \rho_o)_f \}$$

$$\Delta P_{gw} = 0$$

- In the case of gas flood

$$\Delta P_{gw} = c^* l_z g [(S_g \rho_g + S_o \rho_o + S_w \rho_w)_m - (S_g \rho_g + S_o \rho_o + S_w \rho_w)_f]$$

$$\Delta P_{go} = c l_z g \{ (S_g \rho_g)_m + [(S_g + S_o)_f - S_{gm}] \rho_{om} - (S_g \rho_g + S_o \rho_o)_f \}$$

$$\Delta P_{gg} = 0$$

Where;

m- Index corresponding to matrix

f- Index corresponding to fracture

Saturation is to be taken as movable saturation.

The difference of fluid potential, creating flow in case of water flood-

$$(\tau_m - \tau_f)_g = p_{mo} + P_{cgo} + \Delta P_{gg} - (p_{fo} + P_{cgo}),$$

$$(\tau_m - \tau_f)_o = p_{mo} + \Delta P_{go} - p_{fo}$$

$$(\tau_m - \tau_f)_w = p_{mo} - P_{cowm} - (p_{fo} - P_{cowf})$$

The difference of fluid potential, creating flow in case of gas flood-

$$(\tau_m - \tau_f)_g = p_{mo} + P_{cgo} - (p_{fo} + P_{cgo}),$$

$$(\tau_m - \tau_f)_o = p_{mo} + \Delta P_{go} - p_{fo}$$

$$(\tau_m - \tau_f)_w = p_{mo} - P_{cowm} + \Delta P_{gw} - (p_{fo} - P_{cowf})$$

If the quantity of the fluids flowing in or out of the matrix is known, the pressure (P_{mo}) of the matrix at the end of time step can be calculated from the following algorithm:

$$V_{pi-1} [1 - c_p \Delta P] = \left[\left(\frac{V_p S_o}{B_o} \right)_{i-1} - \Delta Q_{oi} \right] B_{oi} + \left[\left(\frac{V_p S_w}{B_w} \right)_{i-1} - \Delta Q_{wi} \right] B_{wi} +$$

$$+ \left\{ \left(\frac{V_p S_f}{B_f} \right)_{i-1} + \left(\frac{V_p S_o}{B_o} R_i \right)_{i-1} - \left[\left(\frac{V_p S_o}{B_o} \right)_{i-1} - \Delta Q_{oi} \right] R_i - \Delta Q_{fi} \right\} B_{si}$$

It is to be noted that each parameter and designation refers to the matrix, where:

$$\Delta P = (P_{mo})_{i-1} - (P_{mo})_i$$

C_p = effective matrix compressibility

9.3 Material balance equation for double porosity reservoirs:

In the cases in which reservoir has intergranular porosity, material balance analysis is widely used in the engineering practice and there is extensive literature on this topic. However, in the cases of double porosity reservoirs the material balance equation has not been worked out satisfactorily and due to its sophistication its application is not widespread. The form of material balance equation of a double porosity reservoir is different to a reservoir having intergranular porosity. This is due to fluid transport between fracture and matrix system caused by gravitational and capillary force and/or depletion. The material balance equation concerning double porosity reservoirs can be deduced by combining the material balance equation, which is valid for intergranular porosity reservoirs with the equations deduced for the matrix (Papay J., 1996, 1998).

The following assumptions are made for setting up the material balance equation:

- production/ injection takes place only through the fracture system i.e. fluid transport is only through fractures
- fluid production is determined by their respective fracture saturations
- pressure measurement is possible in fracture only
- phase boundaries are moving vertically

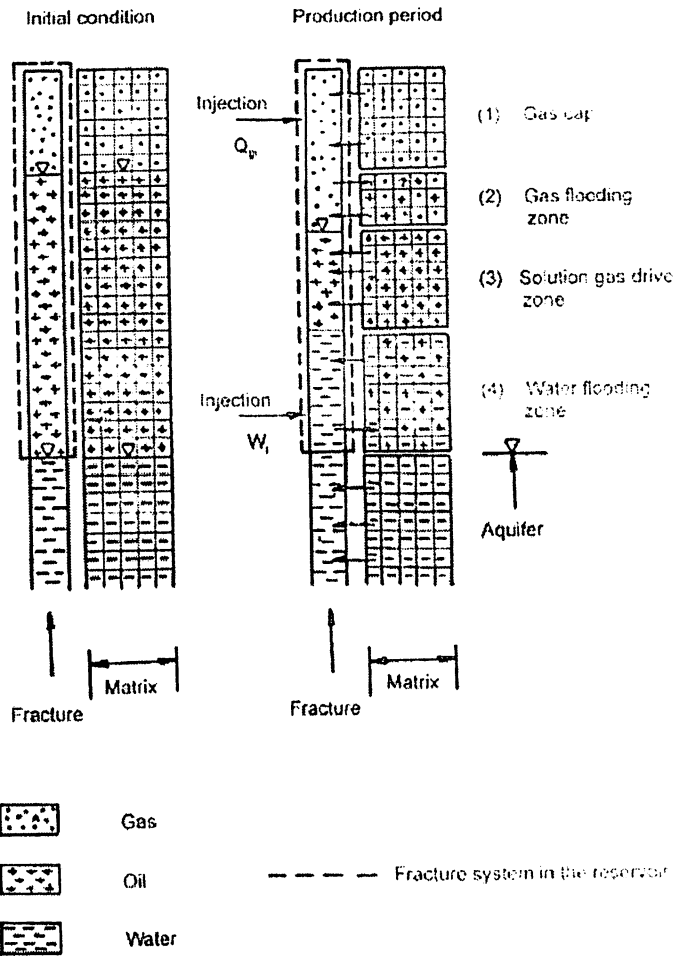


Figure 9.8- Displacement mechanism of double porosity reservoir

The material balance is based on the following model: from the gas cap (1), from the depletion zone (3) and from the aquifer there is an inflow to the fracture; the phase exchange takes place in the gas flooding zone (2) and in the water flooding zone (4), where gas and water displaces oil into the fracture in counterflow.

The material balance for the fracture system is:

$$\begin{aligned} & \{N_p[B_o + (R_p - R_s)B_g]\}_f \\ & = \left\{ V_{pi} S_{oi} \left[\frac{(B_o - B_{oi}) + (R_{si} - R_s)B_g}{B_{oi}} + m \left(\frac{B_g}{B_{gi}} - 1 \right) \right] \right. \\ & \quad \left. + (1 + m) \frac{c_w s_{wc} + c_p \Delta P}{1 - s_{wc}} + (W_s - W_p)B_w + (W_i B_w + Q_{gi} B_g) \right\}_f \\ & \quad + \sum_{x=1}^n (Q B_f)_{o,g,w} \end{aligned}$$

Where:

N_p	- cumulated quantity of the produced oil from the fracture system	$[m^3]$
$B_{o,g,w}$	- reservoir volume factor of oil, natural gas and water at the fracture actual pressure	$[m^3/m^3]$
$B_{oi,gi,wi}$	- reservoir volume factor of oil, natural gas and water at the fracture initial pressure	$[m^3/m^3]$
B_f	- reservoir volume factor of fluids at the actual pressure of the fracture	$[m^3/m^3]$
V_{pif}	- oil saturated total pore volume of the fracture, given at the initial condition	$[m^3]$
S_{oi}	- initial oil saturation in the fracture	$[-]$
m_1	- ration of the gas and oil-filled pore volumes in the fracture, given at the initial condition	$[-]$
R_{si}	- solution gas content of oil in the fracture at initial pressure	$[m^3/m^3]$
R_s	- solution gas content of oil in the fracture at actual pressure	$[m^3/m^3]$
R_p	- cumulative gas-oil ration	$[m^3/m^3]$
c_w	- water compressibility	$[1/atm]$
c_p	- effective rock compressibility in the case of the fracture	$[1/atm]$
ΔP	- difference between initial and actual pressure in the fracture	$[atm]$
S_{wc}	- connate water saturation	$[-]$
W_e	- cumulative water influx from the aquifer in the fracture	$[m^3]$
$W_p; W_i$	- cumulative quantity of water, produced/injected from the fracture	$[m^3]$
Q_{gi}	- cumulative quantity of gas injected into the fracture at normal condition	$[m^3]$
x	- indicating the number of matrix units, where in the matrix the displacement mechanism is the same.	$[m^3]$

It is evident that the classical material balance is simply extended by adding a term for the fluid transmission between fracture and matrix.



Conclusion

Well test analysis has been used to assess well condition and obtain reservoir parameter. Among the different heterogeneous models, the double porosity solutions have been the most widely accepted. This double porosity model is used to explain the pressure behaviour in a naturally fractured reservoir. Also the pressure behaviour in a layered reservoir is studied depending on the existing interlayer pressure and fluid communication between the different heterogeneous layers.

A very important and man-made type of reservoir heterogeneity is hydraulically induced formation fracture. A large percentage of present day well completions employ the hydraulic fracturing technique and thus the pressure behaviour in hydraulically fractured wells is also taken in consideration.

There is an extensive coverage on the phenomena of fracture appearance in the reservoir. We have presented equations dealing with flow from matrix to fracture in all the possible cases and these equations have been used to modify the Material Balance Equation and make it applicable to double porosity system.



References

1. Matthews, C.S. and Russel, D.G.: "Pressure Buildup and Flow Tests in Wells", SPE, 1967
2. Dake, L. P.: "Fundamentals of Reservoir Engineering", Elsevier Science, Amsterdam, 1978
3. Bourdet, D.: "Well Test Analysis: Use of Advanced Interpretation Model", Elsevier Science, Amsterdam, 2002
4. Cosentino, L.: "Integrated Reservoir Studies", IFP Publications, Paris, 2004
5. Lucia, J.: "Carbonate Reservoir Characterization", Springer Publication, Texas, 2007
6. Nelson, R.A.: "Geological Analysis of Naturally Fractured Reservoirs", Gulf Professional Publishing, Texas, 2001
7. Lee, J.: "Well Test Analysis", SPE, 1972
8. Ahmed, T & McKinney P.D.: "Advanced Reservoir Engineering", Elsevier Science, Amsterdam, 2002
9. Fanchi, J.R.: "Applied Reservoir Simulation", Gulf Publishing Company, Texas, 2000
10. Fattah Abdel K.A., Mahmoud E.S., Asaad Y.: "Differential Depletion Performance of Layered Reservoirs", SPE, 1995
11. Uleberg, K. & Kleppe, J.: "Dual Porosity, Dual Permeability Formulation for Fractured Reservoirs", NTNU, 1996
12. Archer, R. & Horne, R.: "Flow Simulation in Heterogeneous Reservoirs using the Dual
13. Reciprocity Boundary Element Method and the Green Element Method", ECMOR 6, 2000
14. Monteiro, J.A. & Pires, A.P.: "Pressure Transient Analysis in Heterogeneous Reservoirs", International Conference 'Inverse and Ill-Posed Problems of Mathematical Physics', 2007